5-2018

Identification of "fhuA" Like Genes in Rhizobium leguminosarum ATCC 14479 and its Role in Vicibactin Transport and Investigation of Heme Bound Iron Uptake System

Sushant Khanal

Identification of "*fhuA*" Like Genes in *Rhizobium leguminosarum* ATCC 14479 and Its Role in Vicibactin Transport and Investigation of Heme Bound Iron Uptake System

---

A thesis

presented to

the faculty of the Department of Health Sciences

East Tennessee State University

In partial fulfillment

of the requirements for the degree

Master of Science in Biology

---

by

Sushant Khanal

May 2018

Dr. Ranjan Chakraborty, Chair

Dr. Christopher Pritchett

Dr. Cecilia A. McIntosh

Keywords: *Rhizobium leguminosarum* ATCC 14479, *fhuA*, vicibactin, heme, iron uptake

ABSTRACT

Identification of "*fhuA*" Like Genes in *Rhizobium leguminosarum* ATCC 14479, and Its Role in Vicibactin Transport and Investigation of Heme Bound Iron Uptake System

by

Sushant Khanal

Siderophores are low molecular weight, iron chelating compounds produced by many bacteria for uptake of iron in case of iron scarcity. Vicibactin is a trihydroxamate type siderophore produced by *Rhizobium leguminosarum* bv. *trifolii* ATCC 14479. This work focuses on identifying an outer membrane receptor involved in the transport of vicibactin. We have confirmed the presence of the putative *fhuA* gene in *R. leguminosarum* bv. *trifolii* ATCC 14479. This bacteria shows mutualistic symbiosis with the red clover plant *Trifoliium prantense*. Leghemoglobin, with its cofactor heme is present in the plant root nodules that surrounds the infecting organism present in the nodules. This work attempts to elucidate the ability of *Rhizobium leguminosarum* bv. *trifolii* ATCC 14479 to utilize heme-bound iron and genes involved in the transport. We have also elucidated the role of energy transducing proteins TonB-ExbB-ExbD on the heme-bound iron uptake system.

ACKNOWLEDGEMENTS

I would like to thank my committee chair, Dr. Ranjan Chakraborty, for giving me an opportunity to work in his lab on this project and learn different laboratory techniques and use the resources in the lab to complete my thesis. I would not have known science better without his support, his mentoring, his austerity, also his friendliness and guidance. I would also like to show my gratitude towards my other committee members, Dr. Christopher Pritchett and Dr. Cecilia McIntosh for their guidance, time/support and their contribution and enthusiasm to my work. I would specially like to thank Dr. McIntosh for helping me with the writing part. I would not have reached this far without the help of Dr. Sean Fox in the lab meetings and presentations and other lab activities with him. I would thank him for all the support/help and his time. I would like to thank Mrs. Robin Grindstaff for the help in the media kitchen and would also like to thank my friends and colleagues who helped me through my MS. I would most of all like to thank my father, my mother, my brother, and other family members, relatives, all my friends who always supported me and pushed me this far and made me believe that I can do it. I would like to thank everyone here in the United States who helped me through this Masters. God bless us all.

TABLE OF CONTENTS

Page

LIST OF TABLES

Table Page

LIST OF FIGURES

Figure Page

CHAPTER 1

INTRODUCTION

Rhizobium leguminosarum

Rhizobium leguminosarum is a gram-negative bacillus. It is an aerobic and motile soil bacterium. It dwells in a symbiotic relationship with legume plants and is present in legume plant roots. The legume roots get infected by these bacteria, that results in the formation of root nodules. This symbiosis facilitates the host plant and the bacteria by providing essential nutrients to each other for survival. The plant provides a habitat and energy for the bacteria to survive. The bacterium provides nitrogen to the plant by performing nitrogen fixation with a process of converting atmospheric nitrogen into nitrogen compounds (Postgate 1998). Nitrogen compounds are essential for growth and development of the plants (Postgate 1998). The abundance of these compounds helps the legume plants to compete with other plants in their surroundings (Postgate 1998). When these legume plants are dead and decayed, the nitrogen is then released into the soil and is available to other plants, which when accumulated in the soil helps to increase the soil fertility (Postgate 1998). Crop rotation can also be done growing legume plants and non-legume plants in turns to increase the soil fertility (Postgate 1998).

Rhizobia are present in free-living form in the soil and they infect legume plant roots. There is an involvement of various flavonoid inducers in this infection process (Peters et al. 1986). The infection of the plant roots is a process which involves quorum sensing mediated via acyl homoserine lactones (AHLs) (Walker and Downie 2000). The symbiosis helps bacteria in various ways viz. growth and development, survival and association with the host (McAnulla et al. 2007). Quorum sensing might also be a factor for successful nodule formation (Walker and

Downie 2000). This symbiotic relationship between the plant and the bacteria is important for both of them to acquire proper nutrients, nitrogen, for the plant; and sugar, minerals and amino acids for the bacteria (Postgate 1998).

Rhizobium leguminosarum biovar *trifolii* ATCC 14479

There are two commonly studied biovars of *R.* leguminosarum; the *R. leguminosarum* biovar *trifolii,* and *R. leguminosarum* biovar *viciae* (Ann and Kim 1998). Both share some common characteristics such as symbiotic nitrogen fixation, root infection and root nodule formation. The strain used in this research is *R. leguminosarum* biovar *trifolii* ATCC 14479 (*R. leguminosarum* ATCC) and is the most effective for nodule formation in roots of the red clover, *Trifoliium prantese* (Ramirez-Bahena et al. 2008). This strain is also known as strains USDA 2046, DSM 6040 and *R. trifolii* Danegeard 1926 (Ramirez-Bahena et al. 2008).

R. leguminosarum ATCC produces a hydroxamate type siderophore, vicibactin, for iron chelation and uptake (Wright et al. 2013). The transport of iron via outer membrane receptors requires energy; however, there is no energy source available in the outer membrane. The inner membrane protein complex TonB-ExbB-ExbD is presumably responsible for energy transduction during the vicibactin transport in *R. leguminosarum* ATCC (Hill 2014; Barisic 2015).

Iron and Its Importance

Iron is one of the most common and abundant elements on earth and is also one of the most important elements for all the living beings, ranging from highly developed multicellular organisms such as humans to unicellular microorganisms such as bacteria. An overdose of iron

in humans causes hemochromatosis, causes damage to lipids, proteins and DNA, damages digestive cells inside the human gut, damages cells in the heart, liver and anywhere else there is excess iron leading to shock, organ failure, coma, and even death (CDC 1998). The unavailability of iron in humans leads to anemia, which leads to insufficient amount of hemoglobin in the blood that makes children and adult women susceptible to various diseases (CDC 1998).

Lack of iron in bacteria affects the bacterial cell composition causing the inhibition of growth and changes the cell morphology in bacteria. It also decreases the rate of RNA and DNA synthesis (Messenger and Barclay 1983). Promotion of sporulation in bacteria is also dependent on sufficient iron concentration and sufficient siderophore production (Grandchamp et al. 2017). It also affects the intermediary metabolism in bacterial cells as they need iron for the tricarboxylic acid cycle (TCA cycle), electron transport, oxidative phosphorylation, nitrogen fixation and aromatic compound biosynthesis (Messenger and Barclay 1983). Metabolic products in various bacteria such as cytochromes, pigments (e.g. bioluminescent *Pseudomonas aeruginosa*), porphyrins, vitamins, siderophores, toxins (e.g. diphtheria toxin produced by *Corynebacterium diphtheria*) and antibiotics are either upregulated or downregulated by the amount of iron available in the cell (Messenger and Barclay 1983; Kunkle et al. 2003; Hannauer et al. 2010). Protein and enzyme synthesis are also dependent on available iron concentration (Messenger and Barclay 1983). The proteins/enzymes that are dependent on iron are peroxidases, ribonucleotide reductase, glutamate synthase, superoxide dismutase, ferritin, nitrogenase, ferridoxins, flavoproteins, hydrogenase and many others (Messenger and Barclay 1983).

Availability of Iron in the Environment and Iron Scavenging Systems in Bacteria

Iron is the fourth most abundant element in Earth's crust after oxygen, silicate, and aluminum (Rudnick et al. 2003). Iron has a wide range of oxidation states from −2 to +7 similar to other transition metals such as ruthenium and osmium in group 8 of IUPAC (International Union of Pure and Applied Chemistry) nomenclature, although +2 (ferrous iron) and +3 (ferric iron) are the most common forms (Meija 2016). It is very reactive in the presence of water and oxygen at physiological pH (Sund 1980). The formation of polymeric iron hydroxides occurs in such environment, which is commonly known as rust (Sund 1980). Soluble iron also reacts with sulfides, chlorides and oxalates to make insoluble complexes, causing depletion of soluble iron in the environment. Hence, the soluble iron concentration in the environment is calculated to be approx. 10^{-18} M which is much lower than what a bacterium has inside the cell (10^{-6} M). This intercellular iron concentration in a bacterial cell should be maintained to survive (Andrews et al. 2003). Therefore, bacteria, fungi, and plants produce iron chelating compounds known as siderophores. These are iron scavenging compounds, and they form complexes with the ferric iron in the environment, that is transported into the cell via complex mechanism (Messenger and Barclay 1983).

Some other sources of iron for pathogenic and some nonpathogenic bacteria are hemin, hemoglobin, ferritin, lactoferrin, and transferrin (Noya et al. 1997). These molecules contain heme as a cofactor. Heme contains a central iron molecule in its porphyrin ring structure. Many bacteria uptake the heme-bound iron by either breaking down the heme-containing compound outside the cell using hemophores or taking in the whole compound inside and breaking it down within the cell (Tong and Guo 2009). The HasA uptake system in *Ps. aeruginosa* involves

hemophore mediated heme uptake; the *phuSTUVW* system in the same organism can uptake heme without using hemophores (Létoffé et al. 1996; Ochsner et al. 2000).

Siderophore Mediated Iron Transport

Siderophores are compounds that are produced by bacteria for iron uptake. These compounds chelate and transport iron from iron complexes. Siderophores are low molecular weight compounds (< 2 kDa) and have the strongest association constant with ferric iron (Loomis and Raymond 1991). The siderophore "enterobactin" in *Escherichia coli* has an association constant of 10^{52} with ferric iron (Loomis and Raymond 1991). The synthesis of siderophore starts when the amount of ferrous iron inside the cell is less than 10^{-6} M, which is a bacterial threshold (Miethke and Marahiel 2007). More than 90 genes that are involved in biosynthesis and uptake of siderophore are controlled by Fur (Ferric uptake regulator) repressor (Wexler et al. 2003). It is hence, considered as a global iron regulator protein. The DNA binding site for Fur is known as the Fur box, and it regulates siderophore synthesis and transport genes using Fe^{2+} and Mn^{2+} as corepressors (Wexler et al. 2003). However, in gram-positive bacteria such as *C. diphtheria,* the DtxR family of proteins replaces Fur and controls iron regulation (Kunkle et al. 2003).

In some gram negative bacteria, other regulator proteins replace the Fur proteins. For example, Rhizobial iron regulator (RirA) controls iron regulation and uptake in the case of nitrogen-fixing *Rhizobium* (Rudolph et al. 2006). Only alphaproteobacteria show the presence of a RirA homolog that has no sequence similarity with Fur proteins (Rudolph et al. 2006). *R. leguminosarum* being in alphaproteobacteria class also shows the presence of RirA proteins that belong to the Rrf2 family of transcription regulators, and it controls the synthesis, uptake, and

regulation of the siderophore vicibactin that is produced by *R. leguminosarum* (Rudolph et al. 2006).

Production of siderophore is found even in plants, though a small number of plants show such character (e.g. mugineic acid produced by Graminaceae) (Loper and Buyer 1991; Miethke and Marahiel 2007). The plants in symbiosis with siderophore producing rhizobacteria have also been found to yield more food products than plants that do not associate with rhizobacteria. *Pseudomonas fluorescens-putida* produces siderophore that helps its host plant's growth and development and increases the host plant food product yield up to 144% (Kloepper et al. 1980).

Graminaceous plants (grasses, cereals, and rice) are among the few plants that are capable of producing siderophores (Sugiura and Nomoto 1984). These plants secrete phytosiderophores into the soil. The secretion is carried out when the soil is calcareous, that means there is a lot of precipitation of calcium carbonate. Maize plants carry out the process of siderophore uptake by using plant roots (Bar-Ness et al. 1992). They also steal the siderophore produced by other microorganisms such as rhizospores (Bar-Ness et al. 1992). As stated earlier, the soil has a lot of free iron, that complex into oxides because of the presence of oxygen and suitable pH. Deoxymugineic acid is an example of a siderophore that is produced by the plant for transport of iron in case of iron unavailability (Sugiura and Nomoto 1984).

Types of Siderophores

Bacteria produce three main types of siderophores namely catecholates (catecholates and phenolates), hydroxymates, and carboxylates (Miethke and Marahiel 2007). There is also the presence of a mixed type of siderophore (Miethke and Marahiel 2007). Siderophores are classified based on their ability to associate with ferric iron and also their chemical properties. The pKa value also differentiates the types of siderophores, e.g. hydroxamate types have a pKa

value of 8-9 (Miethke and Marahiel 2007). The stability of the siderophore and its affinity with ferric iron also define its type (Drechsel and Jung 1988).

Catecholate type siderophores (e.g. enterobactin) have the strongest scavenging ability and are known to be the most efficient iron chelator compared to any other types of siderophore (Drechsel and Jung 1988). The association constant (K_a) between ferric iron and enterobactin is 10^{52} M^{-1} (Loomis and Raymond 1991). Carboxylate type siderophores are produced in extremely acidic conditions which makes them unique. They are not as effective chelators as catecholate type siderophores (Miethke and Marahiel 2007).

Vicibactin

Vicibactin is a cyclic trihydroxamate type siderophore (Fig.1), is produced by *R. leguminosarum* ATCC, and shows similarity to the siderophore produced by other Rhizobial

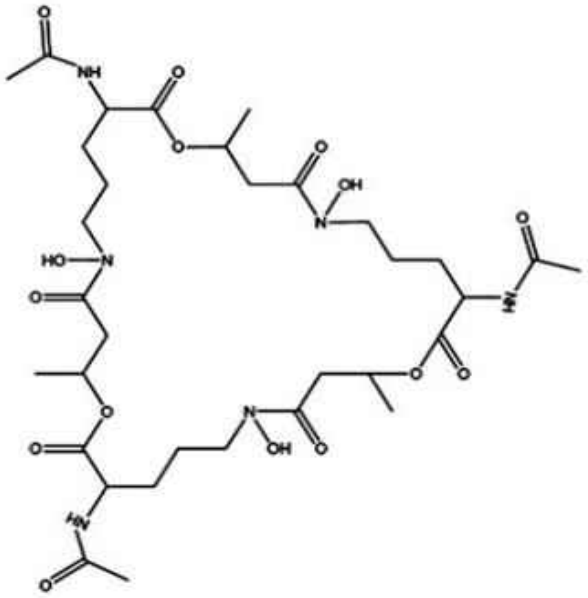

Figure 1: Vicibactin

strains (Wright et al. 2013). Vicibactin is produced in multiple steps and processed through multiple modifications mediated via the gene products of *VbsO, VbsP, VbsA, VbsL, VbsC, VbsG, VbsD*, and ending at *VbsS* which has the central role in synthesizing the cyclic vicibactin (Carter et al. 2002). The proteins that are involved in vicibactin secretion after vicibactin is made are not known.

In *Ps. aeruginosa,* the siderophore pyoverdine (containing a carboxylic group with a chromophore) is secreted by the same system responsible for its uptake (Hannauer et al. 2010). The proteins associated with secretion of pyoverdine are outer membrane protein OmpQ, periplasmic protein PvdR, and inner membrane protein PvdT (Hannauer et al. 2010). Two other outer membrane proteins, FpvA and FpvB, are responsible for Fe-pyoverdine uptake and secretion of newly synthesized pyoverdine (Hannauer et al. 2010).

fhuCDB and *fhuA* Mediated Siderophore Uptake

R. leguminosarum strain 8401 bv. *viciae* has an operon *fhuCDB* that consists of three genes *fhuC, fhuD and fhuB* (Fig. 2). It also has a pseudogene *fhuA* whose expression was undetectable (Stevens et al. 1999). The siderophore produced by *R. Leguminosarum viciae* is also vicibactin (Dilworth et al. 1998). The *fhuA* gene in *R. leguminosarum viciae* was present downstream of the *fhuB* gene that codes for an inner membrane protein required for the transport of siderophore inside the cell (Stevens et al. 1999). Also, the roles of other genes in the *fhuCDBA* operon have been confirmed (Stevens et al. 1999). FhuD was confirmed as a periplasmic transport protein similar to that found in *E. coli* (Stevens et al. 1999). FhuC is an ATPase and FhuB is a cytoplasmic membrane protein that also showed identity with genes from *E. coli* (Stevens et al. 1999).

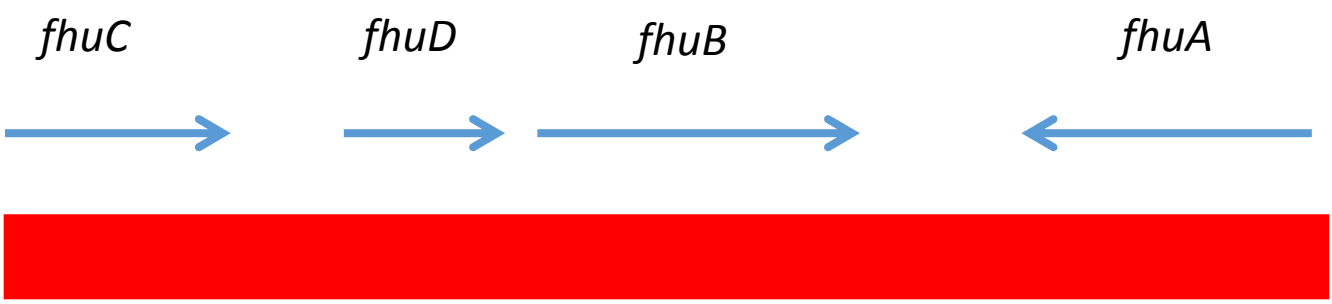

Figure 2: Graphical representation of *fhuCDBA* operon in *R. leguminosarum* 8401

A transposon mutant with a *Tn5::lacZ* reporter showed that *fhuB, fhuC, and fhuD* are in the same transcriptional unit (Stevens et al. 1999). The pseudogene FhuA in *R. leguminosarum* 8401 was identical with *E. coli* FhuA towards the C-terminal end (Stevens et al. 1999). The predicted promoter part of the protein FhuA was cloned in promoter-probe vector pMP220 and plasmid pBIO410 and then was mobilized to *R. leguminosarum* 8401 with *lacZ* marker. This failed to show β-galactosidase activity under low iron concentration in the media (Stevens et al. 1999). This also suggested that *R. leguminosarum* 8401 contains the pseudogene version of *fhuA*.

FhuA is an outer membrane protein of molecular weight 78 kDa. It is a 22 β stranded barrel-shaped protein (Ferguson et al. 1998). Its role in *E. coli* is to bind a hydroxamate type siderophore ferrichrome (produced by fungi *Ustilago tritici*) and transport the ferric-siderophore complex into the cell (Ferguson et al. 1998). The crystal structure of FhuA reveals a structurally distinct domain consisting of the 4β strand and 4α helices located inside the barrel as a "cork" (Ferguson et al. 1998). FhuA in *E. coli* works along with various other inner membrane and periplasmic proteins as a multiprotein complex that involves TonB, an energy transducing protein, as the transport process is energy dependent (Fig.3) (Pawelek et al. 2006). The *fhuCDBA* operon is involved in ferrichrome transport (Pawelek et al. 2006). The siderophore ferrichrome is produced by fungus *U. tritici* and is a hydroxamate type siderophore similar to vicibactin.

Ferrichrome is transported by outer membrane receptor protein FhuA in *E. coli* (Pawelek et al. 2006). The *fhuA* like genes have been reported earlier in *R. leguminosarum* (Stevens et al. 1999).

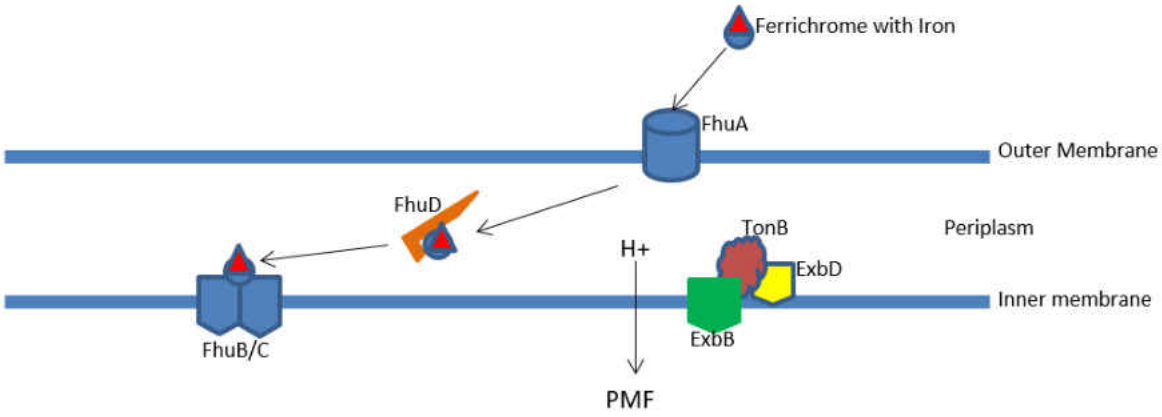

Figure 3: FhuA dependent uptake system in *E. coli*

FhuA is also involved in uptake of phages T1 and Φ80**,** colicin M, antibiotics Viz. rifamycin CGP 4832 and albomycin (Braun et al. 1999; Ferguson et al. 2000).

RosR and FhuF

RosR is a transcriptional regulator protein with a Cys2-His2 type zinc finger motif that belongs to the Ros/MucR family of rhizobial transcriptional regulators (Rachwal et al. 2016). The mutation in *rosR* showed an effect on cellular motility and synthesis of cell surface components. The cells surface became hydrophobic lacking in polysaccharides and the bacteria were defective in symbiotic interaction with clover plants (Rachwal et al. 2016). The gene *rosR* is present upstream of *fhuA* in *R. leguminosarum* Rt 24.2 *trifolii* and codes for a 15.7 kDa protein (Rachwal et al. 2016).

Downstream of *fhuA* is *fhuF,* a 786 Bp gene that codes siderophore-iron reductase protein in *R. leguminosarum* bv. *viciae* (Carter et al. 2002). In *Firmicutes* such as *Bacillus halodurans*, when *fhuF* was mutated, the intracellular ferric-siderophore complexes were not efficiently metabolized. However, their transportation was not affected. As a result, the non-metabolized ferric-siderophore complexes accumulated inside the bacterial cells (Miethke et al. 2011).

Other System for Iron Acquisition

In addition to siderophore-mediated iron uptake, various pathogenic bacteria and some nonpathogenic bacteria are reported to overcome the problem of iron unavailability using different iron uptake systems such as lactoferrin, transferrin, hemoglobin, hemin and ferritin-bound iron uptake (Noya et al. 1997). The hemoglobin, hemin or heme-bound iron uptake system is very common in pathogenic bacteria. Once the bacteria enter the host, they have access to hemoglobin and other heme bound compounds. As bacteria are always in need of iron to support their growth and development, they often use a heme-bound iron uptake system to acquire iron (Miethke and Marahiel 2007). Non-pathogenic *Rhizobium* species can also utilize heme-bound iron (Noya et al. 1997). The leghemoglobin present in the plant roots is also a good source of heme-bound iron (Noya et al. 1997).

Heme Iron Uptake/ *hmuPSTUV* Operon and Its Function

Some known and commonly studied systems for heme uptake are BhuR in *Bordetella pertussis,* HemR in *Yersinia enterocolitic,* HmbR and HpuB in *Neisseria meningitides,* HmuR (Heme utilization receptor) in *Porphyromonas gingivalis,* and ShuA in *Shigella dysenteriae* (Tong and Guo 2009). *R. leguminosarum viciae* has a TonB dependent operon *hmuPSTUV*

(Wexler et al. 2001). The proteins in this uptake system showed similarity with the transporter and degrading proteins that were present in heme uptake system in different pathogenic bacteria (Wexler et al. 2001).

Heme bound iron uptake systems are also found in *Ps. aeruginosa* with a Fur-regulated PhuR outer membrane receptor that binds with heme and then is transported to *phuSTUVW* operon system (Ochsner et al. 2000). Besides the *phuSTUV*W system in *Ps. aeruginosa,* another system, the HasA uptake system, uses hemophore to bind heme (Létoffé et al. 1996). This system consists of a protein known as HasA which is a heme binding and acquisition protein (Létoffé et al. 1996).

Hemophores are heme binding compounds mostly produced by pathogenic bacteria under limited iron availability; they scavenge heme and transport it into the bacterial cell (Tong and Guo 2009). There are only two known types of hemophore associated heme acquisition systems. One is HasA (heme acquisition system), and it is present in *Serratia marcescens*, *Ps. aeruginosa*, *Ps. fluorescens*, *Y. pestis* and *Y. enterocolitica* (Tong and Guo 2009). The other type of hemophore associated heme acquisition system is HxuA (heme/hemopexin utilization) and is only known to be present in *Hemophilus influenza* (Yong Tong et al. 2009). Similar to all other iron uptake systems, the hemophore-mediated uptake system is also TonB dependent and Fur-regulated (Ochsner et al. 2000). The binding affinity of the hemophore to HasA in *S. marcescens* is 5.3×10^{10} M^{-1} (Deniau et al. 2003).

Hemin/ Hemoglobin/ Leghemoglobin and Heme

Hemin is a ligand that contains a ferric iron in a porphyrin IX ring with a chloride (Fig. 4) (Hans 1941). Lyophilized hemin powder is frequently used in research and other medical purposes. It is prepared by treating blood using glacial acetic acid and salt (Elvehjem 1931). Its chemical formula is $C_{34}H_{32}N_4O_4FeCl$. The transport of hemin as a sole source of iron is carried out by bacteria in cases of iron scarcity (Noya et al. 1997).

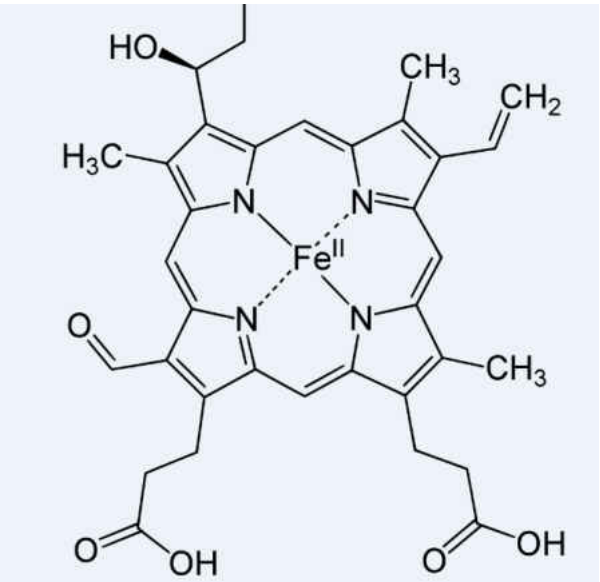

Figure 4: Hemin

Hemoglobin (Hb) is a 65kDa transport protein in red blood cells of vertebrates and contains oxygen and iron (Anthea et al. 1993). The hemoglobin present in blood carries oxygen from respiratory organs such as lungs and gills to almost every part of the body (Anthea et al. 1993). Hemoglobin consists of four globular proteins that are tightly attached to each other. Each subunit contains heme and heme contains the iron (Fig.5). Similar to hemin, heme contains a central iron molecule and has a porphyrin ring structure (Fig. 6). The iron may be either Fe^{2+} or Fe^{3+}, in which the Fe^{3+} ion (also known as met-hemoglobin) cannot bind to the oxygen molecule

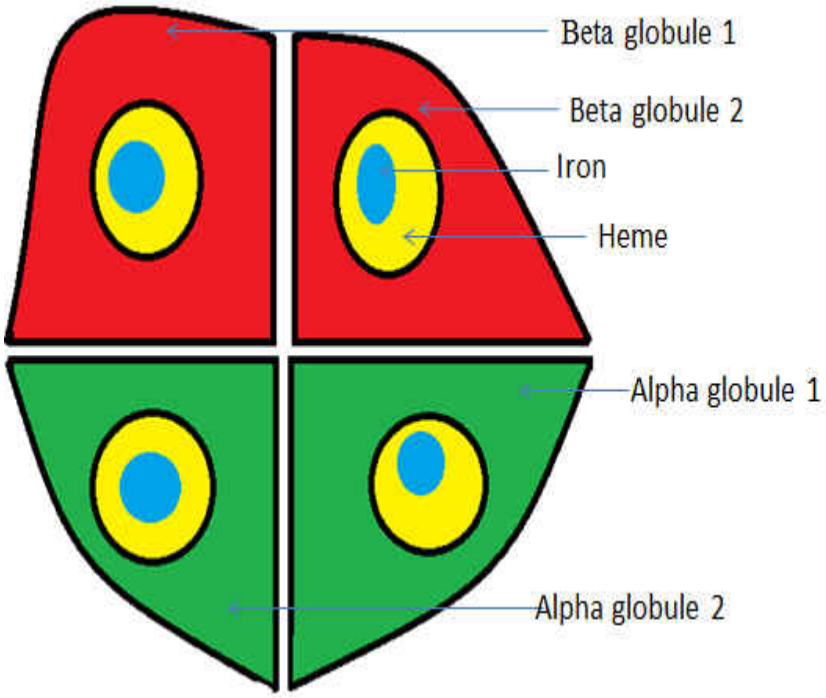

Figure 5: Hemoglobin

(Linberg et al. 1998). The iron molecule in the hemoglobin is targeted by the bacteria in case of iron unavailability and hence some bacteria can uptake hemoglobin in case of iron scarcity (Noya et al.1997).

Leghemoglobin is nitrogen/oxygen carrier and is present in the root nodules of nitrogen

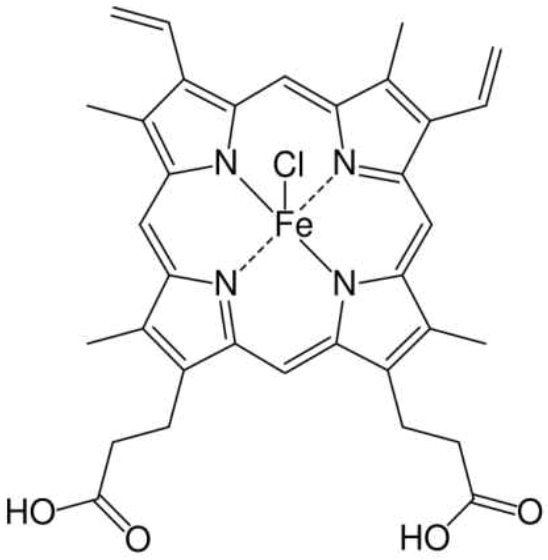

Figure 6: Heme

fixing and leguminous plants. Roots that are not infected by symbiotic rhizobia do not produce leghemoglobin (Ott et al. 2005). The cytoplasm of the plant cells that are infected by *Rhizobium* accumulates leghemoglobin, and they are known to avoid inactivation of oxygen-labile nitrogenase enzyme by acting as a binder/trap for free oxygen (Ott et al. 2005).

Hemoglobin in blood is functionally, structurally, and chemically very similar to leghemoglobin in plants. The cofactor is heme in both hemoglobin and leghemoglobin and is required for formation of these proteins (Ott et al. 2005). The uptake of heme bound iron by soil bacteria such as *Rhizobium* has been reported previously (Noya et al. 1997).

Present Work

As stated earlier, the previous work in *R. leguminosarum* ATCC in our lab has already concluded the presence and involvement of TonB-ExbB-ExbD and Tol-Pal system in the transport of siderophore, vicibactin, a siderophore produced by *R. leguminosarum* ATCC (Wright et al. 2013; Hill 2014; Barisic 2015). The active transport system should have an outer membrane receptor for Fe-vicibactin complex as vicibactin has a molecular weight of 774 Da (Wright et al. 2013), and is larger than the molecules transported via porins (>600 Da). Fe-vicibactin complex is larger than 800 Da. The presence of *fhuA* like genes has been reported by many researchers in *Rhizobium* (Stevens et al. 1999). Outer membrane protein FhuA in *E. coli* is known to transport ferrichrome, a hydroxamate-type siderophore, similar to vicibactin (Ferguson et al. 1998). Therefore, we came up with a hypothesis that, a FhuA like protein is present and is involved in transport of vicibatin in *R. leguminosarum* ATCC.

The body of this work involves identification of *fhuA* like genes in *R. leguminosarum* ATCC and the possible involvement of the protein FhuA in the transport of vicibactin.

Expression of the putative FhuA under different iron concentrations was determined to test its possible involvement in iron transport to test our hypotheses. Deletion of the putative *fhuA* was carried out and the characteristics shown by the mutant and WT were compared.

This work also includes a second hypotheses that *R. leguminosarum* ATCC is able to utilize heme/hemoglobin as a sole source of iron. This research focuses on identification of the genes possibly involved in the heme-bound iron transport. One such TonB-ExbB-ExbD dependent operon, *hmuPSTUV* in *R. leguminosarum viciae,* is responsible for transport of heme bound iron (Wexler et al. 2001). We have also detected the presence of a similar operon in *R. leguminosarum* ATCC for the energy dependent uptake of heme-bound iron. The role of energy transducing protein complex, TonB-ExbB-ExbD, in heme bound iron transport was also studied.

CHAPTER 2

MATERIALS AND METHODS

Bacterial Strain and Growth

Bacterial Strains

The rhizobial strain used in this study is *R. leguminosarum* ATCC 14479 *trifolii* and was obtained from American Type Culture Collection. The *E. coli* strains used were SM10λpir and BL21/DE3.

Table 1: Bacterial strains and plasmids used in this work

Strains	Characteristics	References/Source
E. coli		
SM10λpir	Used during biparental conjugation to mobilize pEXFHU into *R. leguminosarum* ATCC	
BL21(DE3)	used for general cloning and to express pET17b::*fhuA*	Novagen (EMD millipore)
R. leguminosarum		
ATCC 14479	Wild-type strain	ATCC
RL Δ TonB	*R. leguminosarum* ATCC with an in-frame deletion of *tonB*	Hill 2014
RL Δ ExbBD	*R. leguminosarum* ATCC with an in-frame deletion of *exbB-exbD.*	Barisic 2015

Table 1(continued)

RL Δ FhuA	*R. leguminosarum* ATCC with an in-frame deletion of *fhuA*	This work
RL::pBIO1187	*R. leguminosarum* ATCC with pLAFR1-based cosmid, contains vbs genes plus *rpoI*; TetR	Yeoman et al. 2002
Plasmids		
pEX18Gm	Suicide vector; Gm^R	Schweizer et al.
pEXFHU	pEX18Gm plasmid with *R. leguminosarum* SOE fragment with an in-frame deletion of *fhuA* gene	This work
pET17b	Amp^R plasmid	Novagen
pET17b::*fhuA*	pET17b containing *fhuA*	This work

Growth Conditions and Media Used

R. leguminosarum ATCC was grown on Yeast Mannitol Broth (YMB) and Congo Red (CR) agar. The growth of the bacteria under restricted iron concentration was carried out in Modified-Manhart and Wong Medium (MMW) (Manhart and Wong 1979). The LB media was used for growth of all *E.coli* strains. *R. leguminosarum* ATCC was grown at 30°C under static condition or on shaker at 250 rpm when grown in liquid media.

CR agar contained 1% mannitol, 0.05% K_2HPO_4, 0.02% $MgSO_4*7H_20$, 0.01% NaCl, 0.1% yeast extract, 2.5 x 10^{-5} % Congo red dye, and 3% Bacto-agar. Use of 1% aqueous Congo red dye stock solution was done and was added accordingly before autoclaving the media. The pH was adjusted to 6.8 using 6M NaOH before autoclaving (Hammond 2008). Congo red dye is

used for identification of *Rhizobium*. The dye is absorbed very slowly by *Rhizobium* species; while the other organisms take up the dye quickly and form reddish colonies. In case of *Rhizobium*, they form whitish or pinkish colonies (Kneen and Larue 1983). This is also helpful to identify the contaminants such as *E. coli,* which forms reddish colonies.

As stated earlier, YMB was used when iron concentration was not to be restricted. YMB contained 1% mannitol, 0.05% K_2HPO_4, 0.02% $MgSO_4*7H_20$, 0.01% NaCl, and 0.1% yeast extract. The pH was adjusted to 6.8 using 6M NaOH before autoclaving.

Minimal media MMW was used when the amount of iron in the media was to be regulated. MMW media contained the following (w/v): 0.0764% K_2HPO_4, 0.1% KH_2PO_4, 0.15% Glutamate, 0.018% $MgSO_4$, 0.013% $CaSO_4*2H_2O$, and 0.6% dextrose. The pH was adjusted to 6.8 using 12M NaOH, and the media was autoclaved. The media was kept in 55°C water bath to let it cool before addition of vitamin solution and antibiotics. Filter-sterilized 1000X vitamin solution (see appendix) was added to the media after the temperature was brought down to less than 55°C. The vitamin solution was stored at 4°C in container wrapped with aluminum foil to prevent the degradation of certain vitamins by light (Manhart and Wong 1979).

The LB broth contained 1% tryptone, 0.5% yeast extract, and 0.5% NaCl. For the agar plates, 1.5% agar was added to the media. Before autoclaving, the pH was adjusted to 7.5 using 6M NaOH. Antibiotic was added after the media was cooled down to 55°C or lower. LB media was used to grow *E.coli* strains only because *R. leguminosarum* does not grow in LB media. This characteristic was helpful to avoid contamination in *R. leguminosarum*. *E. coli* strains were grown at 37°C. Use of shaker at 250 rpm was done when cells were grown in liquid media.

The final antibiotic concentrations used for *R. leguminosarum* ATCC and other bacteria were as follows:

Table 2: Antibiotic concentrations

Antibiotic	Final concentration
Nalidixic acid (Na_{10})	10 µg/mL
Penicillin G (Pen_{50})	50 µg/mL
Ampicillin (Amp_{100})	100 µg/mL
Gentamycin (Gm_{10})	10 µg/mL
Kanamycin (Kan_{50})	50 µg/mL
Tetracycline (Tet_{10})	10 µg/mL

Iron Concentrations and Growth

As stated earlier, MMW media was used when the organisms were grown under iron restricted conditions. The media was supplemented with the desired iron concentration. The different iron concentrations used were 0 µM, 0_{dipi} (with dipyridyl), 0.05 µM, 0.1 µM, 0.5 µM, 2.5 µM, 50 µM and 100 µM. Conical flasks (250 mL) were treated with concentrated nitric acid overnight to remove any contaminating iron from the glass surface. Next day, the flasks were thoroughly washed with water to remove acid before autoclaving. A total volume of 50 mL of MMW media with 500 µL of inoculum was used for each flask. The inoculum used was prepared in MMW with no added iron (0 µM). To supplement other flasks with different known iron concentrations, the filter sterilized iron was added to each flask separately and carefully. They were incubated at 250 rpm for 2-3 days at 30°C. The cells were used for protein and RNA extraction. The growth of cells was measured using UV/Vis spectrophotometer at $O.D_{600}$ nm and

cells diluted to an $O.D_{600}$ of 0.8 as necessary before extracting either protein or RNA. This was done to maintain approximately equal number of cells while performing protein and RNA extraction.

2'2 dipyridyl was added to achieve absolute zero iron concentration by removing contaminant iron present in the media ingredients. 2'2 dipyridyl is a chelating agent that scavenges the free or soluble iron present in the media. 2'2 dipyridyl was used at 0.25 mM concentration in the media to create an absolute zero iron concentration.

Different concentrations of hemoglobin/hemin were added to the MMW media while studying heme uptake. The media was supplemented with hemoglobin/hemin as the only iron source. Human lyophilized hemoglobin was bought from Sigma Aldrich and was suspended in sterile distilled water. Bovine lyophilized hemin was also bought from Sigma Aldrich.

Amplification of the Putative Genes

Genomic DNA Extraction

A CR plate was used to inoculate *R. leguminosarum* ATCC from a -80°C freezer stock and grown at 30°C for 48-72 hrs. A single isolated colony of the bacteria with a slow absorption of Congo red dye was picked and used to inoculate 3 mL YMB broth supplemented with penicillin G to inhibit the growth of gram-positive contaminants. Nalidixic acid was used to prevent contamination from *E. coli*.

The culture was then transferred to 1.5 mL microcentrifuge tubes and was centrifuged for 10 min. at 13000 rpm (7600 xg). The supernatant was poured off, and the pellet was washed with sterile 0.85% NaCl for three times to remove the exopolysaccharides produced by the bacteria.

After washing, the pellet was used for genomic DNA extraction following a method previously used for bacterial genomic extraction (Kalia et al. 1999).

Agarose gel (1%) in TAE buffer was used to analyze the quantity and quality of the extracted genomic DNA. Nanodrop 2000 from Thermo Scientific was used to confirm the quality and concentration of the genomic DNA. Absorbance at 260 nm, 230 nm, and 280 nm was measured by the nanodrop reader and the ratio of the absorbance at different wavelengths was calculated, confirming the quality of the extracted sample. Any sample with the ratio of less than 1.80 was considered to be an impure sample.

Primers Used for Gene Amplification

List of primers used in this study are as follows. All the primers were designed and analyzed using NCBI primer designing tool/ and were ordered through ETSU core molecular biology facility. The primers were made by Integrated DNA Technologies (IDT). All the sequencing work was performed at ETSU molecular biology core facility.

Table 3: *fhuA* primers from different bacterial species (Primers made by IDT)

PRIMERS	
Name	Sequence (5' – 3')
SMfhuFWDseq 1	TGCTTTATGGCGGGTCCAATCCG
SMfhuREVseq 1	AGGTCCAGCCATTGTCGAAG
SMfhuFWDseq 2	TCGACAATGGCTGGACCTTC
SMfhuREVseq 2	CGCCAAAACGAATCTGGTCC
ECfhuFWD	ATCATGCGTGGTCCGGTATC

Table 3 (continued)

ECfhuREV	AGTGCATCGTCGTCTTTGG
RLfhuFWD	GGCGATGTTCGATTTCGGTG
RLfhuREV	GTCGCATAGGAGACGAAGGG
E. Coli, 2243 Bp forward	ATGGCGCGTTCCAAAACTGCTCAGCC
E. Coli, 2243 Bp reverse	TTAGAAACGGAAGGTTGCGGTTGCAACG
Shinorhizobium meliloti forward	ATGAAGTGCAGGATCCGCGG
Shinorhizobium meliloti reverse	TTACCACTTCTTGCTGAGCTTCAGCG

After amplification of *fhuA*, the primers used for sequencing, RT-PCR, cloning, and SOEing are listed as follows.

Table 4: Primers used for sequencing, RT-PCR, cloning and SOEing of *fhuA* (Primers made by IDT)

PRIMERS	
Name	Sequence (5'- 3')
Rhizobium leguminosarum p1 forward	GACAGATATACTGAGATCTTTCGCTCAGC
Rhizobium leguminosarum p1 reverse	GGATGATCAGCGATCAACGTCGCGG
R. Leg P2 Forward	CAAGTGAGGGCGATGGTCTTTTGC
R. Leg P2 Reverse	TTCTTCGAGGTATTGGCGGTATCC
Primer Forward: P3F	AACTGCCTCTGTTTGGCAGCC
Primer Reverse: P3R	TTCTTGTCGATCGCGCCGAAATCA
P3IIF	TCGTCTCGGTGCGCGCTT
Primer Forward: P4F	ACGTCCGTTGCCGCTAAGAA

Table 4 (continued)

Primer Reverse: P4R	GACGTCTTCCGAGTCGTTCAAC
P5F	CCAGAACCTGCGCTATTCGCA
P5R	AACGTCAGGCCGTTGTCG
P6F	CGAGGGTGAACAGTACGAACT
P6R	TTGATCACCTCGACGCGTTGC
P7F	ATTGCACCCTTCGTCTCCTATGCG
P7R	GATTTTGGTCGCCGCCGAGC
P8F	GTCGAGCTTCTATGTCGATGCATCT
P8R	ACGATCCCGTATTTGCTGCTG
P8IIR	TGGCCAACCTGCCGGTCTTGAC
P9F	ATGCCAATGTCGGCGCGATCAC
P9R_rt	TTGTAGGTGTAGGCCGCAATGATGTCGAG
P10F	ACTCGGAAGACGTCAACAAGAACGC
RT – P1	ATGTTGACAAGGCCAATTTCGCTCCATAGG TTCCG
Rstr1F	AGCTTGGTACCGATGTTGACAAGGCCAATT TCGCTCC
Rstr1R	ATCGGGATCCTTACCACCGATACTTCAGGG TCGC
Forward primer (fhuA1F)	GTGCGCGGTACCAGCTCTGCAAACGACAAT CG
Reverse primer (fhuA1R)	ACTGGGATCCATCGGAGCGGCCCTTCTCG

Table 4 (continued)

Forward primer (fhuSOEF)	GTGACTAAAATAATCATCTTATGTAATAGA TGGCGCCGGAGACGAC
Reverse primer (fhuSOER)	GTCGTCTCCGGCGCCATCTATTACATAAGAT GATTATTTTAGTCAC
Forward primer (fhuIntF)	ATGGGAGTGGCAGTTGCTCAAGTGAGGGC
Reverse primer (fhuIntR)	CTTCGACAAGGGCGGGCTCGTGAC
6KB far primers (RL.F6K)	CGATGGCGAATGAAGGCATC
6KB far primers (RL.R6K)	ACTTTCCCGCATCGCCAATAAGATGG

The primers used for amplification of heme uptake genes are listed as follows.

Table 5: Primers for hemoglobin transport genes from different species (Primers made by IDT)

HM1F	*R. leguminosarum* bv. *trifolii* WSM 2304 - TonB dependent hemoglobin/ transferrin/lactoferrin receptor (2.3 kb gene)	ATGATCGTCCGGTATTGGCG
HM1R		TCAGAACGTCTTGGTGAGCGA
SmH1F	*S. melioti* 1021 – *Sinorhizobium* heme receptor- *shmR* (2.7 kb gene) CAC46967.1	ATTCGTCTCGCTCCGTAAAA
SmH1R		CAAATTGTGCTGAAACTGAGG
ECHm1F	*E. coli* IAI39- outer membrane hemin receptor CAR20113.1 (2.0 kb gene)	TCGAAGCGCCTATGATGGTC
ECHm1R		CGGGTACGGTTATAGGCCAC

Table 5 (continued)

HM2F	*R. leguminosarum* bv. *trifolii* WSM 2304 (TonB dependent hemoglobin/ transferrin/lactoferrin receptor) (2.3 kb gene)	GCGACAATATGGGCGACAAC
HM2R		TGAACTCCGTGAAGCCTGTC
Hm3F	*R. leguminosarum* bv. *trifolii* WSM 2304 (TonB dependent hemoglobin/ transferrin/lactoferrin receptor) (2.3 kb gene)	CCAGCTGGAGCCAGTATAGC
Hm3R		AGAACGTCTTGGTGAGCGAG
Hm5F	*R. leguminosarum* bv. *trifolii*, CB782- hemin ABC transporter substrate protein AHG46540.1 (0.711 kb gene)	AAGAAAACCGCCTGATTGCG
Hm5R		AAATCGCGGTGTTCAGTTCG
Hm6F	*R. leguminosarum* bv. *viciae* 3841- heme uptake protein ANP88820.1, HmuP. (0.183 kb gene)	ATGATGGTTGAAAAGCCAGATAGC
Hm6R		GAATGAGCTTGCCCTGACGG
Hm7F	*R. leguminosarum* bv. *viciae* 3841- putative haem iron transport component , HmuS. CAKO9186.1 (1.05 kb gene)	ATGACCGAACAGACAAGACCG
Hm7R		GCAGGTTTTCCATGATCTCGC
Hm8F	*R. leguminosarum* bv. *viciae* 3841- hemin binding component of ABC transporter, HmuT. CAK09187.1 (0.930 kb gene)	GACGATGCGTAACAATCTGCG
Hm8R		GGTAGACGCCATCCATTCGG
HmuX1F	*tonB* from *R. leguminosarum* bv. *viciae* 8401	TTGGCAAGGAGGTGAAGTTTCTCC

Table 5 (continued)

HmuX1R	*tonB* from *R. leguminosarum* bv. *viciae* 8401	AGCGGCACGTGCTTAAAGCTATC

After amplification, the *hmuPST* genes were sequenced by using the primers as listed below. Some of the primers from Table 5 were also used for sequencing the *hmuPST* genes. Sequencing was carried out at ETSU core molecular facility.

Table 6: Primers for sequencing *hmuPST* genes (Primers made by IDT)

Primers	5'-3'
Forward primer (HM9F)	AGGCGGCCTCATATCAGCAATC
Reverse primer (HM9R)	GATATCACGCTCGCGCATTTTCG
Forward primer (HM10F)	AAGGAAGGCTCCGACG
Reverse primer (HM10R)	CTTGCGCTCGGCCTCC
Forward primer (HM11F)	CGACACGACGAGCATGTATCC
Reverse primer (HM11R)	TGCCTGATTTCGCGGATGTC
Forward primer (HM12F)	AGACATGACGGCTTGGTC
Reverse primer (HM12R)	GGATCCGGCGCAGATTG
Forward Central (Hm12Cen)	AATGTCGAGGCCTATCACGC

Miscellaneous primers used in this study are as follows. These primers were used to confirm the successful cloning of the respective gene fragment in the respective plasmid used. These primers were also used for sequencing and confirming the cloning.

Table 7: Miscellaneous primers (Primers made by IDT)

PEX18FWD	TCTGGAAGGCAGTACACCTTGATAGG
PEX18REV	AAAGCGGGCAGTGAGCGCAAC
RCO12	CGGATATAGTTCCTCCTTTCAGCA
RCO13	TAACCAGTAAGGCAACCCCG
RCpet17bR	ATGGCTAGCATGACTGGT
RCpet17bF	GCTAGTTATTGCTCAGCGG

Polymerase Chain Reaction (PCR)

Polymerase chain reaction (PCR) was used for amplifying the required gene fragment using specific primers. Desired gene fragments are amplified to millions of copies, based on the primers used. This helps in producing enough DNA for further analysis and other experiments.

During PCR reaction, a cyclic process of denaturation, annealing, and extension is carried out for the amplification of the desired gene. If the gene of interest has not been sequenced, the sets of primers were designed based on the known sequence of the similar gene from related species. A master mix was made using the PCR protocol described in a manual from Promega, and the thermal cycler conditions were also followed as described (Promega 2017).

PCR Amplification of *fhuA*

For identification and amplification of *fhuA,* primers were designed based on the published *fhuA* sequence from *S. melioti, E.coli, and R. leguminosarum* bv. *viciae* from more than one part within the gene, so as to test the presence or absence of *fhuA* in *R. leguminosarum* ATCC (Ferguson et al. 1998; Stevens et al. 1999; Cuív et al. 2008). Also, every pair of primers

that did not amplify was used in more than 5 PCR reactions with different PCR conditions to confirm the absence of the genes.

PCR Amplification of Hemoglobin Receptors and Heme Bound Iron Transport Genes

Hemoglobin transport genes from *R. leguminosarum* ATCC were amplified using primers based on known nucleotide sequences of different heme-bound iron uptake genes from different species such as *R. leguminosarum* bv. *trifolii* WSM 2304*, R. leguminosarum* bv. *viciae* 3841*, R. leguminosarum* bv. *trifolii* CB782, *S. melioti* 1021 and *E. coli* IAI39. Different genes that were reported and known to carry out heme/hemin/hemoglobin/lactoferrin transport (See Table 5) were used to design the primers; CAK09187.1, CAR20113.1, CAC46967.1, AHG46540.1, ANP88820.1, CAK09186.1 and others from rhizobase and NCBI online database (NCBI 2016; Rhizobase 2016). The primers were designed from different parts within the gene fragment to confirm the presence or absence of the gene.

Colony PCR

Colony PCR was performed for screening the inserts directly from the bacterial colony. To remove excessive polysaccharides produced by Rhizobia, the colonies were heat treated before PCR. The colony was picked and suspended in 100 µL of sterile distilled water in 1.5 mL microcentrifuge tubes and then was placed in a heat block or water for 10 min. at 95^{o}C. Two µL of the resuspended and heat treated colony was used as a template for the PCR reaction. A master mix for colony PCR reaction included following components.

Table 8: Master mix for colony PCR

33 µL sterile distilled water
10 µL 5X PCR buffer
3 µL 25 mM $MgCl_2$
1 µL 10 mM dNTPs
0.5 µL 10 µM forward primer
0.5 µL 10 µM reverse primer
0.25 µL Taq polymerase
48.25 µL total volume

When heat treatment was not necessary, colonies were picked directly for the PCR reaction using sterile pipette tips. The pipette was set to 20 µL, and the colony was pulled out with just a gentle touch and was then pipetted up and down into the mix directly. The cells were used in smallest quantity possible. For keeping the amount of the bacterial cells minimal, a gentle touch in the colony was sufficient for the PCR reaction. Sufficient mixing and a minimal amount of cells are important to get complete cell lysis and high yields of DNA. The PCR conditions used for colony PCR without the heat treatment/boil prep was as follows.

Table 9: Colony PCR setting

1 cycle	5 min at 95°C (Initial denaturation)
	1 min at 95°C (Denaturation)
30-40 cycles	1.5 min at 54°C (Annealing)
	X min at 72°C (1 min/kb) (Extension)
1 cycle	5 min at 72°C (Final Extension)

Bioinformatics Tools

NCBI/BLAST was used to analyze and align the gene sequence and protein sequence. The sequencing data obtained after SOEing, cloning, sequencing of *hmuPST* and *fhuA* were aligned with the respective known sequences. ClustalW Muscle from EBI-UK was used to align multiple sequences. Chromas software was used to export the sequence data from the sequencer developed file format into Microsoft Word format and to analyze the bases. Chromas software was also used to analyze the peaks of different bases while confirming the sequencing data. ORF finder from NCBI and online promoter analyzer "genome2d" were used to analyze *hmuPST* and *fhuA* sequences to determine the promoter region and the possible ORFs in the region.

EXPASY translation tool was used to convert the DNA sequence into a protein sequence. The protein homology modeling was done independently by using SwissProt 3D modeling tool. After the protein models were obtained, molecular docking was performed by using online modeling tool Swissdock. For viewing the docking files, Swissdock and Chimera software version 1.11.2 from the University of California in San Francisco was used.

Cloning of *fhuA*

Restriction, Digestion and Ligation of *fhuA* in pET17b and Its Transformation

Restriction enzyme sites for the BamHI and KpnI were inserted in 5' regions of the primers (Rstr1F and Rstr1R). The restriction sites were part of the multiple cloning site (MCS) and were not present in the putative *fhuA* gene. The primers were designed to amplify the ORF of the putative *fhuA*.

The *fhuA* gene was amplified via PCR. The PCR product was analyzed in 1% agarose gel. The right sized band at 2.3 Kb was gel extracted using the mol-bio gel extraction kit. The pET17b plasmid and the gel extracted product were digested using 2.1 NEB buffer and the

enzymes BamHI and KpnI. Quiagen plasmid extraction kit was used for plasmid extraction. The digested plasmid and the gene were separated and analyzed using 1% agarose gel electrophoresis. Gel extraction was performed after gel electrophoresis as described earlier. For ligation of the digested and gel extracted products, 10X T4 DNA ligase buffer was used with T4 DNA ligase enzyme and was allowed to ligate at 4°C overnight. The mixture was then heat inactivated for 10 min. at 65°C and was stored at 4°C. Transformation of the newly constructed plasmid was carried out via heat shock method for 30 seconds at 42°C in *E. coli* BL21/DE3 competent cells prepared in the lab. The transformed cells were screened and picked from the ampicillin containing LB plates and were confirmed via colony PCR and sequencing.

These cells could be used for future complementation assays and to check the gene expression in the transformed *E. coli* BL21/DE3 cells. The pET-17b is an expression vector from Novagen, which contains a pBR322 origin of replication with an ampicillin resistant marker and an N-terminal 11aa T7 Tag sequence which is followed by a multiple cloning site (MCS). (Fig. 7)

pET-17b sequence landmarks	
T7 promoter	333-349
T7 transcription start	332
T7•Tag coding sequence	237-269
Multiple cloning sites	
(*Hin*d III - *Xho*1)	141-228
T7 terminator	28-74
pBR322 origin	1480
bla coding sequence	2241-3098

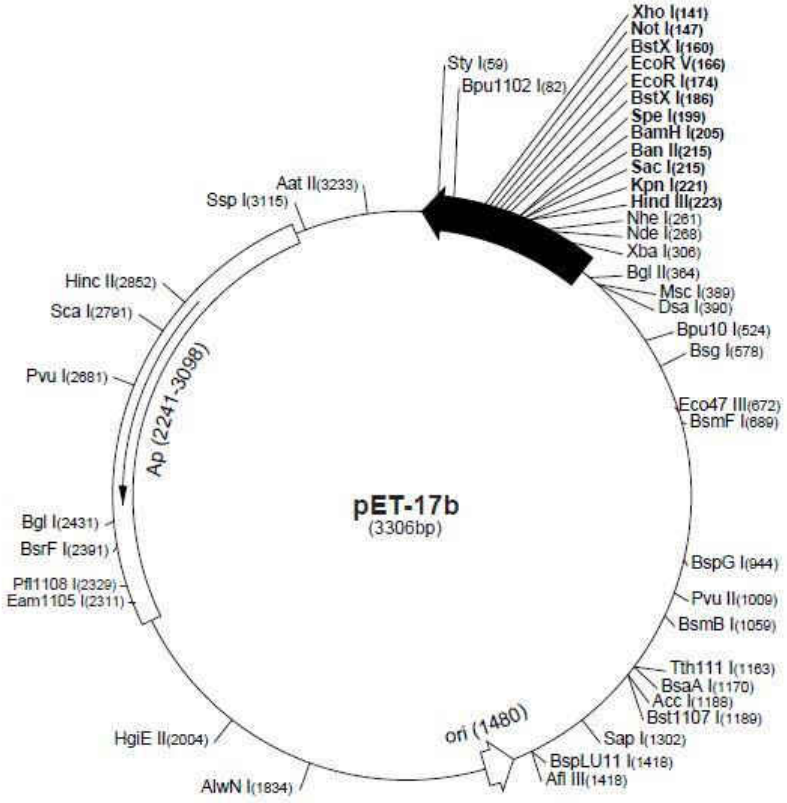

Figure 7: pET17b vector from Novagen, EMD millipore

Competent Cells Using Rubidium Chloride

Competent cells were made by using rubidium chloride salt and bacteria in exponential phase or log growth phase. This helps in making a permeable cell membrane which allows foreign material such as DNA to get in. The *E. coli* strain BL21/DE3 was grown in SOC media for overnight. It was centrifuged, pelleted and washed with TFB1 buffer. The cells were resuspended in TBF2 buffer and incubated on ice. Fifty microliters aliquots were prepared by pipetting in sterile microcentrifuge tubes and were snap frozen using liquid nitrogen and were stored at -80°C for future use.

Growth of the Expression Cells and IPTG Induction

The pET17b::*fhuA* cloned *E. coli* DE3/BL21 cells were grown on a rotary shaker at 250 rpm at 37°C for 5-6 hours in LB_{amp100} until the $O.D_{600}$ reached 0.6-0.8. The cells were induced with IPTG and were allowed to grow for another 3 hours. IPTG mimics a lactose metabolite known as allolactose that triggers transcription of the lac operon. Hence IPTG induction is carried out where the gene is under the control of the lac operator (Marbach et al. 2012). This was done to overexpress the cloned *fhuA* gene under lac operon. The protein extraction was carried out after sonication and expression was analyzed as described.

Expression of the Putative Protein and Gene

Protein Extraction

The bacterial cells grown in different iron concentrations were centrifuged and the pellets were washed with 0.85% NaCl. The pellets were suspended and vortexed in 20 ml of 0.85% NaCl. Outer membrane fragments were isolated after sonication of cells (1 minute pulse and 1 minute pause) using Branson digital sonicator. The sample was placed on ice while performing sonication. The sonicated sample was centrifuged for 10 min. at 10,000 rpm (5000 xg), and the supernatant was collected, discarding the pellet. The supernatant was further ultra centrifuged for 90 min. at 30,000 rpm (30,000 xg) to pellet the outer membrane fragments. The outer membrane pellets were analyzed for protein expression using SDS-PAGE.

SDS-PAGE

The protein expression was checked by using Sodium Dodecyl Sulfate-Polyacrylamide Gel Electrophoresis (SDS-PAGE) (Laemmli 1970). Samples were mixed with 2X loading dye

and were kept at 95°C for 5 min. for the proteins to denature. Eight percent resolving polyacrylamide gel was made, with 4% stacking gel, and the heat-treated samples were loaded on the SDS-PAGE gel. The gel was allowed to run for 75 min. on 35mA and 120V for one gel and 70mA and 180V for two gels. The gel was stained with Comassie Brilliant Blue and was de-stained with de-staining solutions. The samples used were different cell fractions. Whole cell extracts were also analyzed using SDS-PAGE depending on the experiment.

RT-PCR

Gene expression at the transcript level can be detected by Reverse Transcriptase-PCR technique (Freeman et al. 1999). Creation of cDNA (complementary DNA) from the RNA of interest was done by using gene-specific primers and the enzyme reverse transcriptase (superscript III reverse transcriptase, from Thermo Scientific). This synthesizes the first strand cDNA from the RNA of interest that is present in the total RNA extract. Total RNA extraction was done by using Direct-zol RNA miniprep kit by using Trizol reagent from Zymo Research. RNase zap, new sterile tips, and separate sterile work station was used for RNA extraction and the whole process was carried out with extreme precaution by keeping samples on ice all the time (except required by the protocol) to prevent RNA degradation, also by turning of the air vent so that there is very less movement of air in the room and cleaning hands and the work station between every 5-10 minutes using RNase zap to avoid RNase contamination). Complementary DNA (cDNA) was made using the RNA samples. After making the cDNA sample it was treated with enzyme RNase H, this degrades the remaining RNA in the sample. The newly synthesized cDNA was then used as a template for PCR reaction which was quantified based on the band intensity. Multiple cycles of PCR ranging from 15 to 40X were

used to see if the band intensity changes with the increase/decrease of the number of PCR cycles. This experiment was repeated thrice to confirm the results.

Gene Knockout

Splicing by Overlap Extension (SOEing)

The site-directed mutagenesis/in-frame deletion of *fhuA* was carried out using a PCR based technique known as splicing by overlap extension (SOE). It is a process in which multiple PCR reactions are used to engineer a product that contains the fused together 1Kb upstream and the 1Kb downstream regions of the target gene yet eliminating the targeted gene (Horton et al. 1990).

Two sets of primers were designed based on the sequenced data of the putative *fhuA* gene from 1Kb upstream and 1Kb downstream (Fig. 8). The first set of primers designed was SOEF and SOER (Fig. 8). The second set of primer was fhuA1F and fhuA1R. While designing the primers, restriction enzyme sites for enzymes BamHI and KpnI were also inserted in fhuA1F and fhuA1R, respectively. The first set of PCR reactions was carried out using fhuA1F and SOER and the second set of PCR reactions was carried out using SOEF and fhu1R and was used to amplify the 1Kb upstream flanking regions of putative *fhuA* and 1Kb downstream of the putative *fhuA* respectively. The primers SOEF and SOER are complementary of each other, and they are about 40-50 bases long, containing 50:50 regions from the flanking part of the start codon 'AUG' and the stop codon 'TAA' of the putative *fhuA* gene. This leaves an overhang when the flanking regions were amplified using SOEF/fhuA1R and SOER/fhuA1F in separately on both of the PCR reaction.

Both of these PCR products were then loaded in 1% Agarose gel and were allowed to run for 1 hour in 120V and 110mA. After an hour the DNA was extracted from the Agarose gel using Mol-bio gel extraction kit excising the band at 1Kb. The extracted DNA was then used as a template for another set of PCR reaction to generate a 2Kb in-frame deleted SOEΔ*fhuA* fragment with restriction enzymes at two ends. The product produced the desired SOE construct with a deleted *fhuA* fragment which was subsequently ligated into pEX18Gm and sent for sequencing.

The constructed plasmid (pEXFHU) was then transformed into *E.coli* sm10λpir electrocompetent cells which were made in the lab and was confirmed via gentamycin screening and colony PCR and sequencing. The *E.coli* with the construct (pEXFHU in *E.coli*) was then allowed to conjugate with wild-type *R. leguminosarum* ATCC cells to carry out homologous recombination between the plasmid and the WT chromosome.

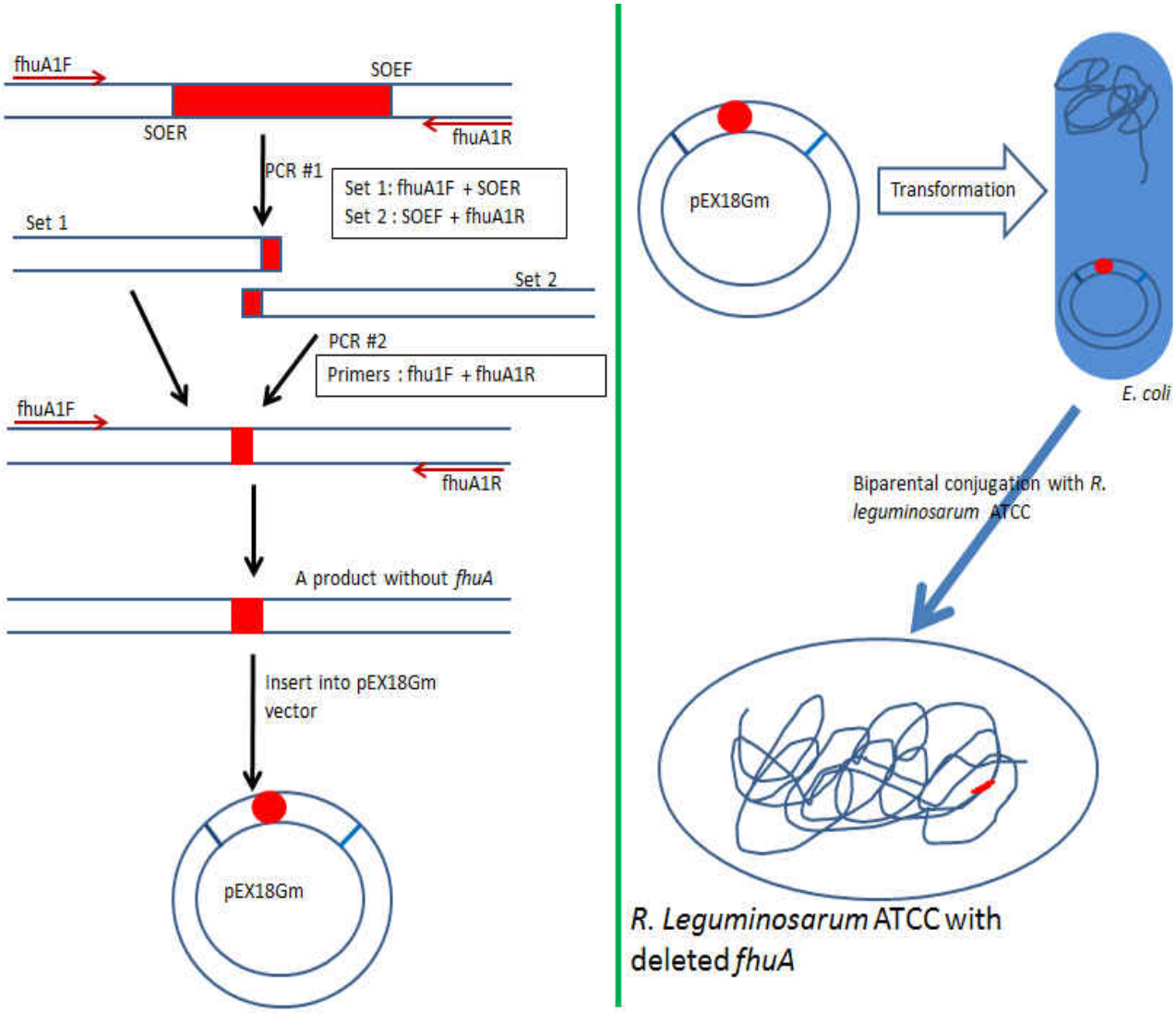

Figure 8: The process of SOEing for site-directed mutagenesis of putative *fhuA*

E. coli SM10λpir Electrocompetent Cells

E. coli SM10λpir contains *tra* gene that allows it to form a pilus to successfully carry out a conjugation process (Simon et al. 1983). The pilus works as a bridge to transfer the plasmid. A 5 mL overnight culture of *E.coli* SM10λpir was grown in LB medium as a starter culture; it was used as inoculum for the 250 mL flask with LB_{kan50} which was grown until the $O.D_{600}$ reached 0.6. Five milliliters of the broth was distributed in each centrifuge tube. Cells were pelleted by

centrifugation for 5 minutes in 6,000 rpm (1500 xg) at 4°C; the supernatant was poured off. The pellet was washed by adding chilled 10% glycerol. The tubes were vortexed vigorously to resuspend the pellet and were centrifuged for 3.5 minutes in 6,000 rpm (1500 xg) at 4°C. The washing step with 10% glycerol was repeated for 4-5 times. Then the cells were resuspended in 100 µL of 10% glycerol. The final mixture was transferred into sterile centrifuge tubes making 30-50 µL aliquots. After the aliquotes were made, they were snap frozen by using liquid nitrogen or directly used for electroporation.

pEXFHU Plasmid and Cloning

pEX18 vectors were used for facilitating homologous recombination between the construct and the chromosome to produce site-directed mutagenesis (Hoang et al. 1998). This series of vectors contain a *sacB* counter selectable marker, *pUC* polylinker, *ori-T* origin of replication and one of the antibiotic resistance markers: tetracycline (Tet), gentamicin (Gm), or ampicillin (Amp) (Hoang et al. 1998). pEXFHU was made in the lab in this work by the integration of the SOE product (which had the deleted *fhuA* with the flanking regions) into pEX18Gm and was then transformed into *E.coli* SM10λpir via electroporation at 2.5kV/cm. The electroporation cuvette with a width of 1-2 mm was loaded with the electrocompetent cells and the constructed plasmid. The cuvette was then inserted inside the electroporation device using a cuvette holder and was exposed to the high voltage. Electroporation is a technique where cell membrane permeability is increased by applying high electric field or high electricity to the cells for a shorter period of time within which, there will be a transfer of DNA, chemicals, drugs,etc. inside the electrocompetent cells (Neumann et al. 1982). When bacteria and plasmid are

combined in a mixture and are electroporated, the plasmid can be transferred inside the bacterial cell.

The electroporated cells were serially diluted onto LB_{Gm15} plates and grown for 24 hrs at 37°C and the colonies were screened via colony PCR. The identification of plasmid DNA isolated from these cells was confirmed via sequencing and restriction digestion using the same enzymes used for cloning (BamHI and KpnI). One of the colonies that contained pEXFHU was used for biparental conjugation with *R. leguminosarum* ATCC.

Biparental Conjugation

Conjugation is the transfer of the bacterial genetic material horizontally via a direct cell to cell contact between two bacterial cells (Baron et al. 1996). In simple words, it can be considered as mating between two bacterial cells to transfer the genetic material; however, there is no exchange of gametes. Transfer of plasmid occurs in this process from a donor cell to the recipient cell. The newly transferred genetic material should be in most cases beneficial for the recipient cell for it to accept it, e.g. antibiotic resistance (Baron et al. 1996).

A pilus is produced by the donor cell because of the F-factor (F-plasmid, F positive or F-pilus) that attaches to the recipient cell to bring them together. This bridge formation leads to the transfer of nicked plasmid that gets transferred as a single-stranded DNA, and both of the cells can synthesize the complementary strand and form a new circular plasmid again (Baron et al. 1996). The plasmid then delivers the gene of interest to the WT strain via biparental conjugation. We used *E. coli* SM10λpir as a donor cell and wild-type *R. leguminosarum* ATCC as a recipient cell in this work.

Five mL of $YMB_{Pg50Nal10}$ was inoculated with *R. leguminosarum* ATCC and placed onto a rotary shaker at 30°C for 48 hours at 250 rpm. Five mL of LB_{Gm15} broth was inoculated with a SM10λpir colony which had pEXFHU. It was grown overnight at 37°C on a rotary shaker at 250 rpm. Both of these cultures mentioned above were centrifuged in microcentrifuge tubes at 8000 rpm for 5 min (2500 xg). and pellets were washed three times with sterile saline (0.85% NaCl) to remove residual antibiotics and media in the tube. This also helps to reduce the exopolysaccharides produced by *R. leguminosarum* ATCC. These cells were then resuspended in 200 µL sterile saline. Two hundred µL of *R. leguminosarum* was combined with 100 µL of *E. coli* SM10λpir containing pEXFHU in a sterile microcentrifuge tube. The mixture was then vortexed. The cells were pelleted via centrifugation in 10,000 rpm (5000 xg) at room temperature, and the supernatant was discarded. The pellet was resuspended in 30 µL of 10 mM $MgCl_2$.

The mixture was pipetted onto sterile 0.22 µm nitrocellulose membrane that was placed on the surface of warmed CR plate. While placing the membrane, the hydrophilic part was facing the agar, and the hydrophobic surface was facing up. This helps in continuous absorbance of nutrients from the media. The CR plates with the nitrocellulose membrane were incubated for 24 hours at 30°C.

After incubation, the nitrocellulose membrane was taken out using sterile forceps, and the colonies were washed off by submerging the membrane in 1 mL of sterile saline (0.85% NaCl) in a 1.5 mL sterile microcentrifuge tube. The tube was then vortexed vigorously so that the cells would get washed off into the solution from the surface of the membrane. The solution with the cells was then serial diluted and plated on $CR_{Gm10Nal10}$ plates and was allowed to incubate for almost 5 days until the colonies were formed. The colonies which successfully carried out the

biparental conjugation can survive, and the rest are killed. Wild-type *R. leguminosarum* ATCC is resistant to nalidixic acid, and the *E. coli* Sm10λpir with pEXFHU is gentamycin resistant. Use of both gentamycin and nalidixic acid allowed the screening of the conjugants which were resistant to both the antibiotics unlike recipient and donor strains. Colonies were further screened via colony PCR to identify the merodiploids.

The *fhuA* Mutant

The PCR identified merodiploid colonies that were able to grow on the $CR_{Gm10Nal10}$ containing plate were picked. Merodiploid is the state in which the bacterial chromosome contains its wild-type region and also the inserted region (Horton et al.1990)). This happens because of homologous recombination. The homologous recombination occurs because the "*fhuA* SOE insert" in the plasmid have a segment which is homologous to the WT chromosome. These merodiploid colonies are the ones with integrated pEXFHU into their genome and thus contained both, *fhuA* from WT and also the *fhuA* SOE product with Gm and *sacB* cassette with the flanking regions. Once merodiploids were identified, they were transferred to 5 mL YMB. The inoculated YMB broth was incubated at 30°C on a rotary shaker for 6 hours at 250 rpm, so that the cells would pass through a recovery process. After incubation, 1 mL YMB broth was transferred in sterile 1.5 mL centrifuge tubes and was centrifuged. The supernatant was discarded, and the pellet was resuspended in sterile normal saline (0.85% NaCl). It was serially diluted before plating on CR media containing 50µg/mL penicillin G and 5% sucrose ($CR_{Pen50Suc5}$). It was done to counter select the mutants against merodiploids that have carried out the homologous recombination and have knocked off the remaining part of pEXFHU keeping the inserted *fhuA* SOE fragment. The colonies were grown at 30°C for 72 hours. The *sacB* cassette in the plasmid produces levan sucrose in the presence of sucrose in the media. Levan sucrose

kills the bacteria by degrading its outer membrane. Hence, the colonies that survive should either have the WT chromosome or the SOE fragment that has "dropped out" the parts from the pEX plasmid and only contains the region flanking the putative *fhuA*. These individual colonies growing on sucrose were then picked and screened via colony PCR to identify the possible mutants which were without pEX fragments but contained the SOE fragment with the flanking regions of putative *fhuA*. A genomic extraction via the CTAB method as described above was performed on each identified potential mutant. The chromosomal DNA of each possible mutant was used as a template for PCR reactions using the primer set fhuIntF and fhuIntR (Table 4). The PCR amplicon with the right sized band at 1 Kb with deleted *fhuA* was sent for sequencing using the fhuIntF and fhuIntR primers. Colonies were confirmed as *fhuA*$^-$ via sequencing with an in-frame deletion of *fhuA* and were called *R. leguminosarum* ATCC *fhuA* mutant (RLΔFhuA).

Vicibactin Isolation and Purification

Atkin's Assay for Vicibactin Detection

Atkin's assay or iron perchlorate assay is a colorimetric assay done to detect the presence of hydroxamate type siderophores in a solution (Atkin's et al. 1970). As mentioned earlier, *R. leguminosarum* produces a hydroxamate type siderophore, vicibactin. Atkin's reagent was prepared by mixing 5mM $Fe(ClO_4)_3$ in 0.1 M $HClO_4$. Two and half mL of reagent was mixed with 0.5 mL of culture supernatant. The mixture is then allowed to incubate for approx. 5 min. at room temperature. A positive reaction forms wine color in the mixture. The intensity of the wine color depends on the amount of siderophore present in the supernatant. Absorbance was measured using a spectrophotometer at 450nm. The spectrophotometric analysis allows the

determination of vicibactin concentration in the samples based on its molar absorbance. The molar absorbance coefficient of vicibactin at 450nm is 1510 M^{-1} cm^{-1} (Carson et al. 1994).

R. leguminosarum ATCC::pBIO1187 and Vicibactin Isolation/Purification

Wild-type *R. leguminosarum* ATCC with cosmid pBIO1187 was used for vicibactin production. The cosmid pBIO1187 is a LAFR-1 based cosmid which contains the whole operon for vicibactin synthesis (Carter et al. 2002). Vicibactin isolation and purification was carried out following a protocol designed and confirmed previously (Wright et al. 2013). Cosmid pBIO1187 was transferred into the wild-type *R. leguminosarum* ATCC by using a helper plasmid pRK2013. A triparental conjugation was carried out for the transfer process.

The tetracycline and nalidixic acid resistant isolated colonies on $CR_{Nal10Tet10}$, were picked and used to make stock and starter cultures. The starter culture was used to inoculate larger batches of MMW media with Nal_{10} and Tet_{10}. Two flasks with 1 liter of MMW were used for inoculation. These flasks were grown on a rotary shaker at 30°C at 250 rpm for 6-7 days until the $O.D_{600}$ reached 1.00. Cells were then pelleted by centrifuging at 14000 rpm (8000 x g) at 4°C for 30 minutes. A longer centrifugation at high speed was needed to reduce the amount of exopolysaccharides produced by the bacteria. The supernatant was collected in 1L bottles. The bottles were acid washed and sterile. The supernatant was acidified to pH of 2.0 by using 6M HCl.

The supernatant was loaded on Amberlite XAD-2 column with bed volume of 5cm X 7.5cm (160 gm) in the column with 5 cm diameter and 30 cm length. The bed volume was calculated, and the column was prepared using methanol. Before loading the sample the column was equilibrated with 3-5 bed volume of deionized distilled water. The column bound vicibactin was washed with at least two bed volume of DDW before eluting. Methanol was used for the

elution process. The elution was done in 5 fractions of 50 mL each. The presence of vicibactin in these fractions was confirmed using Atkin's and Chrome Azurol S (CAS) assay. The eluted fractions with vicibactin were frozen using dry ice and liquid nitrogen and were lyophilized until dry using Freeze Dryer Virtis Freezemobile at ETSU Quillen College of Medicine. The dried samples were resuspended in 5 mL of methanol and were further purified using Sephadex LH-20 columns.

Approx. 45 cm of the Sephadex LH-20 column was packed with 25 g of the beads. The length of the column was 50 cm, and diameter was 1.5 cm. Methanol was used for elution, and total 50 fractions were collected in 1 mL aliquots using a Bio-Rad Model 2110 fraction collector. Five microliters of each fraction was used for Atkin's assay, to confirm the presence of vicibactin. The fractions with vicibactin were combined and poured into a round bottom flask which was further used to evaporate the methanol present using a Buchi R-200 Rotovap. The evaporation was carried out in a water bath at 40°C at the pressure of approx. 300 mm of Hg with a rotation of the flask at maximum rpm. The evaporation was carried out until the entire methanol evaporated. The samples were stored at -20°C until further use.

High Performance Liquid Chromatography (HPLC)

BioRad Biological Duoflow HPLC system was used for further purification of the siderophore. The mobile phases used were filtered 100% methanol and filtered deaerated deionized water. The concentrated sample was suspended using sterile deaerated deionized water and enough methanol to dissolve the sample. The wavelength of the UV detector was set at 240 nm and the column used was Waters 7.8mm x 300mm Novapak HR C_{18} hydrophobic column. The bed volume was calculated, and 3-5 bed volumes of sterile deaerated deionized water were allowed to pass through the column for equilibration. Five hundred microlitres of the sample was

injected into the column. The siderophore was eluted using the gradient of methanol and occurred at 48% methanol. As soon as the methanol was introduced in the column, the elution of the molecules was noted by the UV detector. The molecules eluted were showing peaks similar to the previous results (Wright et al. 2011). The peaks and the fractions were analyzed using Atkin's assay to confirm the purity of the sample.

CHAPTER 3

RESULTS

Growth of *R. leguminosarum* ATCC Dependent on Iron Concentration

R. leguminosarum ATCC was grown in minimal media supplemented with different iron concentrations (0 μM, 0.05 μM, 0.1 μM, 0.5 μM, 2.5 μM, 50 μM, and 100 μM) to determine its influence on growth. The minimal media MMW contained every other nutrients required for growth, but not just the iron. As a negative control, 0.25 mM 2'2' dipyridyl (DIPI) was used to chelate the contaminating iron in the media and to achieve a perfect zero iron concentration (Wright et al.2013). As predicted, the growth of the bacteria in DIPI was almost negligible with $O.D._{600}$ less than 0.2, whereas the growth of bacteria in high iron was much higher ($O.D._{600}$ over 1.6 after 72 hrs). The effect of higher iron concentrations 50 μM and 100 μM on bacterial growth after 36 hrs was similar as shown in Fig. 9. This suggests there is no need of such high iron concentration for a proper bacterial growth. The bacteria were observed to grow differently in different iron concentrations, despite equal amount of bacteria (inoculum) introduced in each flask (Fig. 9). This reveals the effect and necessity of iron in proper bacterial growth and development.

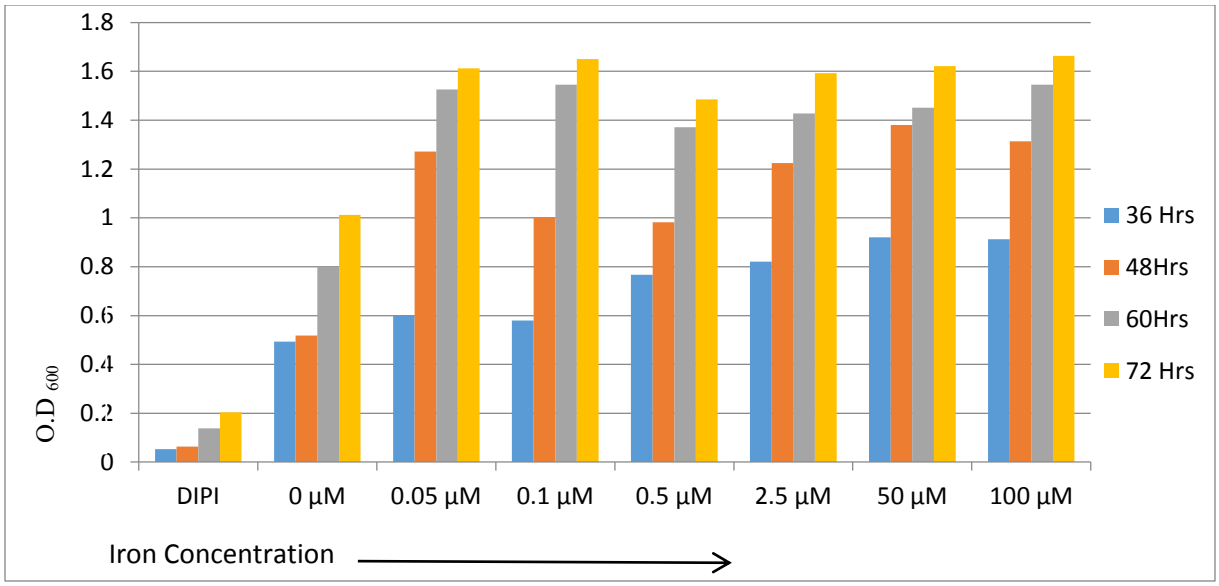

Figure 9: Growth of *R. leguminosarum* ATCC in different iron concentration. The growth of the bacteria is affected by the amount of iron present in the media. DIPI is the absolute zero iron concentration.

Identification of Putative *fhuA* and *In-Silico* Analysis

Presence of *fhuA* Like Genes

Polymerase Chain Reaction (PCR) and agarose gel electrophoresis were used to detect the presence of *fhuA* like genes in *R. leguminosarum* ATCC. PCR primers were designed based on the known gene sequence of *fhuA* from *S. melioti, E.coli* and *R. leguminosarum viciae* (Table 4). Successful amplification was observed only with the primers from *R. leguminosarum* bv. *viciae* 8401. The primers that were based on the gene sequence of *E. coli* and *S. melioti* did not show amplification (Fig. 10). The primers from *E. coli* and *S. melioti* were from within the known open reading frame (ORF) of the *fhuA* gene. The primers based on *R. leguminosarum viciae* 8401were located outside the known *fhuA* sequence. Also, different sets of primers from within the ORF of the respective known *fhuA* sequences showed a similar result to Fig. 10, with

the only amplification from the primers from *R. leguminosarum viciae* 8401. This amplification result suggests that the putative *fhuA* from *R. leguminosarum* ATCC is similar in size to the *fhuA* gene from *R. leguminosarum viciae* 8401.

The PCR amplicon was sequenced further using primer walking technique, designing primers based on the sequenced data and performing PCR and sequencing further forward until the whole sequence was obtained. 1Kb upstream and 1Kb downstream of the putative *fhuA was* also sequenced for future experimental purposes. Sequencing was necessary as the whole genome sequence of the *R. leguminosarum* ATCC has not been performed yet.

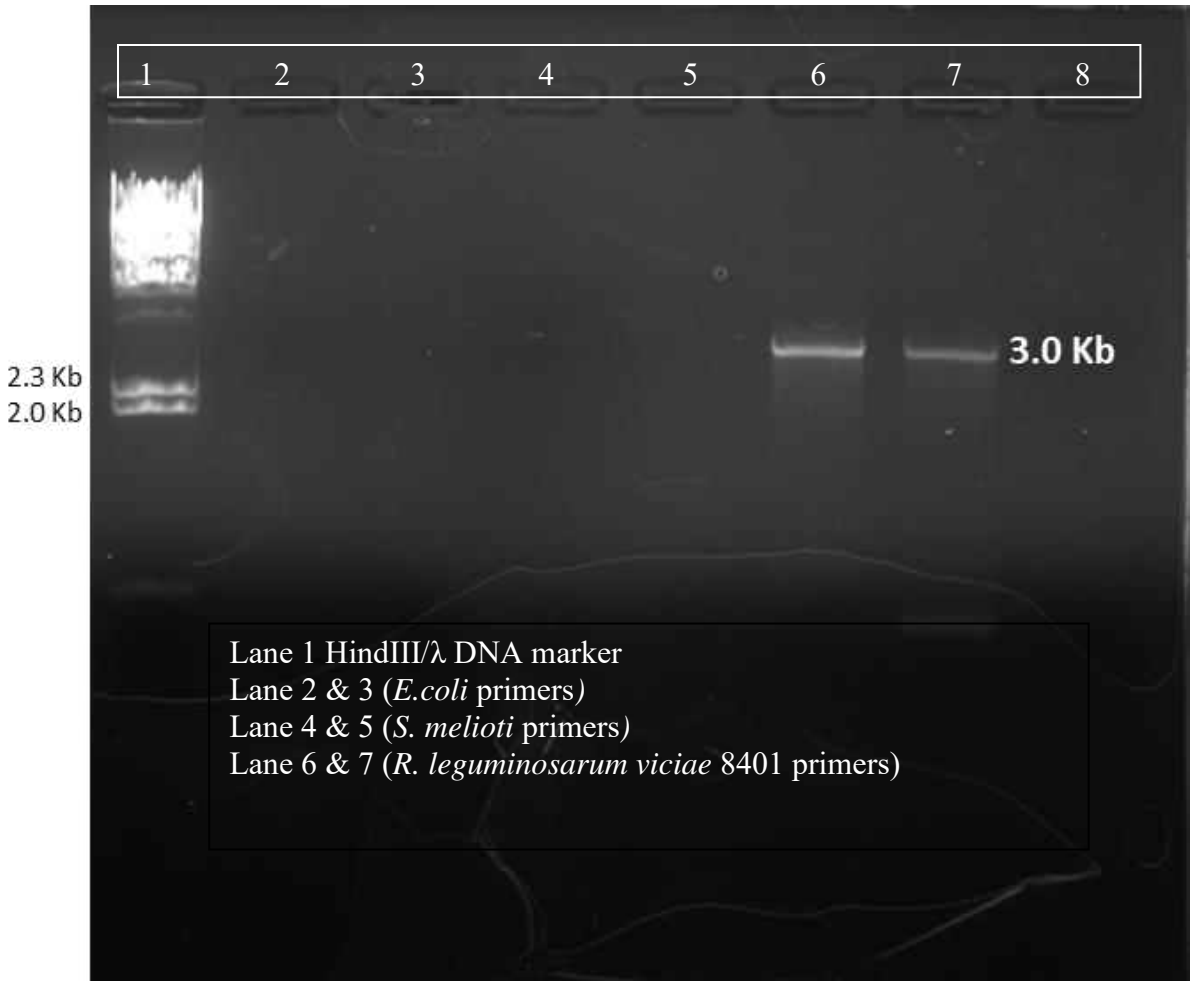

Figure 10: Amplification of the putative *fhuA* in *R. leguminosarum* ATCC. The gel shows amplification of the putative *fhuA* in lanes 6 and 7 only from the primers designed from *R. leguminosarum viciae* 8401 and no amplification from other primers.

Gene Sequencing and Alignment

The putative *fhuA* gene that was amplified in *R. leguminosarum* ATCC was sequenced for further analysis. Sequencing of 3746 bases was performed to obtain the sequence from 1kb upstream, and 1Kb downstream of *fhuA* in order to perform a gene knockout experiment in future. Sequencing was important because a whole genome sequence is not yet available for *R. leguminosarum* ATCC. The sequence data was obtained in parts and hence was put together in a consensus sequence for analyzing the whole 3746 bases. The alignment is shown in parts with two strains of *R. leguminosarum* (see appendix). The genome of relative species *R. leguminosarum* J251 or *R. leguminosarum viciae* 8401 has also not been sequenced yet. Hence, the alignment data is shown in fragments which aligned with different gene fragments of *fhuA* and the flanking regions belonging to *R. leguminosarum* J251 or *R. leguminosarum viciae* 8401.

Nucleotide BLAST (NIH-NCBI) was carried out for the analysis using the sequenced data. Putative *fhuA* shared more than 95% nucleotide identity with *R. leguminosarum viciae* 8401 and *R. leguminosarum* J251. Putative *fhuA* was 70% identical with *R. tropici* and *R. phaseoli fhuA* sequences. Changes in nucleotides at 13 different places were observed within the predicted ORF of 2244 nucleotide bases when aligned with *R. leguminosarum viciae* 8401 (alignment data in appendix). However these changes were not affecting the putative coding region.

In-Silico Analysis

Analysis of the putative sequence was necessary to determine the correct open reading frame (ORF) and to use it for further structural analysis. The prediction was required for cloning and other experiments as well. ORF finder (NCBI) was used to predict the possible ORF from

the putative gene sequence (Fig. 11). The longest ORF2 predicted was 95% identical to the ORF of the published sequence of *R. leguminosarum* 8401 and was 2244 base pairs in length. The online software "genome2d" was used to predict the promoter region (Fig. 12). The promoter region found approx. 10 bases upstream of predicted ORF2 (Fig. 12) also suggested that the predicted ORF2 is the correct ORF. Putative promotor upstream of ORF2 had the highest score (Fig. 12).

The independently generated 3D structure of ORF2 demonstrated a possible barrel shaped model of the putative FhuA using the 3D structural homolog tool SWISS-MODEL 3D (Fig 15). The presence of Pribnow box in front of the ORF2 and observing the consensus -10 sequence and -35 sequence, ORF2 was found to be the best match for the putative FhuA protein.

Label	Strand	Frame	Start	Stop	Length (nt | aa)
ORF2	**+**	**2**	**671**	**2914**	**2244 | 747**
ORF3	+	2	2918	>3742	825 | 274
ORF1	+	2	242	658	417 | 138
ORF4	-	3	2986	791	2196 | 731

Figure 11: Predicted ORF's using NCBI-ORF prediction tool. The possible ORF are shown in the picture. ORF2 is an ORF similar to known and published data.

ID	SeqName	Sequence	start	end	TSS	MotifName	strand	length	Score
p_1	query	TTAAATCGATAAATCCACGCCTTCAACACT	618	648	613	N18b	-	30	6.1
p_2	query	TTGAAGGCGTGGATTTATCGATTTAAAGG	622	651	656	N17	+	29	5.7
p_3	query	TGGATTTATCGATTTAAAGGTGACTAAAAT	631	661	666	N18	+	30	8.7
p_4	query	TTTAAAGGTGACTAAAATAATCATCTTAT	643	672	677	N17	+	29	6.1
p_5	query	TTGACAAGGCCAATTTCGCTCCATAGGTT	673	702	707	N17	+	29	8.3
p_6	query	TATAAATTCGCGATACATTATTAGAAACAT	752	782	747	N18b	-	30	5.8
p_7	query	TAGGCTATCTCTATAAATTCGCGATACATT	763	793	758	N18b	-	30	5.7
p_8	query	TGAACGGATTGGTTTCCTGGAAAGTATAGT	2621	2651	2616	N18b	-	30	5.4
p_9	query	CCGAAAAGTCTGCTGCCTGCGTTACAAT	3619	3647	3652	N16	+	28	5.6

Figure 12: The putative promoter site of the predicted ORF. The site with the highest score upstream of the predicted ORF was considered as a promoter site for the putative ORF. The promoter site p_3 query was upstream of the putative ORF2 with the highest score and a length of 30 nucleotide bases.

The protein sequence was generated by using the translation tool from EXPASY, Swiss Institute of Bioinformatics (SIB) (EXPASY/SIB 2016). The putative protein sequence from *R. leguminosarum* ATCC was aligned with known (crystal structured) amino acid sequences from *E.coli* FhuA (Fig. 13), and known but not crystallized *R. leguminosarum viciae* FhuA (Fig. 14). The alignment showed the similarity of the amino acids with the *E. coli* FhuA with an identity of 32% and similarity of 52% (Fig. 13). The amino acid similarity was interesting because as stated before, the *E. coli fhuA* gene primers did not amplify the putative *fhuA*. The nucleotide sequences between the putative *fhuA* and the *E. coli fhuA* did not align with each other. This similarity between the proteins points out the possibility of these proteins transporting similar types of ligand. As mentioned in earlier sections, the siderophores vicibactin and ferrichrome are both hydroxamate type siderophores. No identity between the gene sequences illustrates that two different genes can code for proteins of similar function. Structural analysis of these proteins was necessary to understand more about them.

Figure 13: Protein sequence alignment of putative FhuA with *E.coli* FhuA. Putative FhuA is the query sequence and *E.coli* FhuA is the subject. Some of many similarities and dissimilarities between these two sequences are shown in the boxes. The sequence was 32% identical and 52% similar.

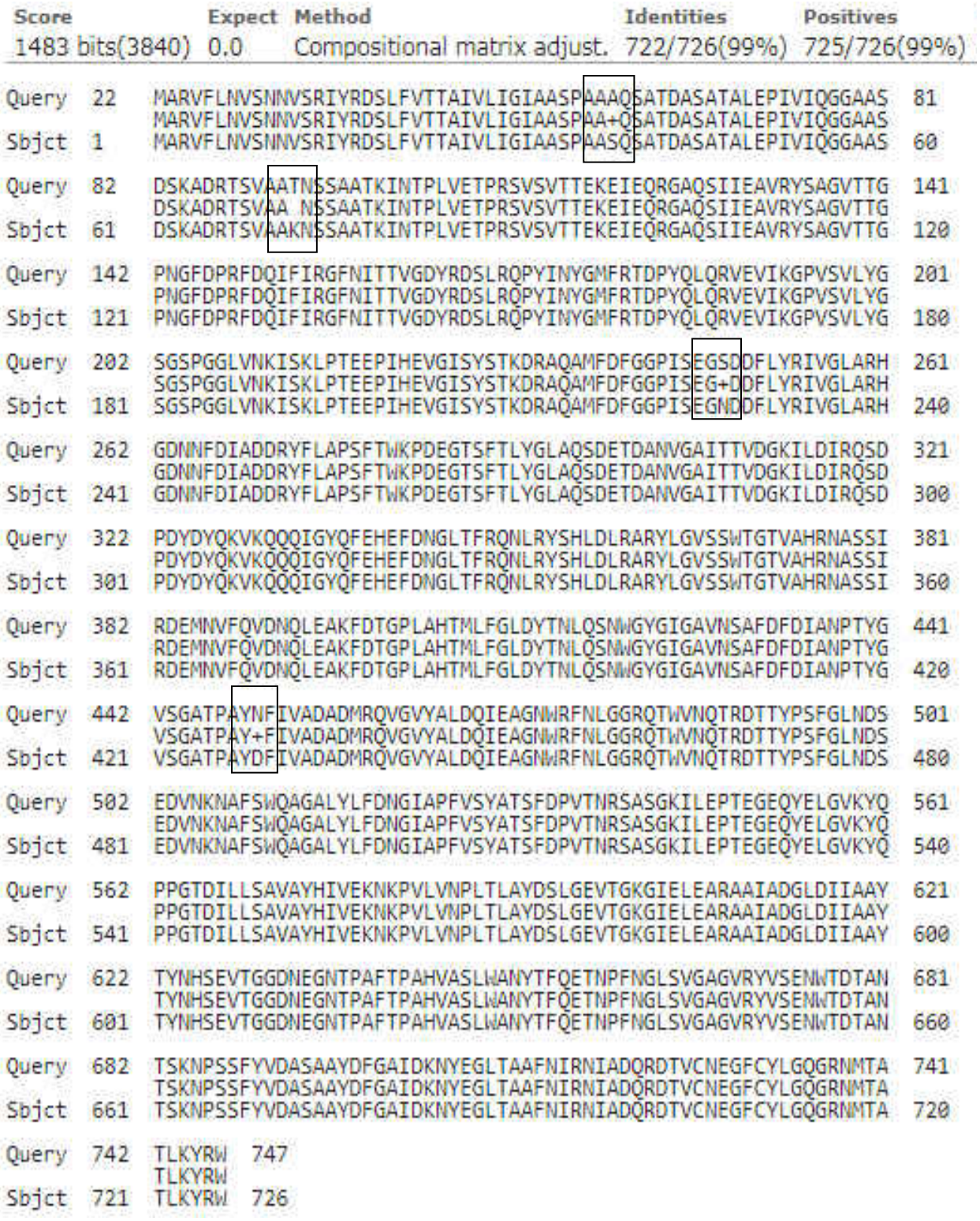

Figure 14: Protein sequence alignment of putative FhuA with *R. leguminosarum viciae* 8401FhuA . Putative FhuA is the query sequence and *R. leguminosarum viciae* 8401FhuA is the subject. The sequence was 99% identical. The only differences were observed in 4 amino acids as shown in the boxes.

SIB-3D SWISS-MODEL tool was used to model the protein structures independently (Fig.15, 16). The putative FhuA protein structure was modelled and was compared with published (solved crystal structure) FhuA model of *E.coli* K12 (Fig. 15, 16) (Ferguson et al. 1998). Both putative FhuA and the *E. coli* K12-FhuA had a 22 β-stranded barrel-shaped structure with a plug domain inside the barrel (Fig. 15, 16, 17, 18). The similarities and differences are shown using the arrows (Fig. 15, 16, 17, and 18). One difference was the N-terminal extension in the putative FhuA for *R. leguminosarum* ATCC, which was not present in *E.coli* FhuA. This extension is seen in the outer membrane transporters such as PupA (*Ps. aeruginosa*) and FecA (*E.coli)* for transduction of energy during the process of siderophore transport (Bitter et al. 1991, Yue et al. 2003). The extension is necessary for interaction with the TonB energy transducing protein (Bitter et al. 1991, Yue et al. 2003). The loop orientation and number of loops was similar with *E.coli* FhuA. Nevertheless, the gene sequence of the crystallized transporter protein from *E.coli* K12 had no sequence alignment with the newly sequenced putative *fhuA* gene (0% alignment).

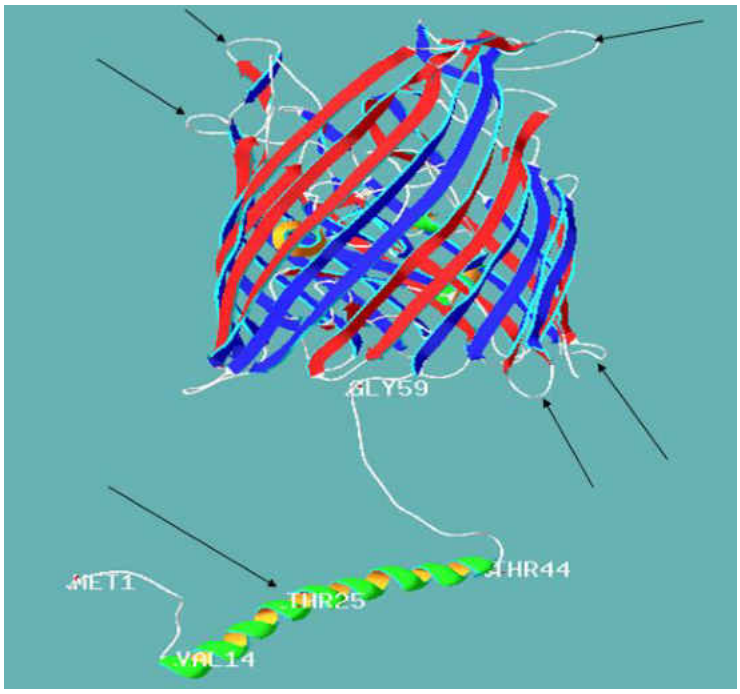

Figure 15: Putative *R. leguminosarum* ATCC FhuA. The similarities and dissimilarities with *E. coli* FhuA are indicated using arrows. Presence of N-terminal extension can be observed in the putative FhuA.

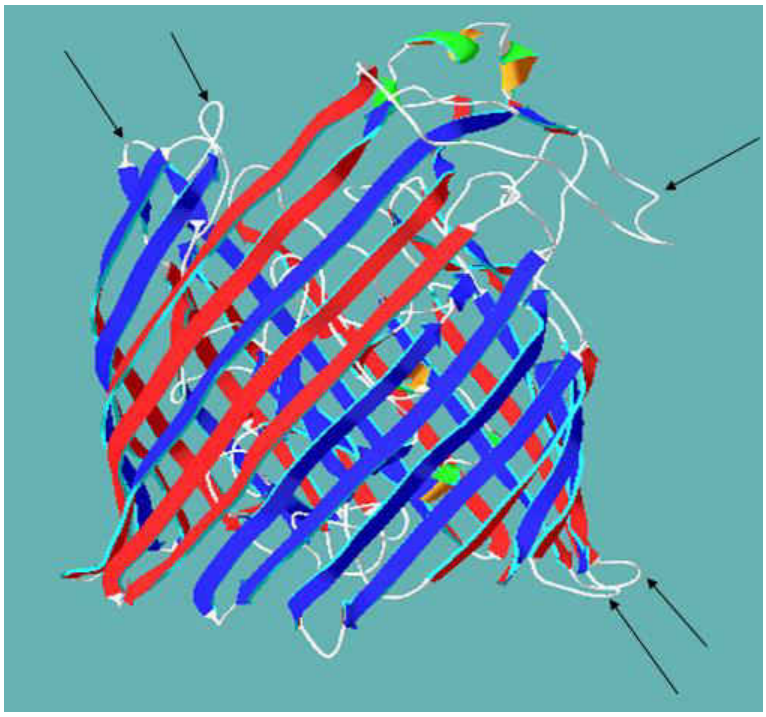

Figure 16: *E. coli* FhuA

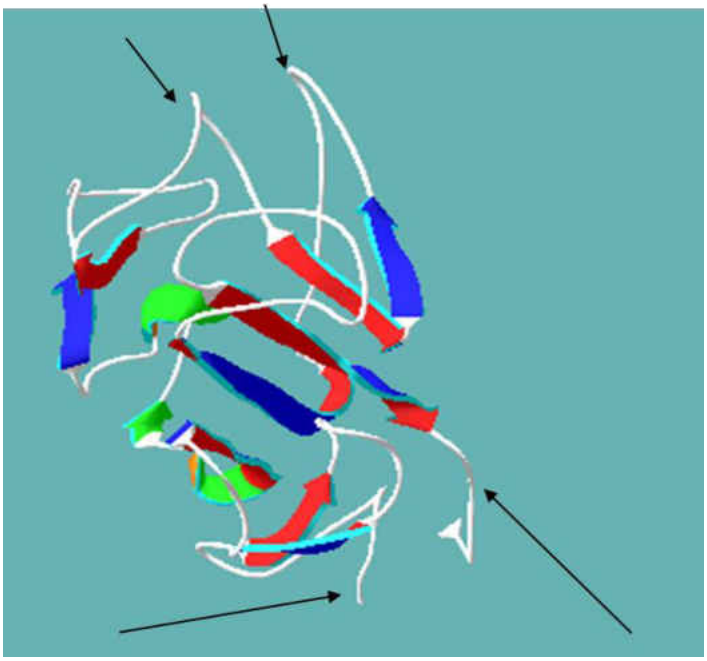

Figure 17: *E. coli* FhuA plug domain

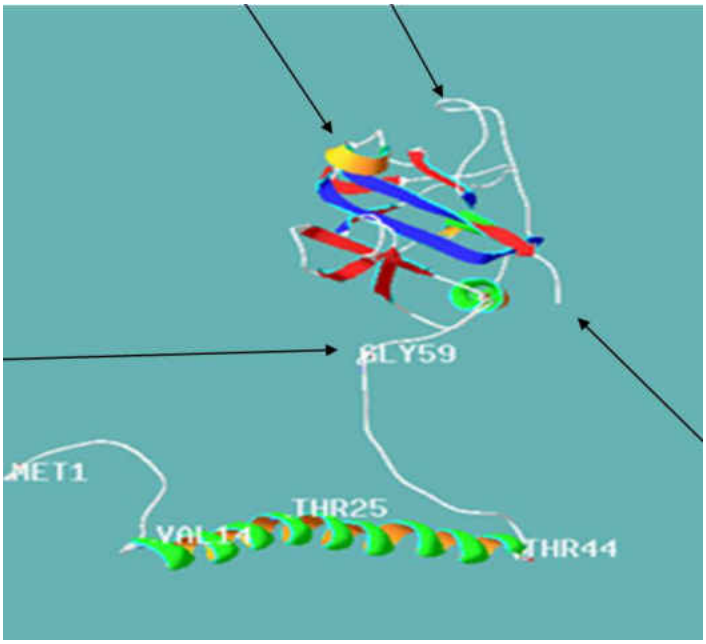

Figure 18: Putative FhuA plug domain. The similarities and dissimilarities with *E. coli* FhuA are indicated using arrows. Presence of N-terminal extension can be observed in the putative plug domain.

Cloning of Putative *fhuA*

Cloning of putative *fhuA* from *R. leguminosarum* ATCC in an expression vector was necessary for future complementation assays. This was also necessary for protein expression and purification for future experiments. The cloning of *fhuA* in the pET17b plasmid was carried out as previously described. The transformation of the pET17b::*fhuA* plasmid into *E.coli* BL21/DE3 was carried out and confirmed via antibiotic selection. Colony PCR and sequencing was done to confirm the cloned insert. The restriction/digestion of the extracted plasmid DNA further confirmed the size as there was a drop out of the same size of the insert (2.3 Kb) and the pET17b vector (3.3 Kb) (Fig.19).

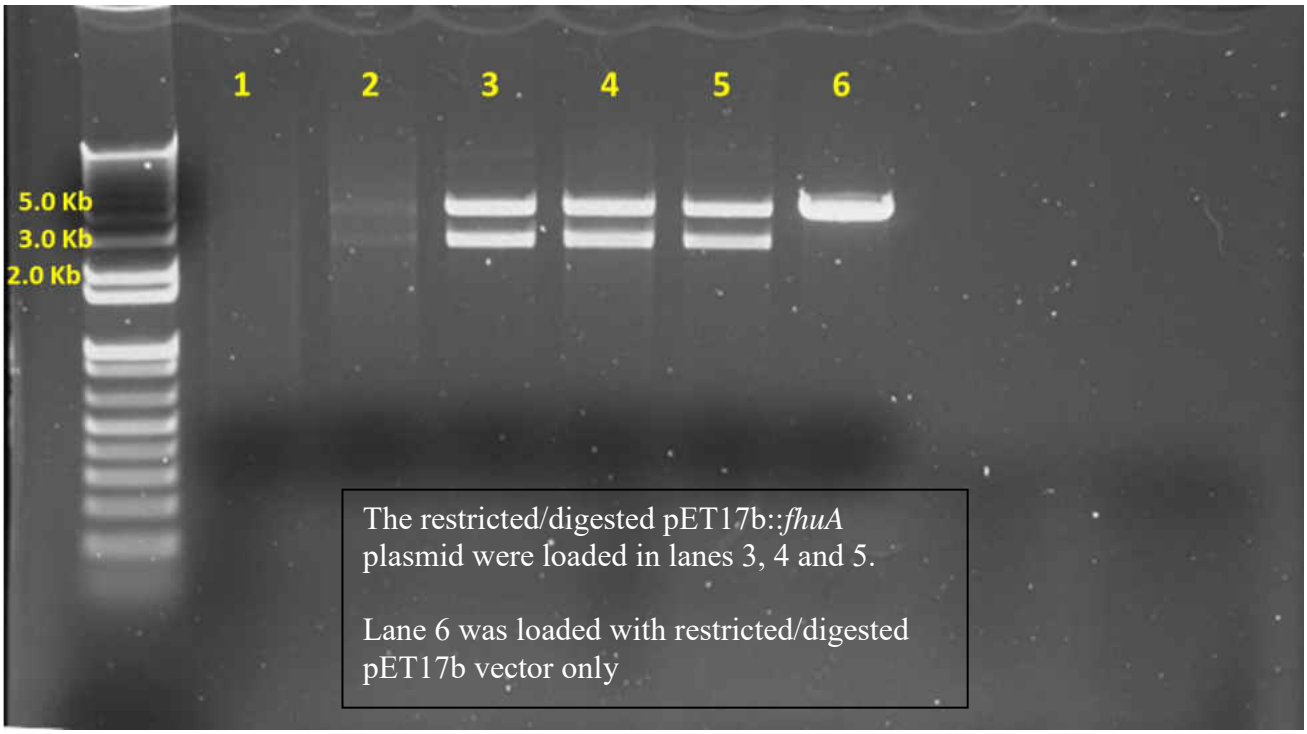

Figure 19: Restriction digestion of pET17b::*fhuA* plasmid and pET17b vector. The drop off of the insert is observed which is absent in lane 6 (Vector only).

The sequencing data confirmed putative *fhuA* was in frame with the T7 epitope. The methionine site in the first line, highlighted yellow in Fig. 20 is the start codon of T7-tag. The

methionine site in the second line, higlighted green, is the start codon for putative *fhuA*. The restriction enzyme site (GGTACC) is highlighted in red.

CCACAACGGTTTCCCTCTAGAAATAATTTTGTTTAACTTTAAGAAGGAGATATACATATG
GCTAGCATGACTGGTGGACAGCAAATGGGTCGGGATTCAAGCTTGGTACCGATGTTGACA

Figure 20: Sequence of the start site of the T7-tag and putative *fhuA*. The in-frame insertion of the putative ORF is confirmed

The same thing as above was done for the stop codon or towards the end of the putative *fhuA* gene. Fig. 21 shows the stop site in purple and the enzyme (GGATCC) right after the stop codon highlighted in red. The inframe insertion is important for protein expression and purification purposes.

CGCAACATTGCCGACCAGCGCGACACCGTGTGCAACGAGGGCTTCTGCTATCTCGGCCAA
GGCCGCAACATGACGGCGACCCTGAAGTATCGGTGGTAAGGATCCACTAGTTAACGGCCTT

Figure 21: The stop codon of the putative *fhuA* in pET17b. The stop codon in purple (TAA) is the stop site of putative *fhuA*. The in frame insertion of the putative *fhuA* in pET17b:: *fhuA* is confirmed.

Location of *fhuA* and *rosR* and *fhuF*

A fragment of the transcriptional regulatory gene *rosR* was found upstream of the putative *fhuA* gene. There is a possibility of the whole gene being present if further sequenced. The whole *rosR* gene is 573 bp and controls various cellular functions as described earlier. It belongs to the TetR family of transcriptional regulators (Rachwal et al. 2015). The alignment of the *rosR* gene from strain *R. leguminosarum* Rt 24.2 showed 95% identity with the putative *rosR* from *R. leguminosarum* ATCC (see appendix). The whole *rosR* gene has not been sequenced yet and it was discovered while sequencing *fhuA* (see appendix).

Downstream of *fhuA*, the *fhuF* gene was present which aligned with the known sequence of *fhuF* from *R. leguminosarum viciae* 3841 and *R. leguminosarum trifolii* 24.2 (see. appendix). The *fhuF* is a 789 bp siderophore reductase gene. As mentioned before, the reduction of siderophore and the ferric-iron complex is carried out by the protein FhuF (Miethke et al. 2011).

To know the location of *fhuA* was necessary as there has been a previous report of a pseudogene *fhuA* in an operon *fhuDCBA* in *R. leguminosarum viciae* 8401 (Yeoman et al. 2000). The pseudogene was present in the operon *fhuDCBA* and was in opposite orientation than *fhuDCB.* The location of putative *fhuA* in *R. leguminosarum* ATCC was analyzed and found to be present between *rosR* and *fhuF*. The study of expression was done after its location was analyzed and confirmed which revealed that it was not present in an operon *fhuDCBA*.

Wild-Type Putative *fhuA* Expression

Expression of Putative FhuA Protein

A 7.5% SDS-PAGE was performed to determine if there are proteins with different level of expression present in the outer membrane fragments of cells grown at low and high iron concentrations (Fig. 22). Any proteins in the outer membrane fragments that are controlled by iron concentration with a size ranging about 70-90 kDa are likely candidates for OM receptors in bacteria for iron transport (Morton and Williams 1989). Two such bands were found in SDS-PAGE gel analysis. The molecular weight of the putative FhuA protein was calculated to be 82 Kilo Daltons (kDa) using EXPASY molecular weight calculator. There was one such band present in the polyacrylamide gel which was similar to 82 kDa. This band was a band of interest also because the *E.coli* FhuA is approximately the same size (78 kDa) (Fig. 22). The experiment

was repeated more than three times to confirm the under expression of this protein in the outer membrane at higher iron concentration. The expression of proteins involved in siderophore biosynthesis and transport are known to be repressed at higher concentration (Morton and Williams 1989). This suggests that the protein of size 82 kDa in the gel is more likely to be the putative FhuA or another protein regulated by iron concentration which is more likely to be required for siderophore transport. A second band in the gel at approximately 70 kDa was not a possible candidate for putative FhuA because as stated earlier, the calculated molecular weight based on the sequence data was 82 kDa and not 70 kDa.

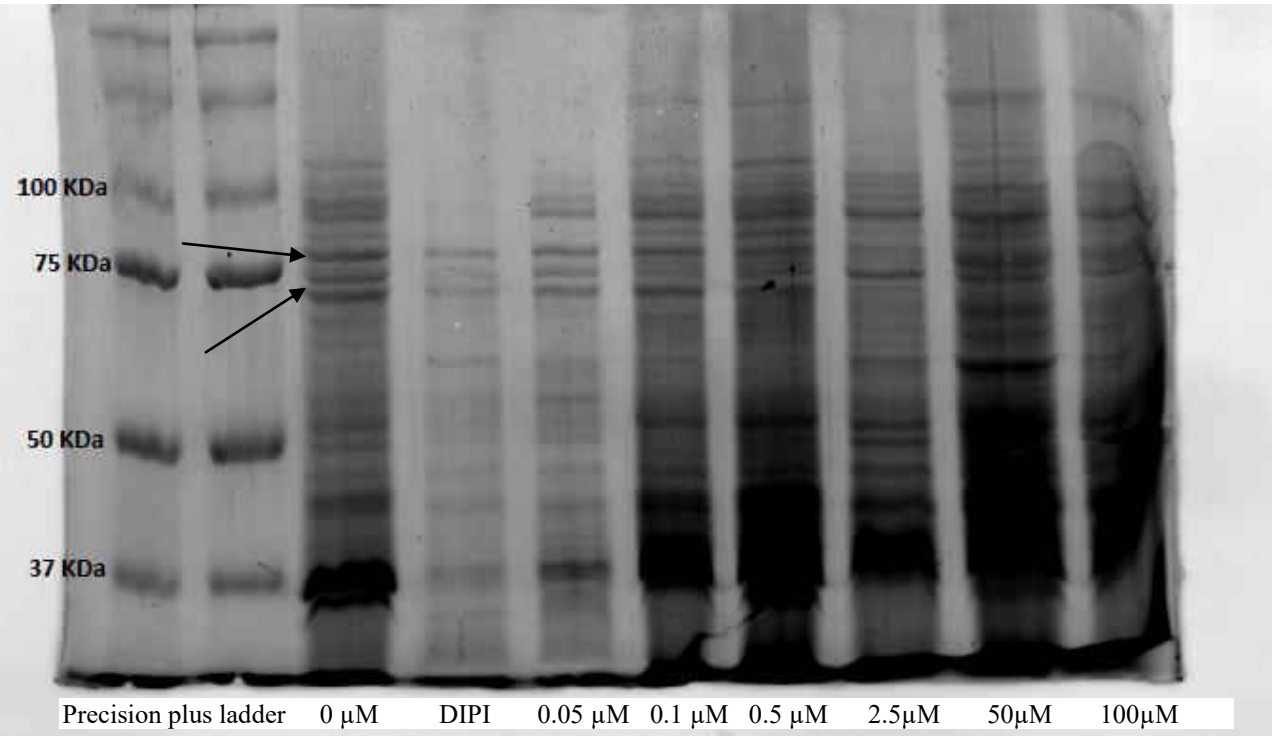

Figure 22: Expression of outer membrane protein fragments controlled by $FeS0_4.7H_2O$. The outer membrane fragments from bacteria grown in 0µM iron is loaded in 3rd lane, dipiridyl in 4th lane, 0.05µM in 5th, 0.1 µM in 6th, 0.5 µM in 7th, 2.5 µM in 8th, 50 µM in 9th and 100 µM in 10th lane. The bands shown by the arrow resemble sizes 70-90 kDa and are being under-expressed in high iron. The putative FhuA is most likely to be the band resembling the mol. wt. size of approximately 82 kDa since the calculated mol. wt. was 82 kDa.

Expression of Putative *fhuA* Gene

RT-PCR was performed to determine if the putative *fhuA* mRNA transcript was being produced (Fig. 23). The RNA extraction was done when the $O.D_{600}$ was 0.6 to 0.8 and the amount of total RNA loaded for synthesis of the cDNA was exactly same for all the samples grown at different iron concentrations. The expression of putative *fhuA* was seen to be high in low iron concentrations and very low/almost undetectable in higher iron concentrations. This expression was very similar to that of the 82 kDa protein in the SDS-PAGE gel (Fig. 22). Furthermore, the quantification of this data was done by performing the RT-PCR experiment in various PCR cycles (15X, 20X, 25X, 28X, 29X, 30X and 40X). The 1% Agarose gel shown below (Fig. 23A) is from the PCR run for 30 cycles. The expression of the putative *fhuA* is decreasing when the iron concentration was increased. Lane 6, 7 and 8 have almost no amplification showing that the amount of mRNA synthesized were very low which were specific to the putative *fhuA*. Fig 23B, Fig 23C, Fig 23D are the gel from 20X, 25X and 40X, respectively. In Fig. 23B, the expression of the putative *fhuA* is very low when PCR was performed for 20 cycles. In Fig. 23C, the expression is visible until lane 4 (0.1 μM iron). In Fig 23D, the expression of the putative *fhuA* is seen in all the lanes.

There was no amplification at all in PCR runs for 15 or less cycles. The presence of the mRNA specific to the putative *fhuA* caused the amplification in all cases. The high iron lanes have the amplification in all the lanes in 40X because, there is definitely going to be very low expression of the putative *fhuA* even if iron concentration is very high as it is required for iron transport. The expression would not be halted completely. The abundance of high iron will make the expression lower when compared to the cells grown in low iron concentration. That would be the reason behind the band in all lanes in Fig. 23D.

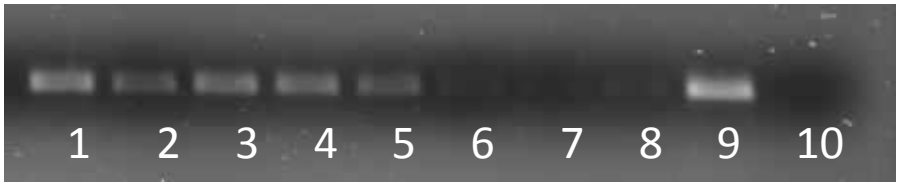

Figure 23A: 1% agarose gel after RT-PCR of the putative *fhuA* for 30 cycles

Lane 1: 0 µM
Lane 2: Dipiridyl
Lane 3: 0.05 µM
Lane 4: 0.1 µM
Lane 5: 0.5 µM
Lane 6: 2.5 µM
Lane 7: 50 µM
Lane 8: 100 µM
Lane 9: Chromosomal DNA
Lane 10: No RT-Enzyme

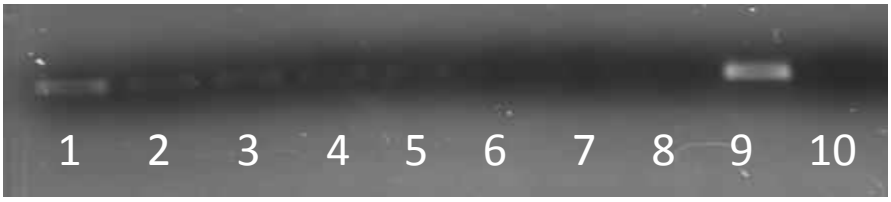

Figure 23B: 1% agarose gel after RT-PCR of the putative *fhuA* for 20 cycles

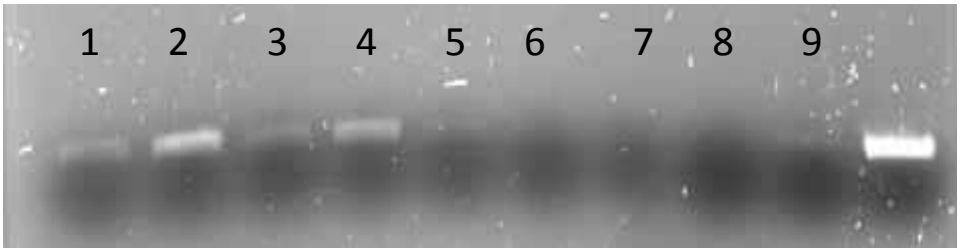

Figure 23C: 1% agarose gel after RT-PCR of the putative *fhuA* for 25 cycles

Lane 1: 0 µM
Lane 2: Dipiridyl
Lane 3: 0.05 µM
Lane 4: 0.1 µM
Lane 5: 0.5 µM
Lane 6: 2.5 µM
Lane 7: 50 µM
Lane 8: 100 µM
Lane 9: No RT- Control
Lane 10: Chromosomal DNA

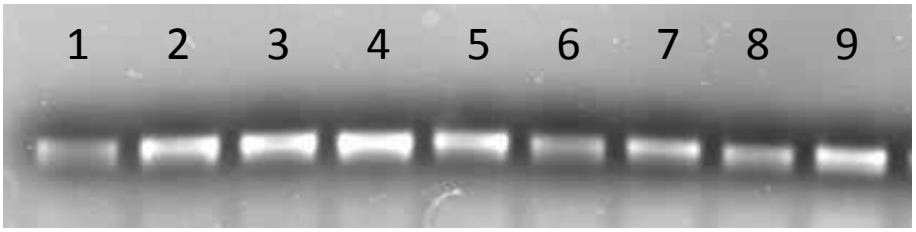

Figure 23D: 1% agarose gel after RT-PCR of the putative *fhuA* for 40 cycles

Lane 1: 0 µM
Lane 2: Dipiridyl
Lane 3: 0.05 µM
Lane 4: 0.1 µM
Lane 5: 0.5 µM
Lane 6: 2.5 µM
Lane 7: 50 µM
Lane 8: 100 µM
Lane 9: Chromosomal DNA

Figure 23: Expression of putative *fhuA* gene. Use of 1% Agarose gel to show different levels of expression of the putative *fhuA* in different iron concentrations. The decrease of expression of the putative *fhuA* in increasing iron concentration and vice versa elucidates its possible involvement in iron transport.

R. leguminosarum Putative *fhuA* Mutant

Cloning and Construction of pEXFHU and Its Confirmation

Cloning of pEXFHU and its confirmation was done following the same procedure used for cloning *fhuA* into pET17b as described in the earlier sections. The restriction digested and ligated pEXFhu plasmid with the "SOE fragment" was introduced into *E.coli* SM10λpir electrocompetent cells via electroporation. The colonies were screened on gentamycin plates and confirmed via colony PCR using the primers specific to the inserted SOE fragment. The plasmid DNA was further digested with the appropriate enzymes to confirm the size of the fragments that dropped out which was the similar to the size of the insert in lane 4 (1.6 Kb) (Fig. 24). However the digested vector did not show such drop out (Fig. 24). Successful cloning was confirmed via sequencing using appropriate primers (Fig. 25).

Figure 24: Restriction digestion of pEX::FHU and pEX18Gm vector. Lane 3: whole plasmid with the SOE fragment, Lane 4: restriction digested plasmid DNA, Lane 6: Whole plasmid/vector DNA only, Lane 7: restriction digested vector DNA only, Lane 9 : Whole plasmid/vector DNA only, Lane 10: restriction digested vector DNA only.

Figure 25: In-frame deletion of the putative *fhuA* and the alignment of the flanking region. The box shows the putative start codon and the putative stop codon of the putative *fhuA* with the flanking region (query) in the pEX18FHU plasmid aligning with the flanking region of the (Subject) WT putative *fhuA*.

Construction of *R. leguminosarum* ATCC *fhuA* Mutant (RLΔFhuA)

Biparental conjugation was carried out between wild-type *R. leguminosarum* ATCC and *E.coli* SM10λpir with pEXFHU. The conjugated cells were selected using gentamycin/nalidixic acid. Gentamycin was used to kill the wild type *R. leguminosarum* ATCC which were unable to carry out the conjugation process. Nalidixic acid was used to kill the *E.coli* strains. The *R. leguminosarum* ATCC colonies with the pEX::FHU (Gm^R) were the only ones which were able to grow in the antibiotic selection process. Colony PCR was done to confirm the successful conjugation followed by integration of the SOE fragment. As described before, the colonies were counter-selected in 5% sucrose as the cassette *sacB,* if present, produces levan sucrose in presence of sucrose which kills the bacteria by degrading its cell membrane. The colonies that

can survive are either WT colonies or the colonies that went through successful recombination and have dropped off the fragments from pEX::FHU.

After performing selection and counter selection of the mutants, colony PCR was done to confirm the mutants (Fig. 26). The primers used (Fig. 28) for colony PCR were IntF and IntR (Fig.26). Mut1, Mut2, Mut3, Mut4, Mut5 and Mut6 are mutants. The wild type was used as a control during colony PCR. The primers used were the primers outside the putative *fhuA* ORF and are approx. 0.5 Kb away from each start and stop site of the putative *fhuA* (Fig. 28). These primers were also used for sequencing the RLΔFhuA mutants. Sequencing data revealed the in-frame deletion was carried out successfully (Fig. 27). The smaller bands sizes (1.0 Kb and 0.4 Kb) in both the gels (Fig. 26, Fig. 29 respectively) show that the putative *fhuA* has been deleted in *R. leguminosarum* ATCC. The WT colony with the putative *fhuA* is showing the band size 3.5 Kb and 3 Kb (Fig. 26, Fig. 29 respectively). The sequencing of the mutants also confirmed this deletion (Fig. 27, Fig. 30). The in frame deletion of putative *fhuA* is highlighted in blue showing just the start and stop codons (Fig. 27, Fig. 30).

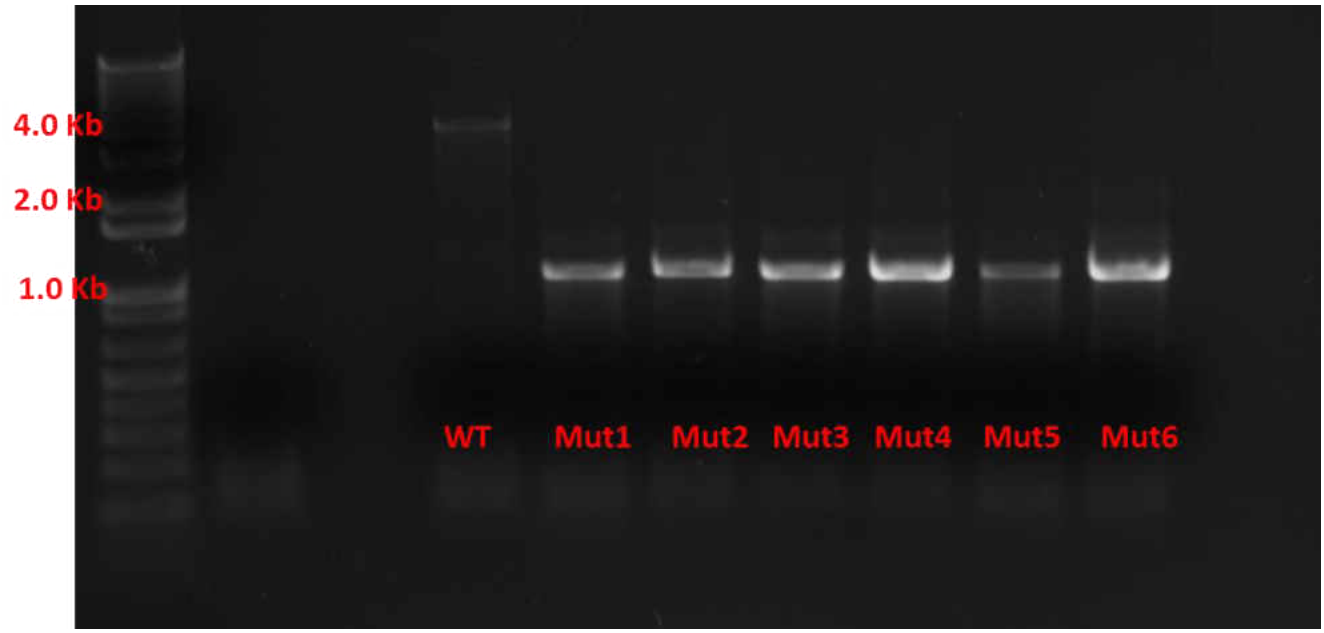

Figure 26: The amplification of the fragments flanking putative *fhuA* in RLΔFhuA. WT is wild type *R. leguminosarum* amplified with putative *fhuA*. Mut1, Mut2, Mut3, Mut4, Mut5 and Mut6 are the mutants showing the smaller band size 1.0 Kb without *fhuA*. WT, with putative *fhuA* shows a band at 3.5 Kb.

Figure 27: Sequencing to confirm the in-frame deletion of putative *fhuA* in RLΔFhuA. The Start codon and stop codon are shown in the alignment and hence it is confirmed that the putative *fhuA* has been deleted in-frame. Query is the sequence from the RLΔFhuA.

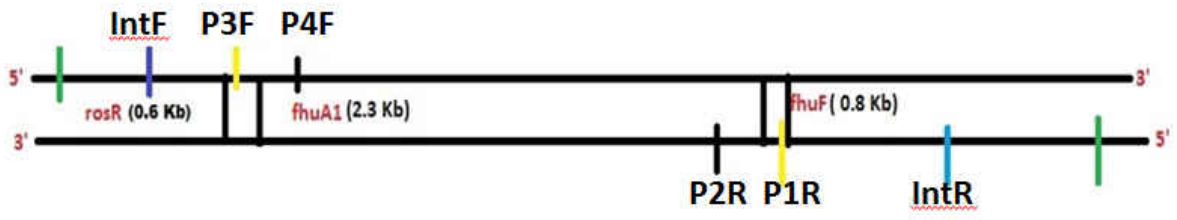

Figure 28: Schematic representation of the primers used for confirming the mutants

The same mutants were used for Colony PCR and sequencing by using another primer set P3F and P1R (Fig. 28 and Fig 29). The mutant colonies showed a band size of 0.5 Kb as the primers used were outside the putative ORF. This indicates that a deletion occurred in the mutants. The WT showed the bigger band size of 3.0 Kb as there had been no deletion in the WT (Fig. 29). The deletion was confirmed via sequencing as well. The sequencing using the same primers also showed an in-frame deletion of the putative *fhuA* (Fig. 30).

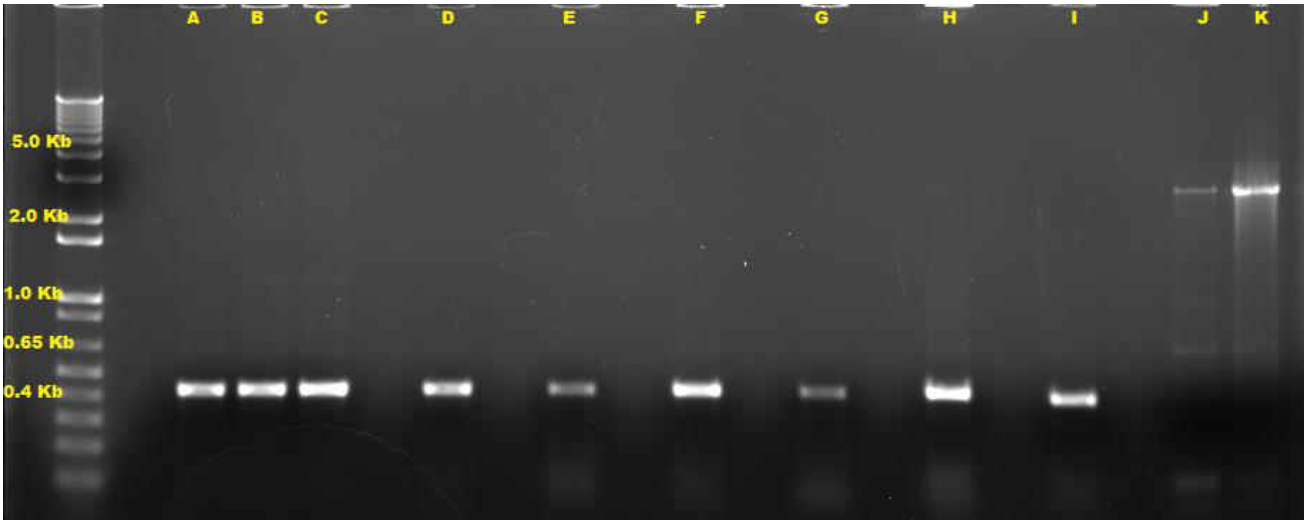

Figure 29: Amplification of the mutants and WT with the primers outside the putative *fhuA* ORF. Lane A to lane I are the mutants that were picked. Lane J and Lane K are the WT chromosomal DNA and colony, respectively.

Figure 30: Alignment of the sequenced data from the mutants. The primers used were P3F and P1R, outside the putative *fhuA* operon. The deletion is observed to be in frame and is supported by the flanking regions. Query is the sequence obtained from the RLΔFhuA and subject is the sequence of the flanking regions of putative *fhuA*.

Possibility of a Duplicate *fhuA* Like Gene

Genomic DNA from RLΔFhuA and isolated colonies was used as a template for PCR amplification using primers within the ORF (Fig. 28) of the putative *fhuA* (Fig. 31). This is the part that has been deleted. These were the same primers used for sequencing of the putative *fhuA* (P4F/P2R). The primers amplified the chromosomal DNA showing the exact band size as the wild-type (Fig. 31).

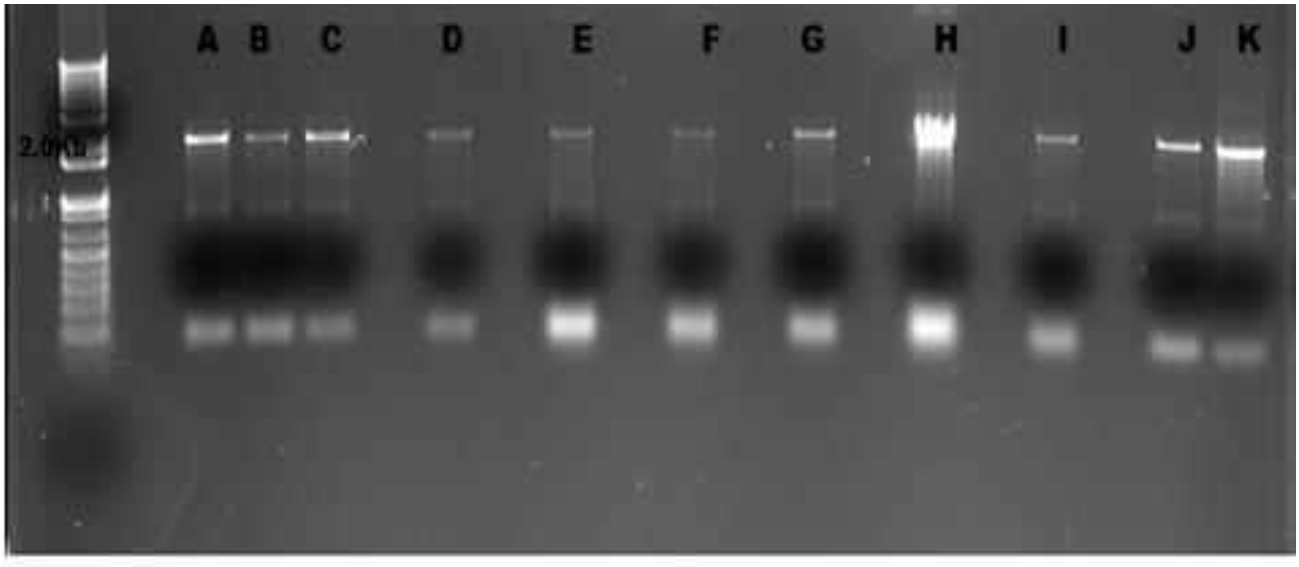

Figure 31: Amplification in RLΔFhuA using the gene specific primers. Lane A to Lane I: RLΔFhuA mutants created via SOEing. Lane J to Lane K: wild type. All mutants and WT still showed the presence of *fhuA* gene.

The deletion mutants were not expected to have shown this amplification as the putative *fhuA* gene was deleted and confirmed with sequencing data. The deletion was confirmed by sequencing the region of deletion using primers outside the putative *fhuA*. However, the result of the colony PCR of the mutants using inner primers indicates the possibility of another *fhuA* like gene in the chromosome. The amplified fragment from the figure above was sequenced, and the sequence was more than 97% similar to the nucleotide sequence of the putative *fhuA* that was sequenced in this work (Fig. 32). However, the presence of gaps in the ORF was high and random. This possibly points out a fact on this gene being a pseudogene as the ORF was not continuous. This might also be possible because of impure DNA sample or other sequencing errors. Also, Sanger sequencing tends to give some random results towards the end of the sequencing in a longer sequencing data. Further experiments are required to solve/ diagnose this problem.

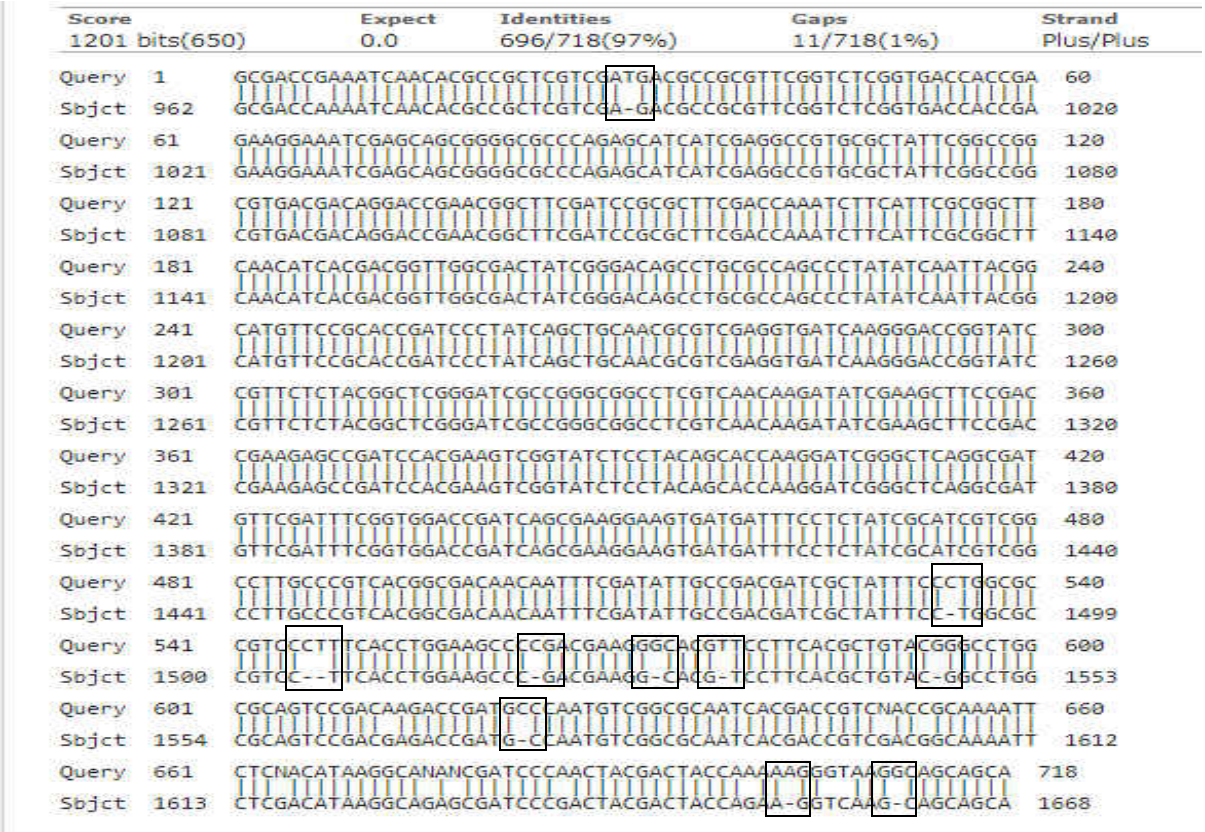

Figure 32: Sequencing of possible second *fhuA*. Amplification was done using the in frame primers P4F/P2R. The alignment with the deleted putative *fhuA (fhuA1)* shows the sequence identity of 97% along with some mismatch. This suggests there is a homolog present in the bacterial chromosome and very similar to the putative *fhuA1*. The gaps are shown in boxes. Also, the random gaps and discontinuity might as well indicate that this ORF is a pseudogene or perhaps there was a sequencing error.

Study of the *fhuA* Mutants

Effect of Iron on the Growth of *fhuA*⁻ *R. leguminosarum ATCC*

The putative *fhuA* mutants were not affected by the amount of iron present in the media. The media used was minimal media MMW. The mutants grew similar to wild-type. This suggested that iron acquisition was not affected in the mutants and the organism grew normally

(Fig. 33). Mutant 9 showed less growth after 72 hours and 96 hours as compared to others. The experiment was repeated to check if Mut9 showed less growth and again it did not.

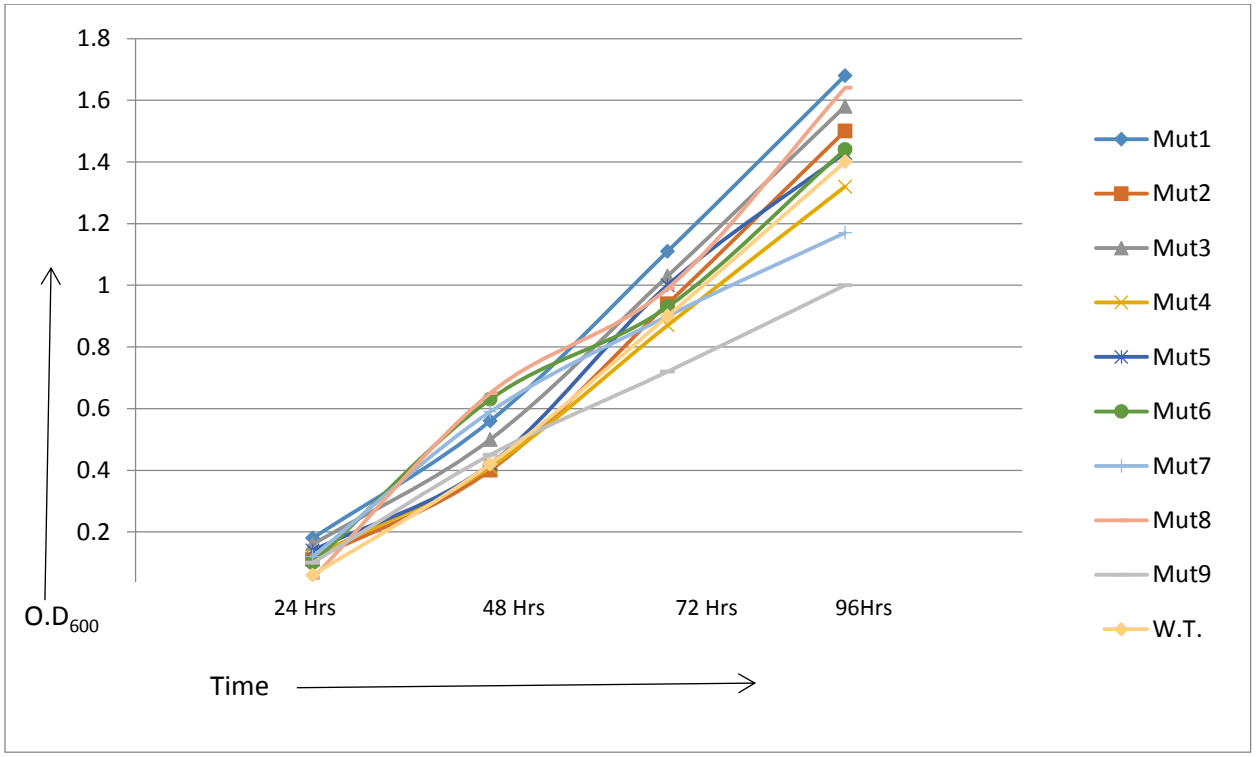

Figure 33: Growth of mutants and wild type in low iron media. The mutants were growing the same as the wild type. This shows that the iron transport has not been affected in the mutants.

Vicibactin Synthesis by the RLΔFhuA Muants

The putative *fhuA* mutants should generally produce more vicibactin if the iron transport has been affected. As described earlier, iron regulation and uptake in *R. leguminosarum* is controlled by the transcriptional regulatory protein RirA that is controlled by iron concentration (Rudolph et al. 2006). The iron transport mutants should be vicibactin overproducers. An Atkin's assay was performed to calculate and observe the amount of vicibactin being produced by mutants and wild-type. The production of vicibactin was found to be similar to wild-type. Thus, the mutants were not found to be overproducers (Fig. 34). This means that the mutants were

easily fulfilling their iron scarcity or iron requirement by some other mechanism. The deletion in the putative *fhuA* did not affect the iron transport and hence the growth of the mutant was similar to WT.

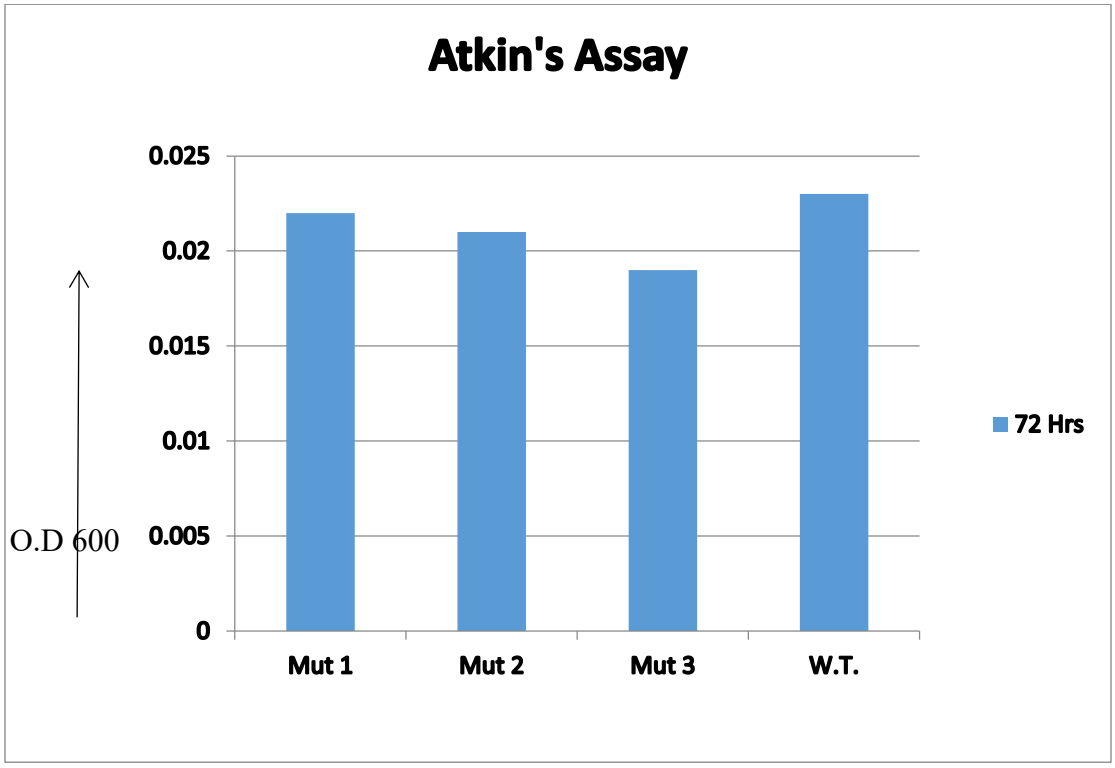

Figure 34: Atkin's assay for vicibactin produced by mutants and the WT. The effect of the deletion in *fhuA* was not observed in the mutants, thus, no vicibactin overproduction was recorded.

Analysis of Outer Membrane Proteins From the Mutants

SDS-PAGE was carried out to determine if some proteins are missing in the mutants when compared to the WT. If the protein coding ORF has been deleted, there should have been no band in a range of 82 kDa which should be just present in the WT. The polyacrylamide gel (Fig. 35) however, shows that no such band is absent in the mutants. Both whole cells and OM fragments were loaded to check this. The cells were harvested from MMW broth after 48 hours and 96 hours. The amount of whole cells were measured via spectrophotometer and the cells

were diluted accordingly before loading in the polyacrylamide gel. The amount of cells used for OM fragments are equal.

In Fig. 35A, Lanes M1 to M9 are mutants while WT is a wild-type. Lanes were loaded with whole cells from 48 hours (M1to M9). Last 3 lanes ; M1 to M3 are whole cells from 96 hours. There are no missing protein bands in mutants which are present only in WT. In Fig. 35B, Lanes M4 to M9 are whole cells from 96 hours and WT is wild type. Last 6 lanes are outer membrane fragments from the WT and mutants (M1 to M5).

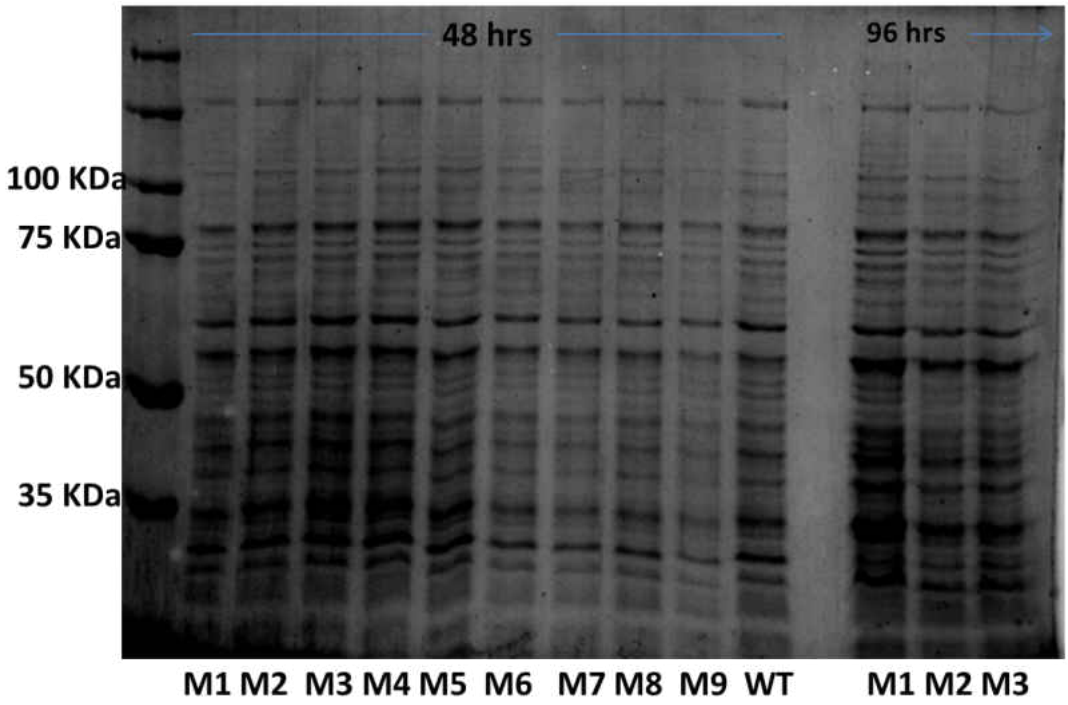

Figure 35A: SDS-PAGE of whole cells

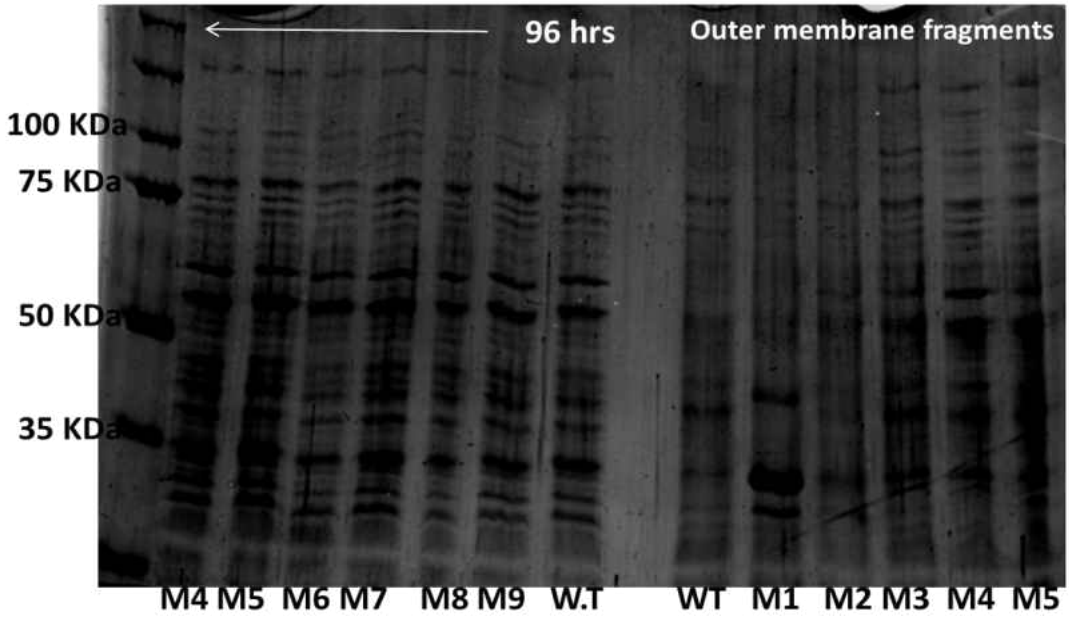

Figure 35B: SDS-PAGE of whole cells and outer membrane fragments

Figure 35: SDS-PAGE of whole cells and outer membrane fragments of mutants and WT. They were harvested in different growth phases. The comparison of a band ranging 82kDa was done with the WT and the mutant. The calculated mol. wt. of the putative FhuA was 82 kDa. There was no such protein present in WT and absent in the mutant.

Vicibactin Isolation and Purification for Transport Assays

Vicibactin Purification Using Amberlite XAD-2 and Sephadex-LH20 Columns and HPLC

Cosmid pBIO1187 containing *R. leguminosarum* was used for vicibactin production. Vicibactin was purified using multiple chromatographic columns. In all chromatographic methods, methanol was used for elution of vicibactin from the columns. The 2nd and 3rd fractions eluted highly concentrated vicibactin from Amberlite XAD-2 column (Fig. 36). The presence of vicibactin in the fractions was determined by CAS and Atkin's assay as described in methods section (Fig. 36, Fig. 37 and Table 10, respectively). The change in color in CAS plates from blue to orange shows the presence of sideophore in the loaded sample (Fig.36). The changes in color of Atkin's reagent shows that a hydroxamate type siderophore is present in the sample (Fig. 37) (Atkin et al. 1970). Table 10 shows the optical density of the Atkin's reagent for the fractions from Amberlite XAD-2 column and shows similar result to the CAS assay showing elution of siderophore in fractions 2nd and 3rd. These fractions with the siderophore were combined, lyophilized and then concentrated as described in methods section. The concentrated sample was loaded on to LH-20 column. Methanol was used for elution of vicibatin. Vicibactin was eluted in fractions 9-13. It was confirmed via CAS and Atkin's assay as described. These fractions were further concentrated using Buchi R-200 rotavapor. The concentrated fractions were suspended in a small volume of methanol until dissolved and was syringe filtered to remove the bigger particles if present.

The filtered vicibactin samples were loaded on HPLC. Approx. 0.5 ml sample was loaded during each run. The peaks were observed in HPLC at fractions 4-7, 14-18, 19-23 and 34. However, the Atkin's assay showed the presence of vicibactin in fractions 6-7, 15-19, 20-22 only. All these fractions showed wine color in Atkin's assay. The peak at 34th fraction was

obtained at elution in 100% methanol, which didn't show any reaction with Atkin's. All other peaks were obtained at elution with 48% methanol. The highest O.D and the strongest wine color was seen in fractions 6, 7 fractions 16, 17, 18 and fraction 21. These early elutions in fractions 6^{th} and 7^{th} might either be some unbound vicibactin or some other molecules that are being eluted. The detection of degraded vicibactin products A and B have been reported previously (Wright et al. 2012) in 16^{th} to 21^{st} fractions (Fig. 38) along with the intact cyclic vicibactin known as vicibactin C. All these samples were furthure purified using HPLC and were saved carefully at -20°C for future use (Fig. 38).

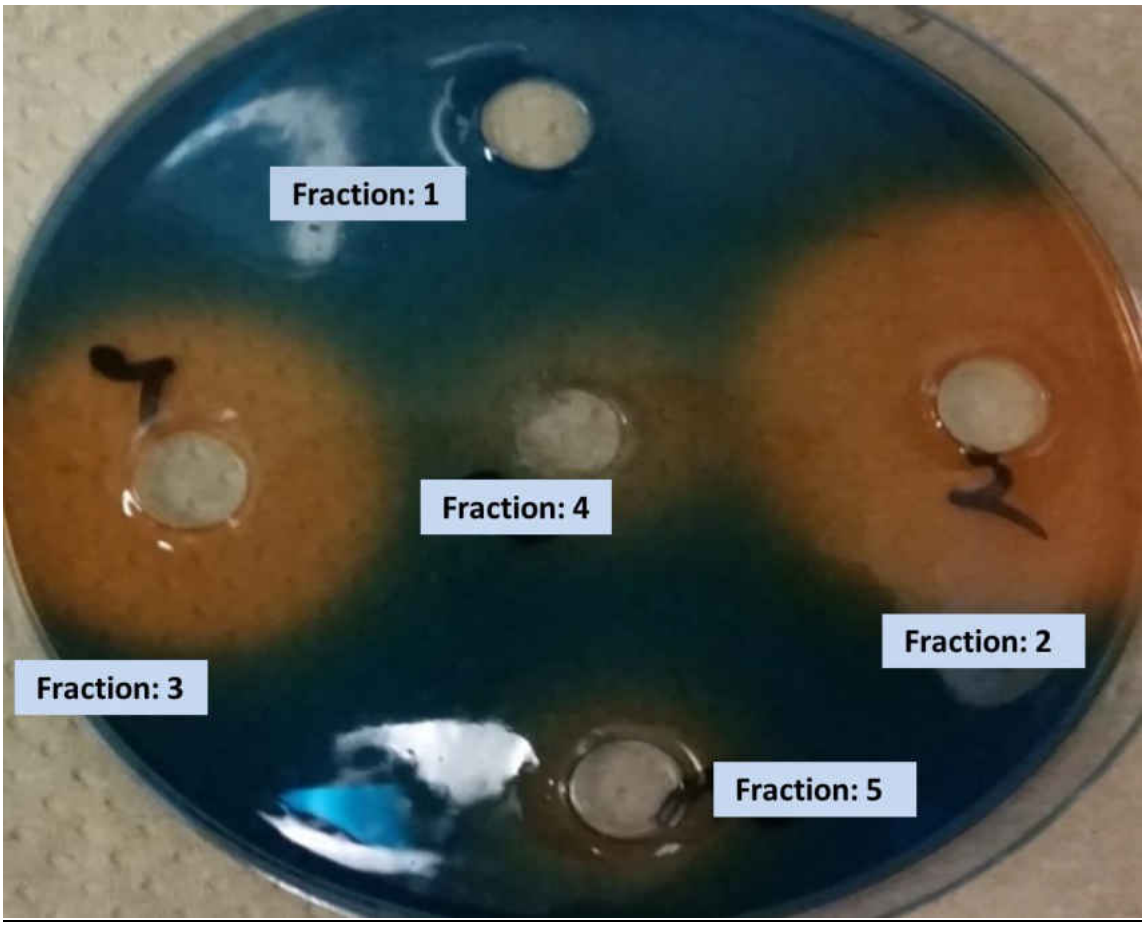

Figure 36: CAS assay for Amberlite XAD-2 fractions. Fractions 2^{nd} and 3^{rd} are showing lot of vicibactin. The elution of vicibactin occurred as soon as methanol was introduced in the column eluting the hydrophobic molecule in the early fractions.

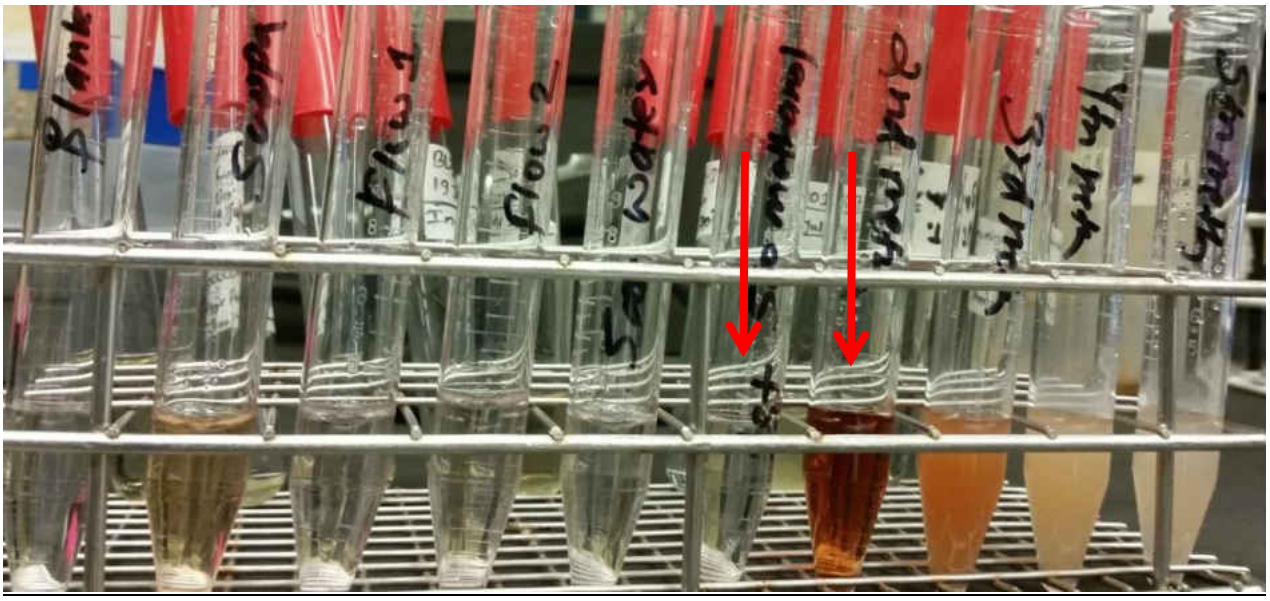

Figure 37: Atkin's assay for Amberlite XAD-2 fractions. The fractions (2^{nd} and 3^{rd}) in red arrow are showing the wine red color after the elution and were taken for further purification.

Table 10: Atkin's assay for XAD-2 fractions. The high O.D 2^{nd} and 3^{rd} fraction with the wine red color confirms the presence of vicibactin in these fractions. The calculated concentration of vicibactin for 2^{nd} fraction was 0.00145 moles/litre.

Samples	O.D at 450nm	Concentration of vicibactin (moles/liter)
Supernatant	0.223	1.47×10^{-4}
Flowthrough1	0.047	0.31×10^{-4}
Flowthrough2	0.052	0.34×10^{-4}
500ml H_2O	0.037	0.24×10^{-4}
1st fraction	0.026	0.17×10^{-4}
2nd fraction	2.198	14.5×10^{-4}
3rd fraction	2.593	17.1×10^{-4}
4th fraction	2.102	13.92×10^{-4}
5th fraction	1.65	10.92×10^{-4}

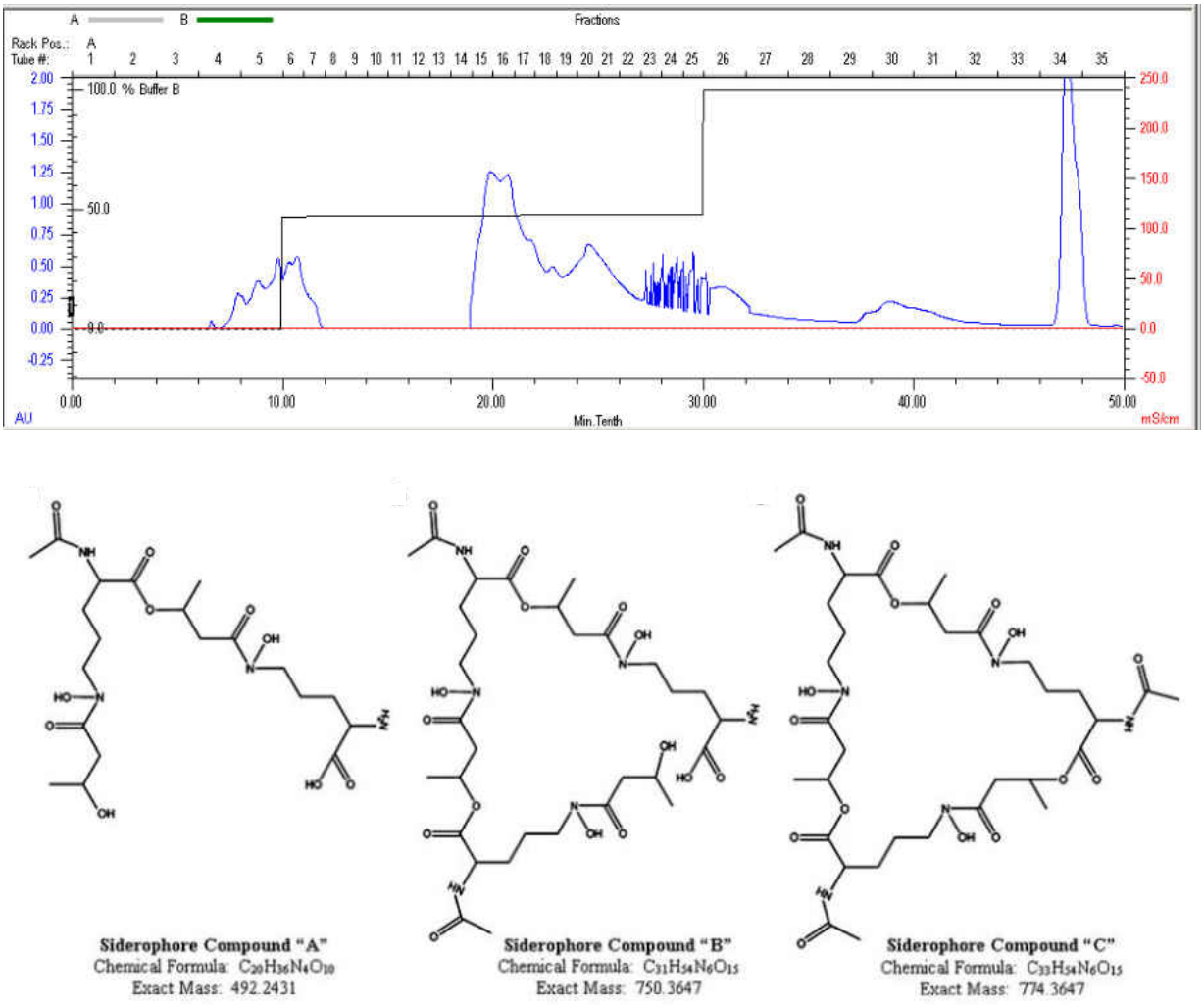

Figure 38: HPLC to purify vicibactin and three different vicibactin products. The undegraded vicibactin is siderophore C. Others, siderophore A and siderophore B, are degraded products of vicibactin (Wright et al. 2013). Fractions 16 to 21 eluted all three products of vicibactin.

Use of Other Iron Sources

Growth of *R. leguminosarum* ATCC with Hemin and Hemoglobin as Iron Source

As described before, to determine if *R. leguminosarum* ATCC can utilize various other sources of iron, *R. leguminosarum* ATCC was grown in MMW minimal media and growth was measured in different concentrations of hemin and hemoglobin (Fig. 39 and Fig. 40). As stated,

hemin and hemoglobin were used because of their similarity with leghemoglobin. A significant difference in growth was only observed in the minimal media supplemented with different concentrations of hemoglobin (Fig. 39). Increasing concentrations of hemin did not significantly affect the growth of the bacteria (Fig. 40). The growth of the bacteria was affected by the increasing hemoglobin concentration. The hemoglobin concentration higher than 1 µM did not show a lot of effect in the growth of the bacteria at 48 hrs. However, hemoglobin concentrations from 0.025 µM to 1 µM showed a significant effect in bacterial growth.

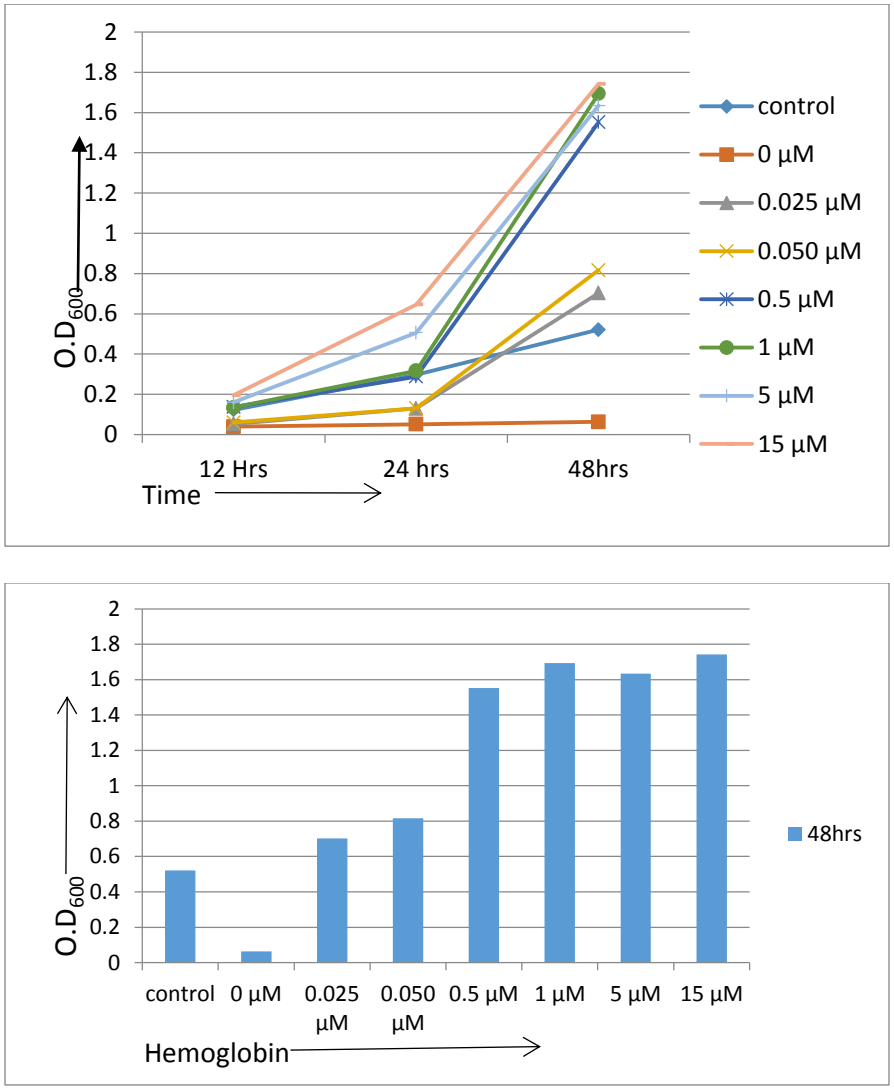

Figure 39: Growth of *R. leguminosarum* ATCC in different concentration of hemoglobin in MMW. The growth shows that the hemoglobin can be utilized as a sole source of iron by *R. leguminosarum* ATCC.

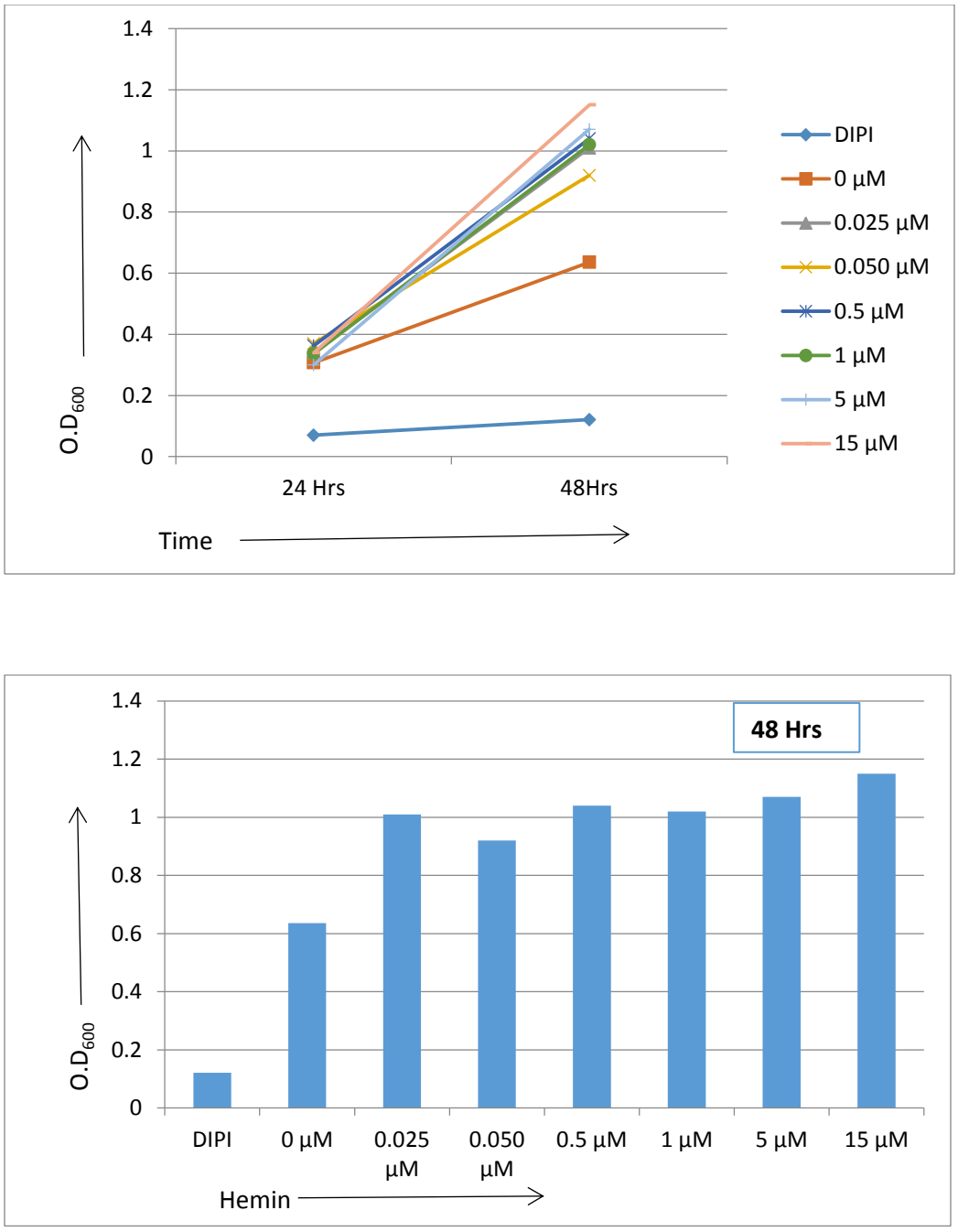

Figure 40: The growth of *R. leguminosarum* ATCC in different concentrations of hemin in minimal media MMW. The growth of the bacteria was not significantly changed by the increasing concentrations of hemin

Proteins Responsible for Hemin/Hemoglobin Uptake

It was our interest to determine the effect of different concentration of hemin and hemoglobin on protein expression. Identification of such heme bound iron transport proteins

were necessary in *R. leguminosarum* ATCC. Therefore, the whole cell extract from cells grown at different hemin/hemoglobin concentrations were used for analyzing protein expression using SDS-PAGE. We observed that many proteins were controlled by different hemin/hemoglobin concentrations. It was interesting to note that some of them were downregulated with the increasing hemoglobin/hemin concentration and some were upregulated (Fig. 41). The ranges of the proteins are from 35 kDa to 100 kDa which are controlled by different hemoglobin concentrations.

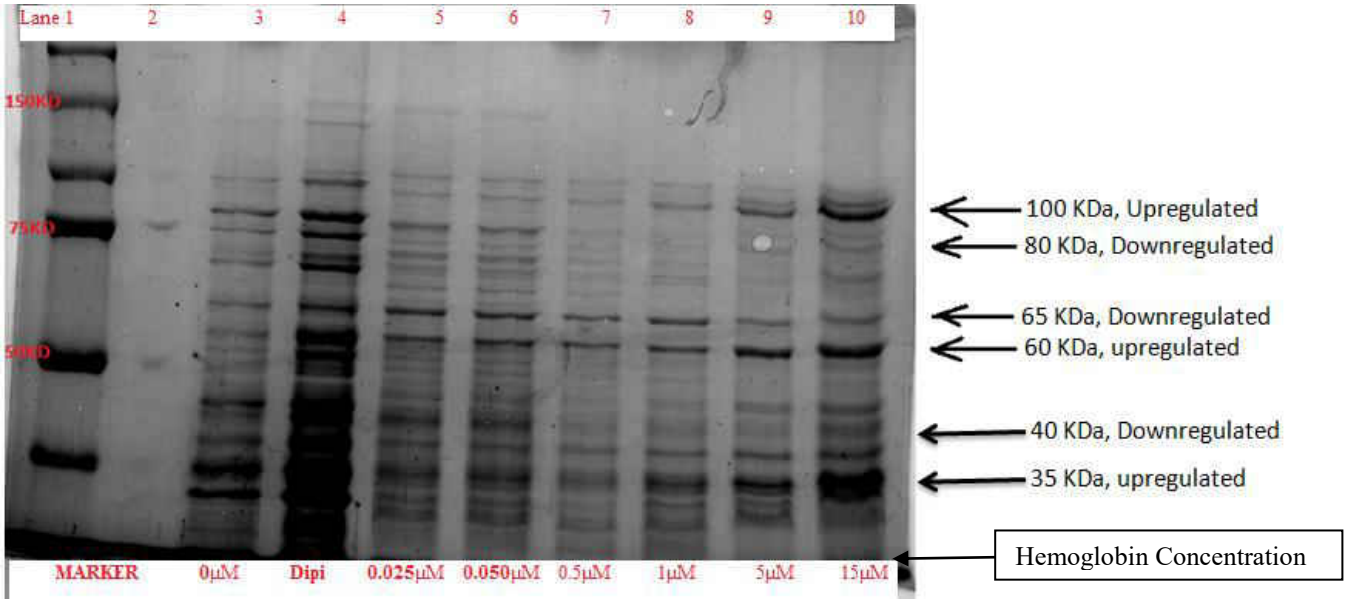

Figure 41: Effect of hemoglobin in protein expression. Some of the proteins were either up-regulated or down-regulated by the different concentration of hemoglobin. This guides to a presence of a possible system for heme-bound iron uptake and the control of expression of the proteins associated with different heme concentration.

Further studies on the effect of hemin as the sole source of iron was suspended due to its insignificant effect on the bacterial growth when compared to the effects of hemoglobin. However, similar to hemoglobin, protein expression was affected by different concentration of hemin in the medium (Fig.42). There were four major proteins downregulated with different

hemin concentration. All of them ranged between 70-90 kDa. These proteins might be involved in hemin bound iron uptake.

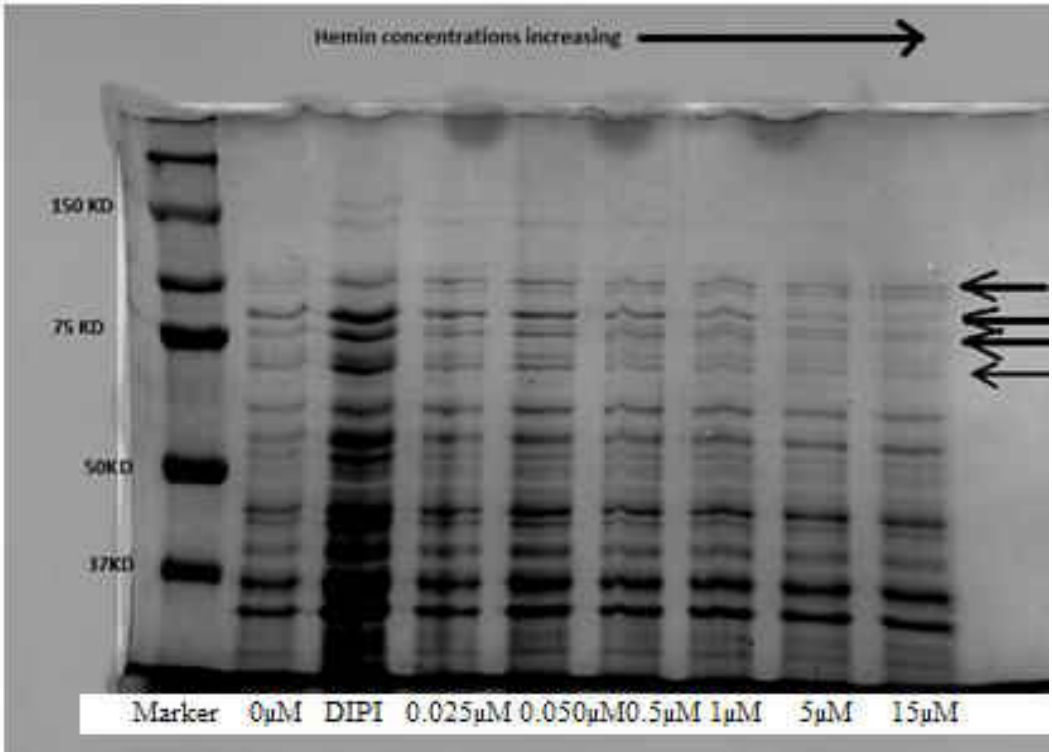

Figure 42: Effect of hemin on the expression of different proteins. Only four proteins were seen to be down-regulated with the increasing hemin concentration is shown by the arrow. These are the proteins most likely to be involved in hemin transport.

Heme-Bound Iron Uptake Putative Genes and the Proteins

hmuPSTUV Operon

Multiple sets of primers were designed based on published sequences of heme uptake genes from *E.coli* and different species of rhizobia (See list of all primers in Table 5). Primers were also designed from different heme uptake genes present in the same species. We identified three genes using PCR with the primers designed from the bacterial strain of *R. leguminosarum viciae* 3841 (Fig.43). These three genes namely *hmuP (hemP), hmuS, hmuT* belonged to the same

operon *hmuPSTUV* from the *R. leguminosarum viciae 3841.* The amplification and identification of putative *hmuU and hmuV* in *R. leguminosarum* ATCC are in progress in our lab.

The outer membrane receptor *hmuR* was also a gene of interest. Heme receptor genes for *E. coli* and *S.melioti* were also used as a template for designing primers. However, *hmuR* was not present in this strain based on the results of PCR amplification. The primers were not able to amplify the possible heme receptor. As stated earlier, different sets of primers for outer membrane heme receptor gene from various other strains were also designed and used for PCR. We were not able to identify any of those mentioned genes which were coding for the outer membrane heme receptor protein (See Table 5 for list of primers and genes). There are chances that these particular genes are absent in *R. leguminosarum* ATCC. However, other techniques could be followed to further look after the unknown outer membrane receptor that transports heme bound iron.

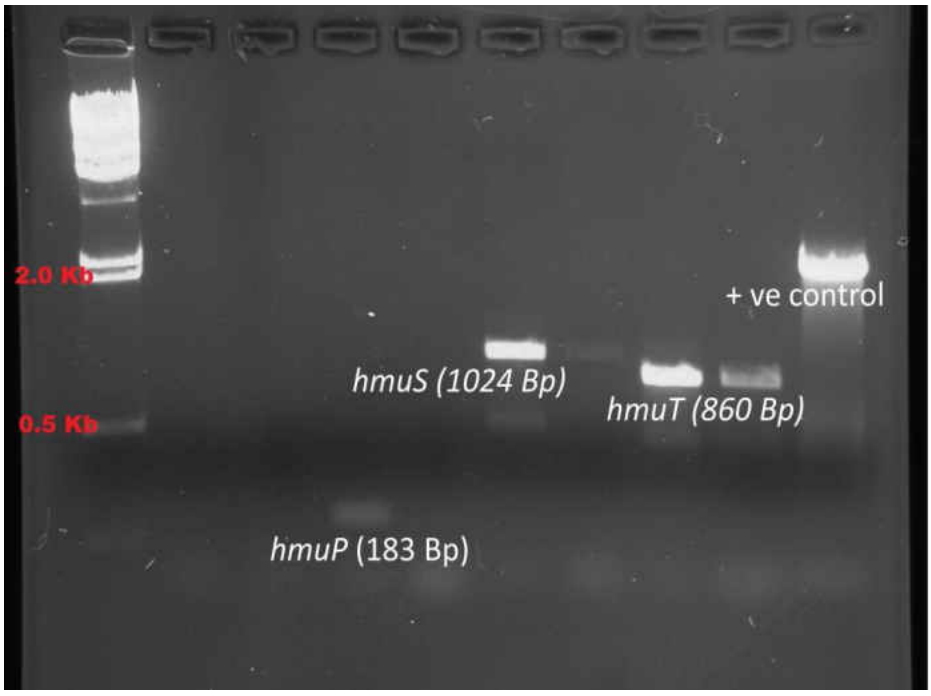

Figure 43: Amplification of heme receptor genes from *hmuPSTUV* operon. The only heme transport genes amplified were from the primers based on *hmuP, hmuS* and *hmuT.* These genes belonged to the operon *hmuPSTUV* from *R. leguminosarum viciae* 3841.

The PCR products which gave amplification from primers based on *hmuP, hmuS* and *hmuT* were sequenced and studied further using *in-silico* analysis tools. The primers used for sequencing are listed in Table 6. The sequenced genes showed more than 98% identity with the published/known gene sequences of different heme uptake genes from different bacteria such as *R. leguminosarum* WSM 2304*, R. leguminosarum* 3841*, R. leguminosarum* WSM 1325*, R. leguminosarum* WSM 1689 and various other strains. The sequencing results are presented in sections below.

HmuP

hmuP is a 183 Bp long gene and is known as heme uptake protein gene and shows sequence similarity to the genes from the various rhizobial strains. It is a TonB dependent heme uptake protein (Wexler et al. 2002). In *Yersinia sp.* there is a similar gene named *hemP* and codes for a small protein of 81 amino acids. When the *hmu* operon was cloned in *E. coli*, a Fur box regulated protein of size 6.5 kDa, HemP, was expressed (Thompson et al. 1999). It is reported/annotated as a heme binding/transport cytoplasmic protein protein (Thompson et al. 1999).

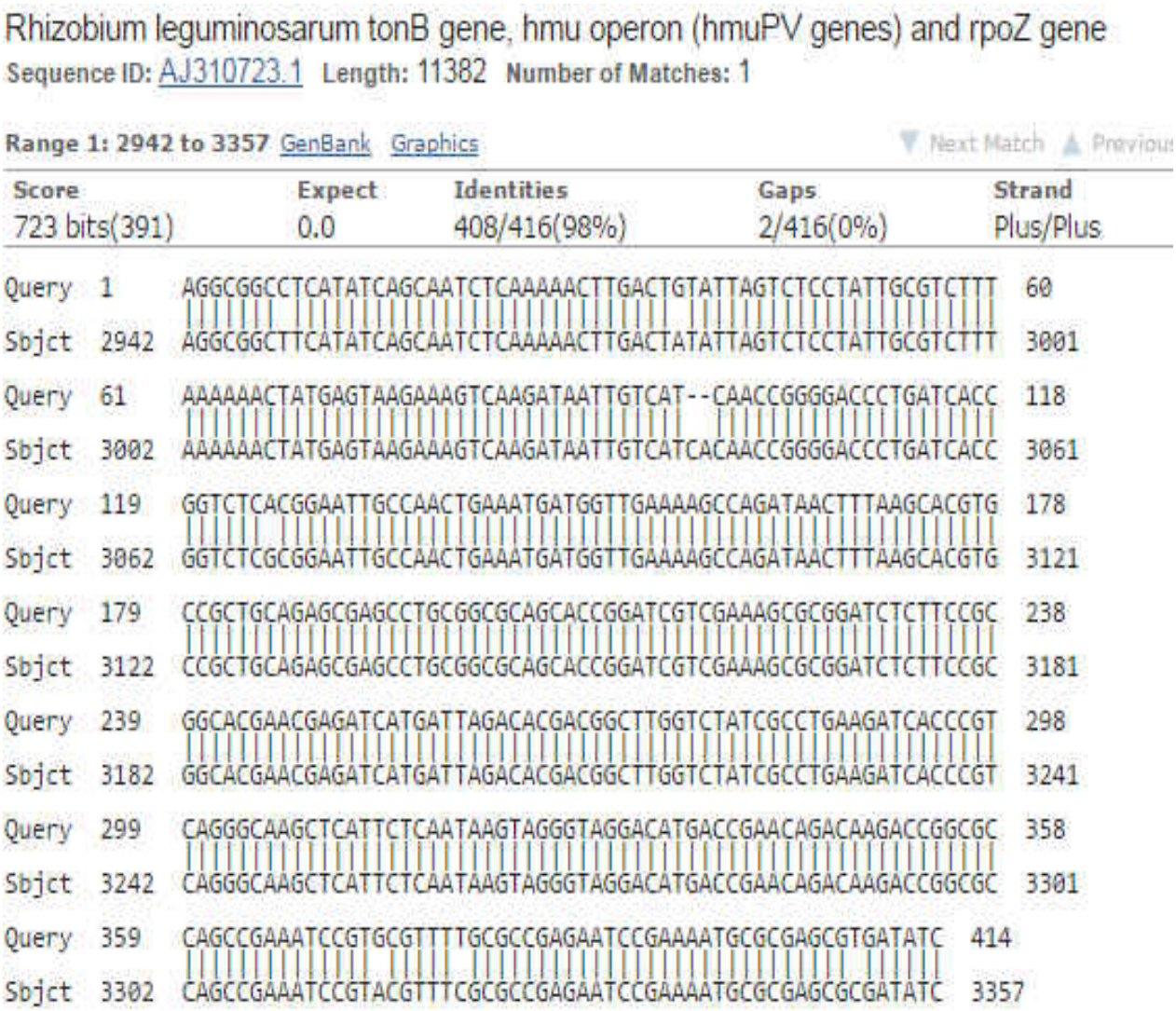

Figure 44: Alignment of putative *hmuP* with the *hmuP* gene of *R. leguminosarum* 3841. The nucleotide identity of 98% was seen when the two sequences were aligned. The query sequence is the putative *hmuP* gene. The ORF which was identical to known sequence of *R. leguminosarum* 3841 was used for further study.

The 3D structure of the putative HmuP protein was generated independently using SWISS-MODEL, and molecular docking was performed by using the SWISS-DOCK online tool. The 3D Structure and docking are shown below in Fig. 45 and Fig. 46. There was no crystal structure in the database for this protein HmuP, hence comparison could not be performed.

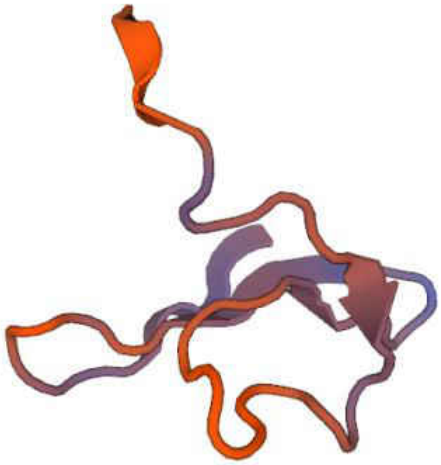

Figure 45: Putative HmuP heme binding/transport protein. The structure was generated independently using SWISS-3D modeling tool which generated a globular protein.

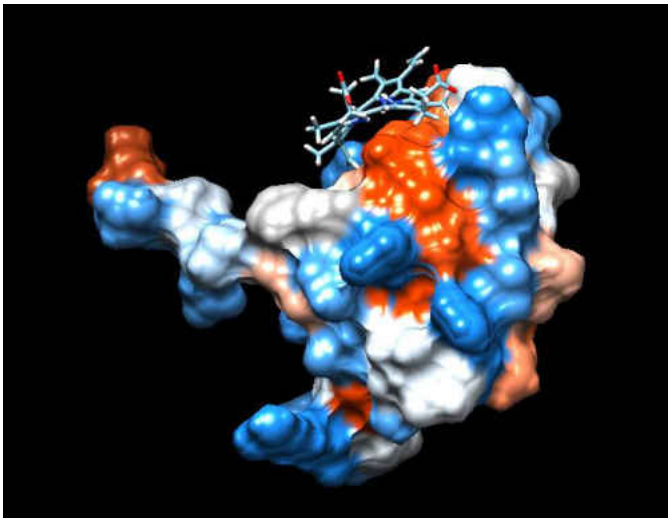

Figure 46: Docking of the heme molecule with putative HmuP. This was done to check if the heme molecule could bind with the putative HmuP. The binding of heme and the putative HmuP occurred in docking analysis showing that this protein could be involved in heme uptake.

HmuS

The gene *hmuS* also amplified as shown in Fig. 43 and was further sequenced. It is a 1024 bp long gene coding a protein of 349 amino acids, with a molecular weight of 39 kDa. It is reported/annotated as a periplasmic heme degradation protein, present in many other bacteria

(Wexler et al. 2002). It is also a TonB dependent protein (Wexler et al. 2002). The sequence alignment showed identity of 99% with more than 10 relative species and also with *R. leguminosarum viciae* 3841 (Fig. 47). A similar protein is also present in *Roseobacter* and *Yersinia* (Thompson et al. 1999; Hogle et al. 2017).

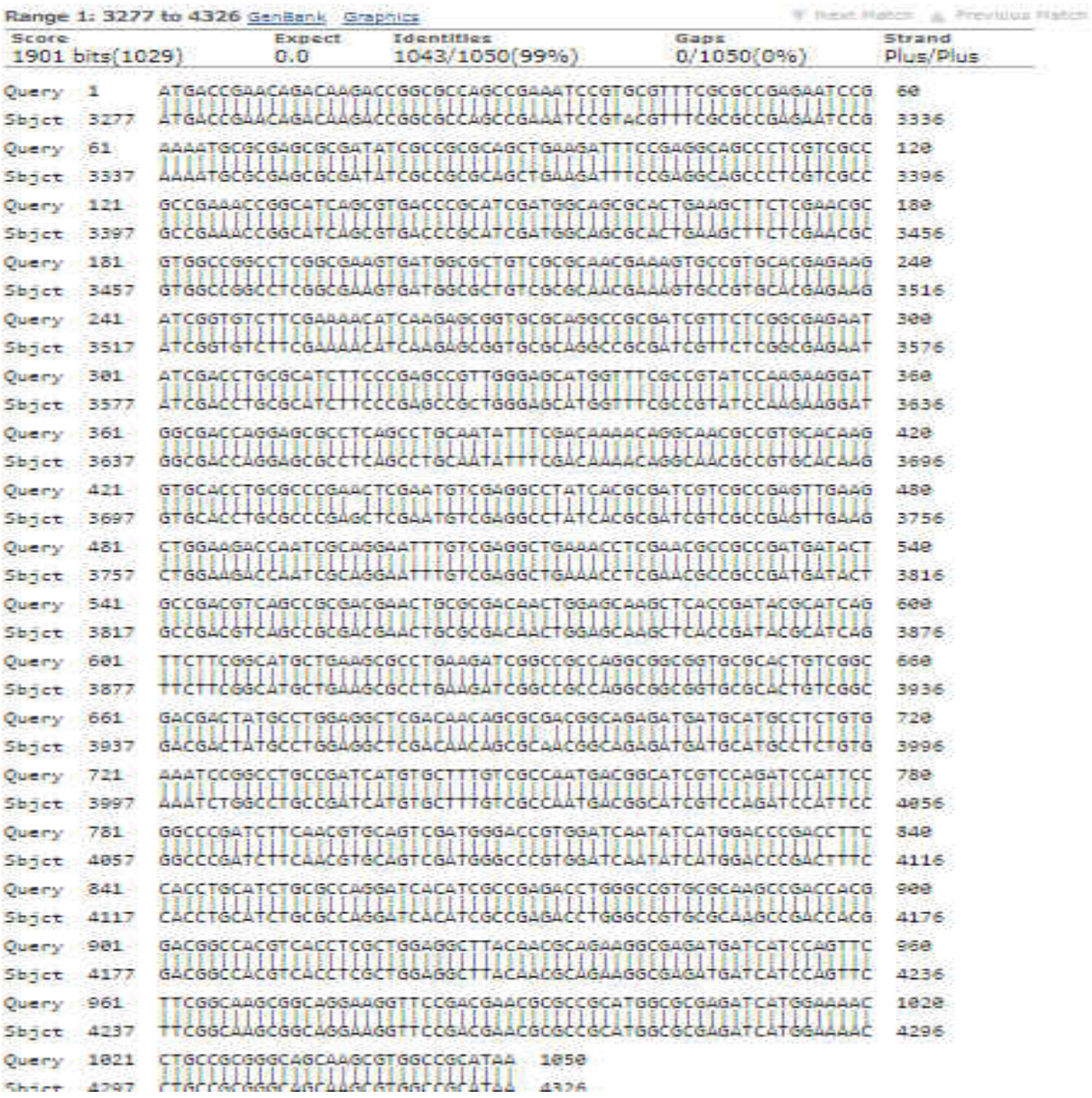

Figure 47: NCBI-Blast of putative *hmuS* with *R. leguminosarum* 3841. It shows 99% identity with the known nucleotide of *hmuS* from *R. leguminosarum viciae* 3841(subject). When the alignment was observed, the sequence identical to the known ORF was used for further analysis.

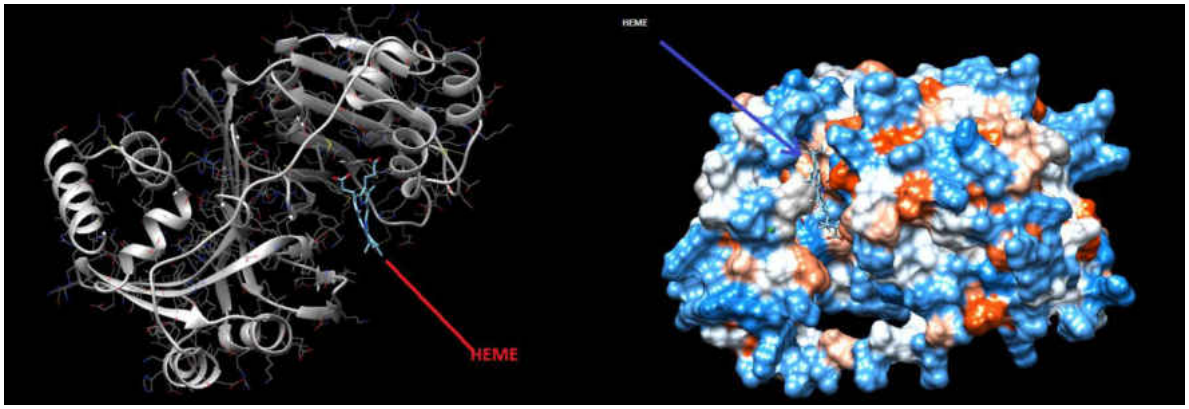

Figure 48: Putative HmuS from *R. leguminosarum* ATCC and its docking with heme. The docking showed that the heme molecule binds with the putative protein. This suggests that the putative protein is more likely to be involved in heme transport.

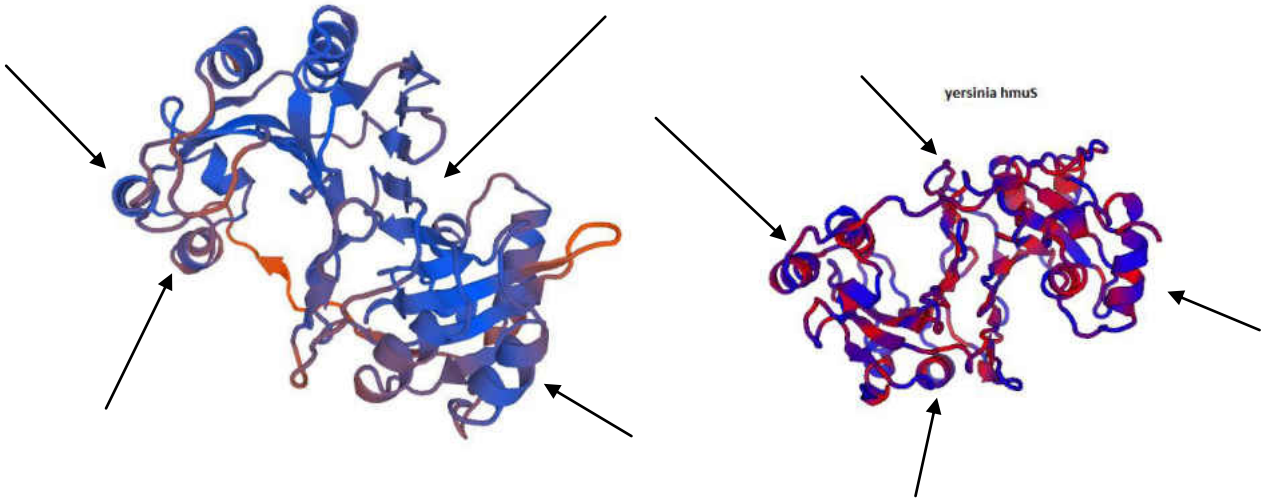

Figure 49: Putative HmuS from *R. leguminosarum* ATCC and crystal structure of HmuS from *Yersinia sp.* The arrows point out some of the many differences and similarities between these two proteins.

The arrows point out some of the similarities and dissimilarities between these two independently generated structures (Fig. 49). The α-helices look similar to each other and are present in the same number. However, the pocket in the putative protein seems to be in opposite orientation in *Yersinia.* The study of similarities is very interesting because *Yersinia* is a pathogenic strain and *R. leguminosarum* ATCC is not (Fig.49).

HmuT

This is a 930 bp long gene and codes for protein of length of 310 amino acids which is known as hemin ABC transporter substrate binding protein (Wexler et al. 2002). The putative gene from *R. leguminosarum* ATCC shows sequence similarity with the heme uptake gene of another rhizobial strain (Wexler et al. 2002) (Fig. 50). It is also a TonB dependent heme uptake protein (Wexler et al. 2002). In *Cornybacterium glutamicum* there is a similar gene named *hmuT* and codes for a HmuT transport protein (Muraki et. al 2015). However, nucleotide BLAST analysis showed there was no sequence similarity between these two genes. The nucleotide sequence was 96% identical (Fig. 50) with *hmuT* from *R. leguminosarum* 3841 (Wexler et al. 2002).

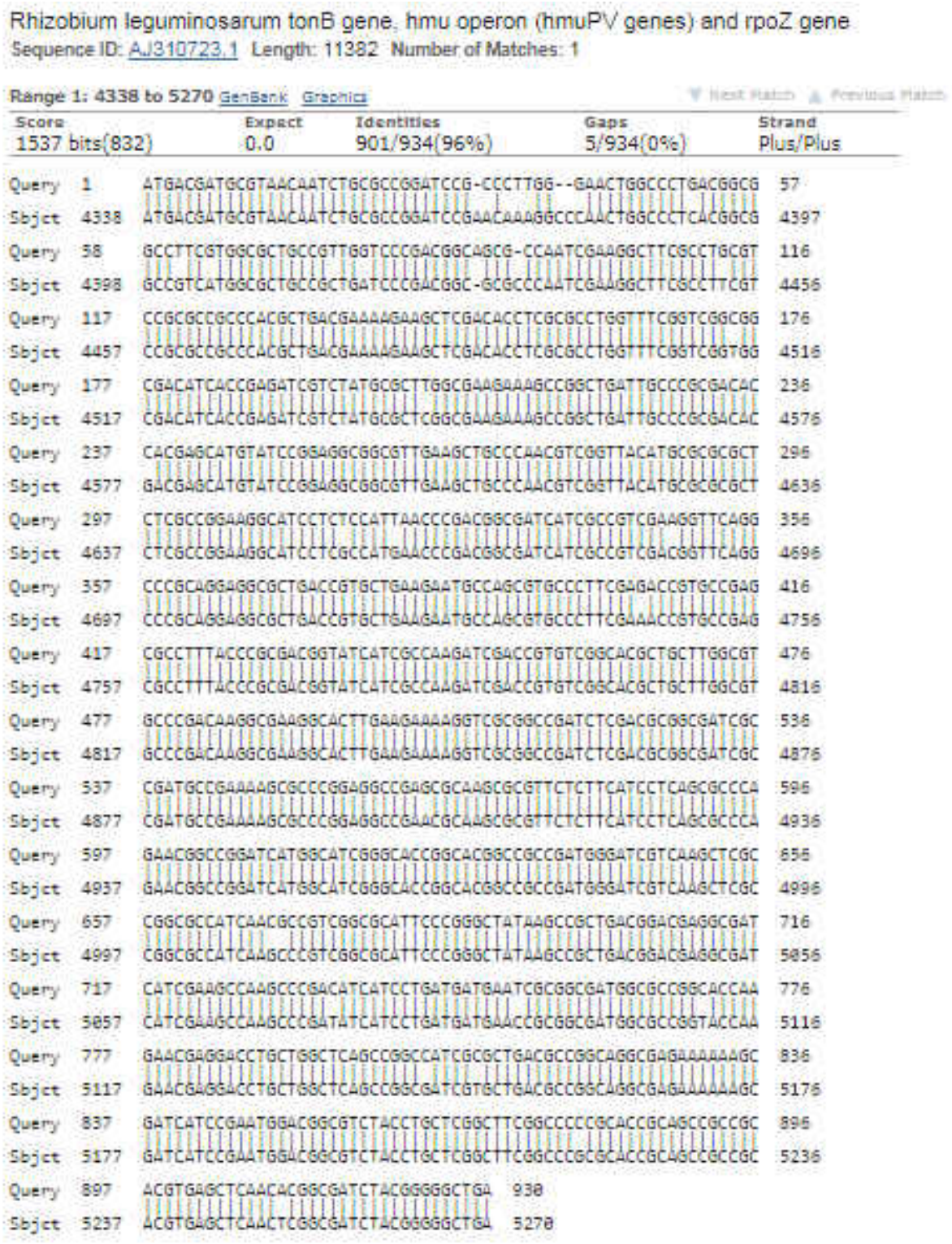

Figure 50: Putative *hmuT* alignment. It was present in the same operon of TonB dependent heme transport genes from *R. leguminosarum* 3841. The query is the putative gene sequence and the subject is the gene from *R. leguminosarum* 3841. The putative ORF was 96% identical with the known gene sequence.

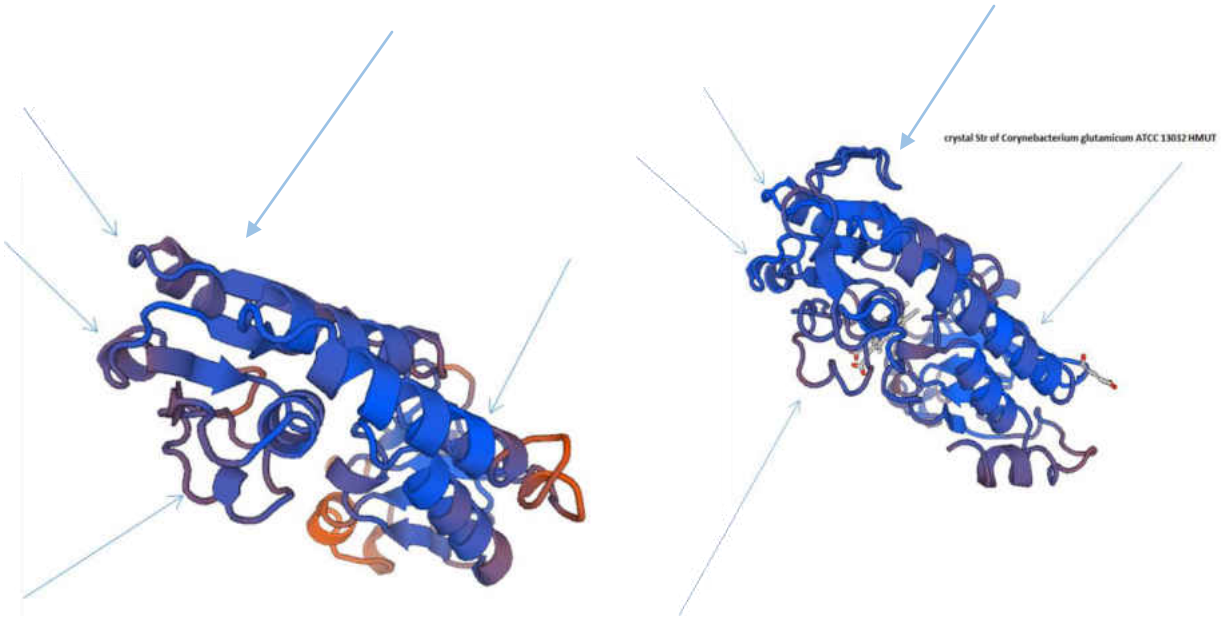

Figure 51: Putative *hmuT* from *R.leguminosarum* ATCC and *hmuT* from *C. glutamicum.* Some of many similarities and differences are shown using the arrows.

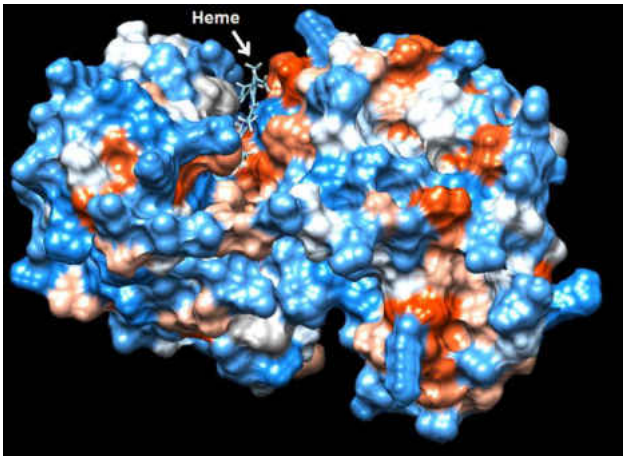

Figure 52: Molecular docking of heme with putative HmuT protein. This docking indicates the possible involvement of the HmuT protein in heme uptake.

The no. of α-helices are shown using arrows (Fig. 51). The no. of loops is also similar between the independently generated structure of pathogenic and non-pathogenic bacteria (Fig. 51). One of the differences to notice is a loop that is present in the *C. glutamicum,* HmuT, but is absent in the putative protein HmuT. This comparison pointed out the evolutionary aspect of non-pathogenic bacteria and pathogenic bacteria and showed how closely the proteins are related.

TonB Dependent Heme Uptake

The TonB Dependent Operon *hmuPSTUV*

The sequence data we obtained matched with a TonB dependent operon *hmuPSTUV* for hemoglobin/heme transport from *R. leguminosarum viciae* (Fig. 52) (Wexler et al. 2002).

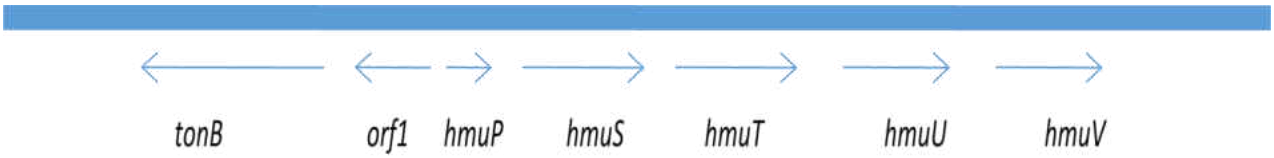

Figure 53: Graphical representation of *hmuPSTUV* operon

The *tonB* mutant strain (Hill 2014) was used for hemoglobin uptake assay to determine if the hemoglobin transport in *R. leguminosarum* ATCC is TonB dependent. Fig. 54 below shows that the mutant was unable to uptake hemoglobin during first 24 hours. This suggests that the hemoglobin uptake is dependent of TonB, energy transducing protein and requires energy. The difference in hemoglobin concentration showed difference in growth of WT as mentioned previously (Fig. 39). Despite the different hemoglobin concentration no difference in growth was seen in the TonB mutant after 48 hrs (Fig. 55).

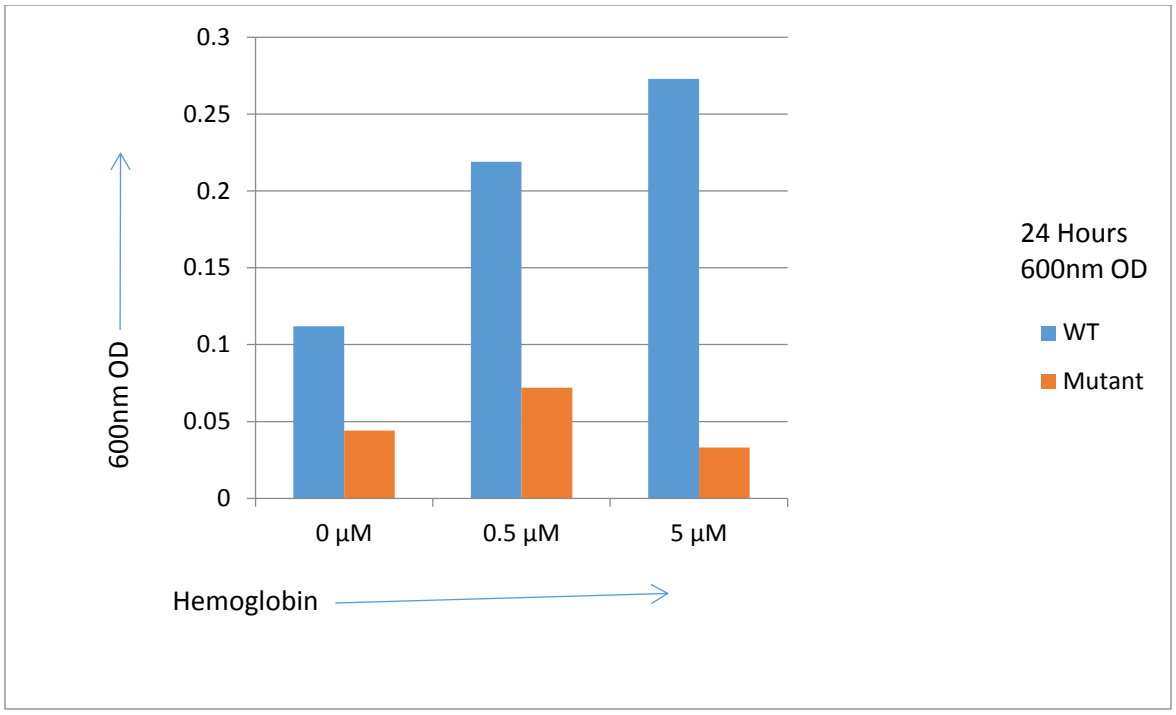

Figure 54: RLΔTonB and WT *R. leguminosarum* ATCC in hemoglobin transport in 24 hrs. The defect in growth was observed for first 24 hrs.

However, after 48 hours the mutant was able to regain its growth. The growth was not exactly the same as the wild-type but was growing well at 48 hrs in the presence of hemoglobin as the only source of iron. This phenomenon (Fig. 55) was earlier reported in *R. leguminosarum* 3841, stating that the *hmuPSTUV* mutants grew very similar to the WT after a few days (Wexler et al. 2002). We used *tonB* specific primers from *R. leguminosarum 3841* and performed PCR. We were unable to identify a *tonB* gene upstream of *hmuPSTUV* operon in *R. leguminosarum* ATCC as confirmed in *R. leguminosarum* 3841.

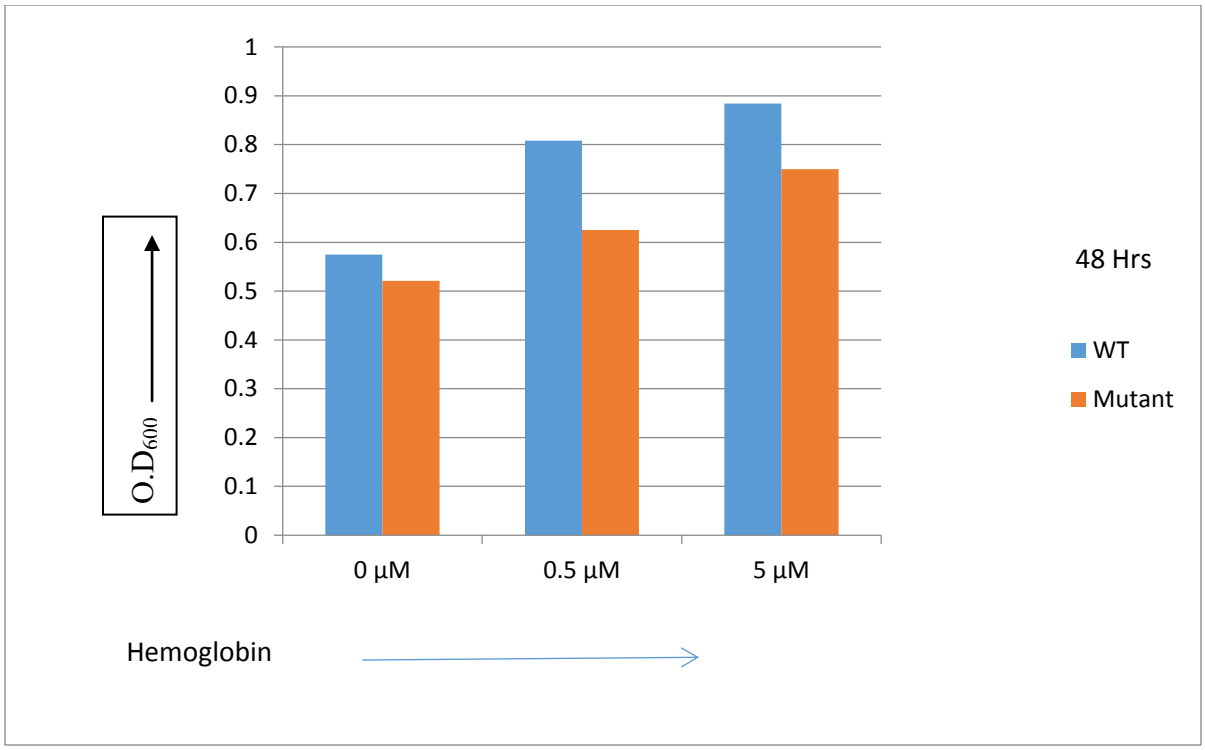

Figure 55: RLΔTonB and WT *R. leguminosarum* ATCC in hemoglobin transport in 48 hrs. The growth in 48 hrs was very well when compared to WT.

Role of RLΔExbB-ExbD in Transport of Hemoglobin

The ExbB-ExbD mutant was also tested for its ability to use hemoglobin as a sole source of iron. The ExbBD protein is a TonB associated energy transducing protein (Barisic 2015). The ExbBD mutants showed similar results to the TonB mutant and were unable to grow properly for the first 24 hours (Fig. 56). However, showing similarity to the TonB mutants, they were able to regain their growth after 48 hours (Fig. 57). Both TonB and ExbBD mutants were growing very similar to the WT after 96 hours (Fig. 58).

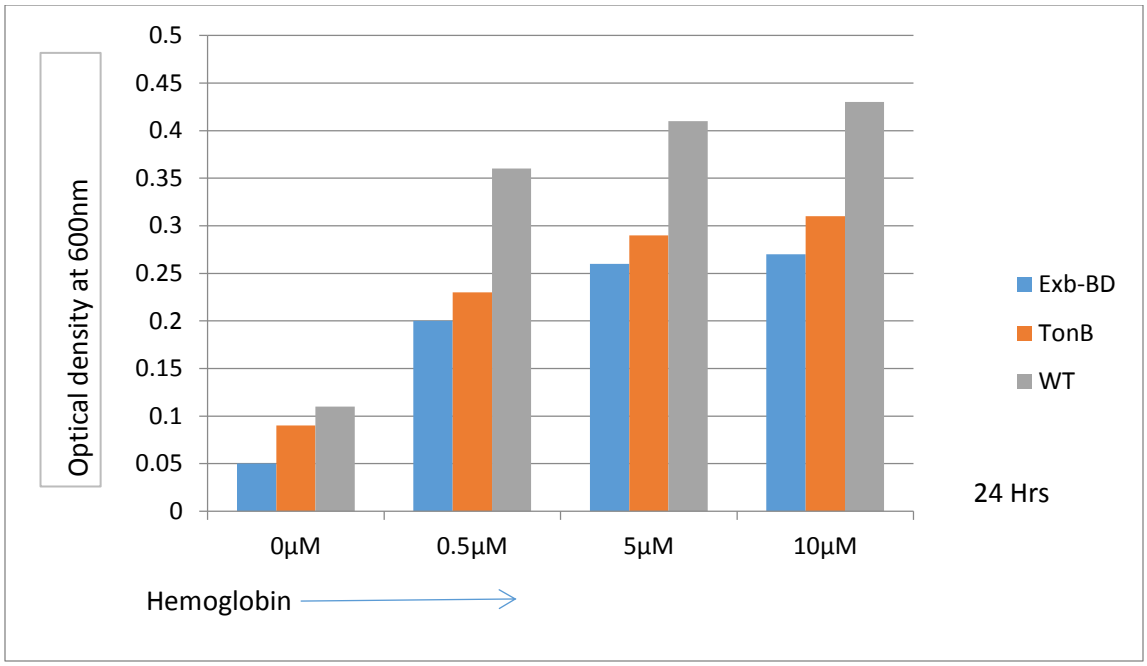

Figure 56: RLΔExbBD and RLΔTonB growth with hemoglobin as iron source in 24 hrs. WT is growing very well in different hemoglobin concentration. The mutants are not able to grow as well as WT.

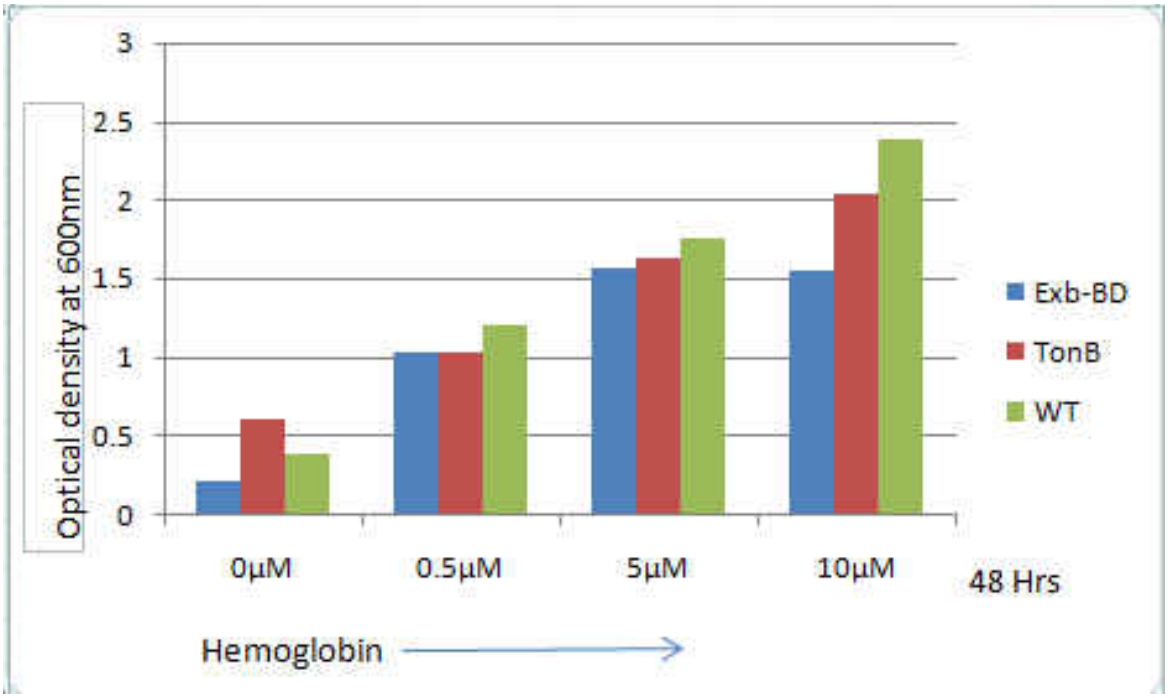

Figure 57: RLΔExbBD and RLΔTonB growth with hemoglobin as iron source it 48 hrs

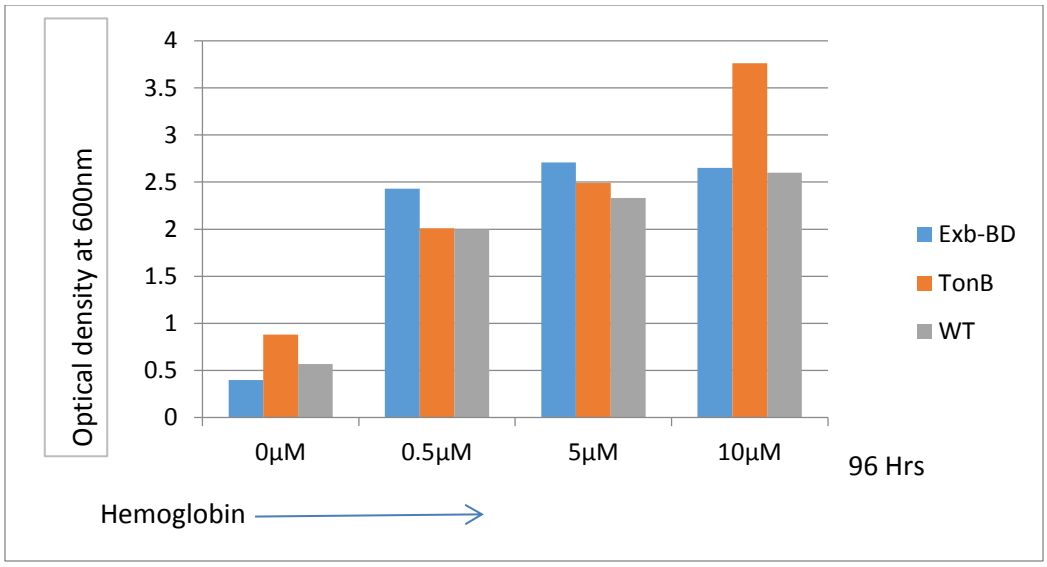

Figure 58: RLΔExbBD and RLΔTonB growth in 96 hrs with hemoglobin as iron source

Hemophores

To determine if this strain can produce hemophores, we used the supernatant and performed a 10% SDS-PAGE gel and observed the change in protein expression (Fig. 59). There was no such notable change in expression in protein size ranging 18-30 kDa. The size of hemophore ranges from 18 kDa to 30 kDa depending on its type (Tong and Guo 2009).

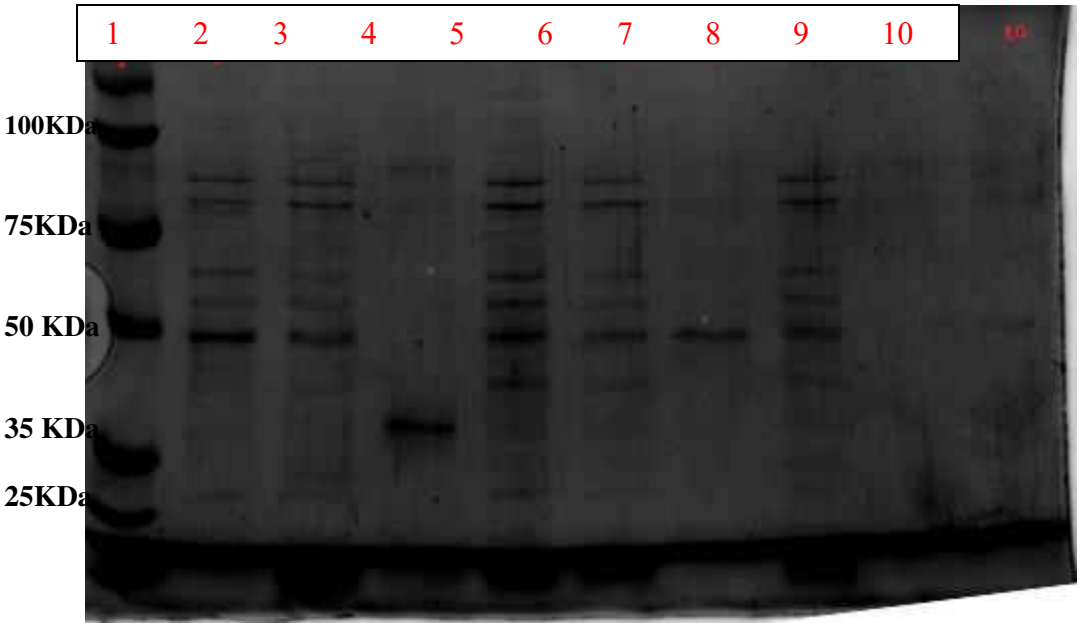

Figure 59: Absence of hemophores in heme utilization. The SDS page gel was 10% SDS gel and the supernatant was loaded to see if hemophore can be detected. Lane 1 is the ladder, Lane 2 contains supernatant from the cells grown at 2.5µM $FeSO_4$ (No hemoglobin), Lane 3; 15 µM hemoglobin, Lane4; 5µM hemoglobin, Lane5; 1µM hemoglobin, Lane6;0.5µM hemoglobin, Lane 7; 0.05µM hemoglobin, Lane 8; 5µM hemoglobin + 5µM $FeSO_4$, Lane 9; Dipirydil, Lane 10; Control (No dipiridyl, No Iron)

CHAPTER 4

DISCUSSION AND CONCLUSION

Iron is essential for normal bacterial growth and development. Production of siderophores in an iron deprived condition is a common way to scavenge iron for many microorganisms. Siderophores cannot be transported through porins and require an outer membrane receptor because of their larger size (Liu et al. 1993). Uptake and transport of the trihydroxamate type siderophore, vicibactin, in *R. leguminosarum* ATCC requires such an outer membrane receptor protein. The receptor protein for vicibactin has not been classified yet. In *E.coli,* receptor FhuA transports a hydroxamate-type siderophore "ferrichrome" (Ferguson et al. 1998). Vicibactin and ferrichrome both are hydroxamate type siderophore; this was one of the reasons to look for FhuA receptor protein in *R. leguminosarum* ATCC. Previous studies have reported the presence of FhuA and iron-dependent expression of FhuA in *R. leguminosarum* 8401 *viciae* (Yeoman et al. 2000). However, there is also a presence of a pseudogene version of *fhuA* in *R. leguminosarum viciae* (Stevens et al. 1999).

The genome sequence of *R. leguminosarum* ATCC is not available hence primer walking technique was used to sequence the *fhuA* gene based on primers from the relative *R. leguminosarum* species. Primers based on *S. melioti* and *E. coli* didn't amplify the putative *fhuA* in *R. leguminosarum* ATCC. This means that there is a presence of a putative *fhuA* in *R. leguminosarum* ATCC. When amplified, the gel extracted PCR product was sent for sequencing. Sequencing was necessary to know about the gene and to perform *in-silico* analysis. Also sequencing of the flanking regions of the putative *fhuA* was necessary for whole gene knockout mutation. A regulatory gene *rosR* was present upstream of the putative *fhuA*, and a siderophore

reductase gene *fhuF* was present downstream of the putative *fhuA*. The pseudogene version of the *fhuA* was present after *fhuB* in an operon *fhuBCDA* in *R. leguminosarum viciae* (Stevens et al. 1999).

The ORF of putative *fhuA* was predicted using online prediction tools and looking at the -10 and -35 elements in the putative sequence data. The ORF was further analyzed by using *in silico* softwares. ORF of the putative *fhuA* was translated into amino acid sequence (ExPasy) that was 32% identical and 50% similar to that of *E.coli* (Ferguson et al.1998), and both nucleotide and amino acid sequence was more than 97% identical with the respective sequences from *R. leguminosarum viciae* (Stevens et al. 1999). When the independently predicted structure was compared to the crystal structure of FhuA of *E. coli*, putative FhuA showed many similarities including the shape and the orientation (22 β stranded barrel, the number of α helices, loop orientation, and the plug domain). Despite the fact that the nucleotide sequence of the putative *fhuA* was not identical with the nucleotide sequences of *E.coli fhuA* the structural similarity between the two proteins was indeed surprising. This suggests that these proteins are required for transport of similar type of ligand. FhuA is an outer membrane receptor in *E.coli* transporting ferrichrome, a hydroxamate type of siderophore produced by the fungi *Ustilago tritici.* Vicibactin is also a hydroxamate type syderophore and hence it is possible for a similar protein to transport these hydroxamate type ligands.

To answer the question if the putative ORF is related to iron transport, the effect of different iron concentrations was studied on the expression of putative gene *fhuA* and the putative protein FhuA. The expression of proteins involved in iron transport is regulated by the iron concentrations in the medium (Morton and Williams 1989).

SDS-PAGE and RT-PCR were carried out for determining the iron dependent putative FhuA protein expression and *fhuA* gene expression, respectively, in *R. leguminosarum* ATCC. The molecular weight of the putative protein coded by the putative ORF was calculated to be 82 kDa. One such protein, of size 82 kDa, in the SDS-PAGE, showed its dependence on iron concentration and was also similar to the size of known FhuA from *E.coli* (78 kDa). FhuA is an outer membrane receptor in *E.coli* transporting ferrichrome, a hydroxamate type of siderophore produced by the fungi *Ustilago tritici.* The concentration of iron in the media controlled the expression of the particular protein of approximately 82 kDa, downregulating it when the iron concentration was high. The expression of that 82 kDa band was high when the iron concentration was low. The Fe^{2+} in the media works as a corepressor and regulates the RirA transcription regulatory proteins, which regulate the genes associated with iron transport (Rudolph et al. 2006). As mentioned earlier, proteins involved in iron transport are known to be repressed at higher iron concentration in the media (Morton and Williams 1989). The results were further confirmed by RT-PCR assessing the expression of mRNA specific to the putative ORF. Equal amounts of total RNA were used and reverse transcribed to synthesize cDNA specific to the putative ORF. The cDNA was further amplified using gene specific primers. The amplification of the template occurs depending on its quantity. This shows difference in the amount of mRNA synthesized. The mRNA transcript showed the results similar to the putative band in SDS-PAGE gel. The expression of the 82 kDa protein in SDS-PAGE was repressed by iron concentrations of $\geq$ 2.5μM. A similar result was observed in RT-PCR when the difference in the band intensity was observed in a 1% agarose gel. The results supported the possible involvement of the putative ORF and the protein of interest in vicibactin mediated iron transport.

To determine if the putative FhuA was actually involved in vicibactin transport, an in-frame deletion/knockout of the gene was performed. As FhuA was known to transport a hydroxamate type siderophore, it was reasonable to hypothesize that a putative FhuA would be involved in hydroxamate type vicibactin transport. PCR based SOEing technique, cloning, and biparental conjugation as described were used to engineer a RLΔFhuA strain. The mutants were identified using colony PCR and antibiotics screening as previously described.

The primers designed outside the predicted/putative ORF and the sequencing results confirmed the in-frame deletion of putative *fhuA* in the mutant when compared with WT *R. Leguminosarum* ATCC. However, the primers within the ORF (gene-specific primers) showed amplification of *fhuA* gene using chromosomal DNA from the mutant. This suggested the presence of a *fhuA* homolog in the organism. Presence of more than one *fhuA* has been reported earlier in bacterial strains *S. melioti* (*fhuA*1 and *fhuA*2), *Azoarcus sp.* BH72 (*fhuA*1 and *fhuA*2), *Cupriavidus taiwanensis* LMG 19424 (*fhuA*1, *fhuA*2, *fhuA*3, and *fhuA*4), (Amadou et al. 2008; Po et al. 2008; Moldes et al. 2015). Similar results were obtained during the knockout studies involving *exbB-exbD* genes in *R. leguminosarum* ATCC, which led to the discovery of a Tol-Pal system (Barisic 2015). The presence of a pseudogene *fhuA* (*fhuA* homolog) has also been reported in previous works in *R. leguminosarum* 8401 *viciae* (Yeoman et al. 2000). This led us to a conclusion that a whole genome sequencing and southern blotting for the wild-type *R. leguminosarum* ATCC could help to confirm the presence of a homolog of *fhuA* gene or also maybe a pseudogene as the sequencing data obtained contained a lot of gaps in the codon.

The RLΔFhuA mutant strain was used for phenotypic studies. We wanted to determine if there is any phenotypic change or differences in the mutant. The mutant strain was used to test whether the deletion of the putative *fhuA* gene affected the growth under low iron concentration.

The mutant strain, however, did not show lower growth as compared to the WT under iron restriction. If iron transport had been disturbed, the mutants should have grown poorly as compared to the WT. The result clearly indicated that the mutants are acquiring iron similar to the WT cells. SDS-PAGE analysis of the whole cell or outer membrane extracts did not reveal the absence of a protein band around 82 kDa when compared to the WT. If a protein coding gene was deleted, there should have been no protein in the mutants and only present in the WT. This suggests that the deleted ORF is most likely not expressed or there is a presence of a protein of the similar size or perhaps a FhuA homolog.

Usually when an iron acquisition pathway is affected in an organism; it produces an increased level of siderophores (Takase et al. 2000). However, in this mutant the Atkin's assay confirmed that the cells didn't overproduce vicibactin, indicating that the mutant strain was still able to acquire sufficient iron. The mutant strain was not under iron restriction and was hence not overproducing vicibactin.

To perform a radiolabeled iron-vicibactin transport assay, vicibactin was isolated and purified using a series of chromatographic techniques including HPLC (Wright et al. 2012). The purified vicibactin can be used in future to perform transport assays using radiolabelled iron. The radiolabelled vicibactin transport assay using both the WT and a putative *fhuA* mutant strain could help determine the involvement of putative FhuA in vicibactin transport, if responsible. Also, for the future complementation assay and protein purification, the putative *fhuA* was cloned using a pET17b plasmid and transformed in *E.coli* BL21/DE3 competent cells. The complementation assay is required to transfer or repair the putative *fhuA* in the *fhuA*$^{-}$ mutants. This assay can be done after we confirm the role of putative *fhuA* in vicibactin transport. The expression cells can also be used for purifying the FhuA protein and use the purified protein for

crystallization, mass-spectrophotometr, HPLC and many other experiments which require concentrated and pure protein samples.

According to our second hypothesis, *R. leguminosarum* ATCC is able to utilize heme-bound iron. Various pathogenic and non-pathogenic bacteria can utilize heme-bound iron for regular growth and development (Yamamoto et al. 1995). Non-pathogenic Rhizobial species can also utilize heme-bound iron (Noya et al. 1997). *R. leguminosarum* ATCC is surrounded with leghemoglobin in root nodules, and leghemoglobin contains heme. This may explain *R. leguminosarum* ATCC's ability to uptake the human lyophilized hemoglobin, that also contains heme. *R. leguminosarum* ATCC was grown in MMW media supplemented with various concentrations of hemoglobin and hemin. The only source of iron in the media was hemoglobin or hemin. 2'2- dipiridyl was used to eliminate/chelate any trace amount of iron in the media. The results showed that *R. Leguminosarum* ATCC was able to utilize hemoglobin bound iron and the growth was dependent on hemoglobin concentration in the media. Different hemin concentrations, however, did not significantly affect the bacterial growth as hemoglobin did. Thus, hemoglobin was the better source of heme bound iron for *R. leguminosarum* ATCC.

It was necessary to identify the genes and proteins involved in heme bound iron uptake system. The TonB dependent hemoglobin transport system, with various genes associated has been reported previously in other rhizobial species (Wexler et al. 2001). The operon *hmuPSTUV* is required for heme-bound iron transport and utilization in *R. leguminosarum* (Wexler et al. 2001). Very similar to the siderophore uptake system, expression of the proteins required for heme-bound iron transport system is also controlled by the iron concentration in the media (Gao et al. 2005). The SDS-PAGE analysis of cell extracts grown at different concentrations of hemoglobin revealed that the expression of more than five proteins in size range of 35 kDa – 100

kDa, was controlled by the concentration of hemoglobin in the media. PCR amplification using primers based on the DNA sequences of the genes *hmuP, hmuS and hmuT* from a TonB dependent operon *hmuPSTUV* from *R. leguminosarum viciae* and sequencing revealed the presence of these genes in *R. leguminosarum* ATCC. The putative nucleotide sequence alignment with known gene from other species was 98% identical. Various other pathogenic strains also contained similar genes for heme-bound iron uptake. Molecular docking and *in-silico* analysis showed how heme could bind to each of these proteins and how their structure is similar to other known proteins from various other bacterial strains.

The heme bound iron uptake system in *R. leguminosarum viciae* is TonB dependent (Wexler et al. 2001), and the transport requires energy. RLΔTonB and RLΔExbB-ExbD were not able to utilize heme and showed slower growth as compared to the WT. This showed that TonB/ExbBD is required in *R. leguminosarum* ATCC for hemoglobin transport. The production of hemophores was not detected in the supernatant revealing that there could be a heme uptake system without any possible requirement of hemophores. The production of hemophores has not been reported in nonpathogenic strains of bacteria (Tong and Guo 2009). The *tonB* gene upstream of *hmuPSTUV* operon was also not present in this strain of *R. leguminosarum* ATCC. The presence of a *tonB* upstream of *hmuPSTUV* in *R. leguminosarum viciae* has been reported earlier (Wexler et al. 2001). Therefore, to find out about the energy transduction in heme-bound iron uptake, the whole genome sequencing could be used to locate a *tonB* gene. If present, this could be facilitating the heme-uptake in *R. leguminosarum* ATCC. It would also reveal other genes associated with the hemoglobin uptake system. The presence of *hmuV* and *hmuU* genes is yet to be confirmed in *R. leguminosarum* ATCC. We were also not able to detect the presence of the outer membrane receptor "ShmR" for hemoglobin transport in *R. leguminosarum* ATCC.

ShmR is an outer membrane receptor involved in hemoglobin transport in *S. melioti* (Battistoni et al. 2002).

There are many questions that need to be answered in this research for identifying the outer membrane receptor for vicibactin transport and understanding the iron transport system as a whole. As mentioned before, a southern blot analysis is very important using putative *fhuA* mutants and WT to check if there is more than one *fhuA* present in the bacterial genome. Another experiment that could be done is the transport assay using radiolabeled iron and vicibactin with WT and the putative *fhuA*$^{-}$ mutants. This would reveal the role of the deleted putative *fhuA*.

The preliminary work done on the hemoglobin bound iron uptake system will provide opportunity to explore the system further. This will help us to better understand the bacteria's ability to use the hemoglobin bound iron. It may also help us to understand the evolutionary aspects of the use of heme as a source of iron by non-pathogenic soil bacteria.

REFERENCES

Amadou C, Pascal G, Mangenot S, Glew M, Bontemps C, Capela D, Carrere S, Cruveiller S, Dossat C, Lajus A, Marchetti M, Poinsot V, Rouy Z, Servin B, Saad M, Schenowitz C, Barbe V, Batut J, Medigue C, Masson-Boivin C. 2008. Genome sequence of the beta-*Rhizobium cupriavidus taiwanensis* and comparative genomics of Rhizobia. Genome Research 18:1472-1483.

Ann J, Kim Y. 1998. A gene cluster encoding malonyl-CoA decarboxylase (MatA), malonyl-CoA synthetase (MatB) and a putative dicarboxylate carrier protein (MatC) in *Rhizobium trifolii*. Cloning, sequencing, and expression of the enzymes in *Escherichia coli*. European Journal of Biochemistry 257:395-402.

Andrews S, Robinson A, Rodríguez-Quiñones F. 2003. Bacterial iron homeostasis. FEMS Microbiology Reviews 27:215-237.

Anthea M, Hopkins J, William C, McLaughlin, Johnson S, Quon MW, LaHart D, Wright JD. 1993. Human Biology and Health. Englewood Cliffs, New Jersey, US. 0-13

Atkin CL, Neilands JB, Phaff HJ. 1970. Rhodotorulic acid from species of *Leucosporidium, Rhodosporidium, Rhodotorula, Sporidiobolus, and Sporobolomyces*, and a new alanine-containing ferrichrome from *Cryptococcus melibiosum*. J. Bacteriol. 103: 722-733.

Barisic V. 2015. Characterization of putative ExbB and ExbD leads to the identification of a potential Tol-Pal system in *Rhizobium leguminosarum* ATCC 14479 [MS thesis]. [Johnson City (TN)]: East Tennessee State University. Retrieved: 01/2016. http://dc.etsu.edu/etd/

Bar-Ness E, Hadar Y, Chen Y, Shanzer A, Libman J. 1992. Iron uptake by plants from microbial siderophores: A study with 7-Nitrobenz-2 Oxa-1,3-Diazole-Desferrioxamine as fluorescent ferrioxamine B analog. Plant Physiology. 99:1329-1335.

Baron S, Holmes RK, Jobling MG. 1996. Genetics: Conjugation: Baron's Medical Microbiology (4th ed). Univeristy of Texas Medical Branch, Austin. (Chapter 5)

Battistoni F, Platero R, Duran R, Cervenansky C, Battistoni J, Arias A, Fabiano E. 2002. Identification of an iron-regulated, hemin-binding outer membrane protein in *Sinorhizobium meliloti*. Applied and Environmental Microbiology 68:5877-5881.

Bitter W, Marugg J, Weger L, Tommassen J, Weisbeek P. 1991. The ferric-pseudobactin receptor PupA of *Pseudomonas putida* WCS358: homology to TonB-dependent *Escherichia coli* receptors and specificity of the protein. Molecular Microbiology 5:647-655.

Braun M, Killmann H, Braun V. 1999. The beta-barrel domain of FhuADelta5-160 is sufficient for TonB-dependent FhuA activities of *Escherichia coli*. Molecular Microbiology 33:1037-1049.

Carter R, Worsley P, Sawers G, Challis G, Dilworth M, Carson K, Lawrence J, Wexler M, Johnston A, Yeoman K. 2002. The vbs genes that direct synthesis of the siderophore vicibactin in *Rhizobium leguminosarum*: their expression in other genera requires ECF σ factor RpoI. Molecular Microbiology 44:1153-1166.

Centers for Disease Control and Prevention (CDC). 1998. Recommendations to prevent and control iron deficiency in the United States. U.S. Dept. of Health and Human Services, Atlanta, Ga. Retrievd 01/2017. https://www.cdc.gov/mmwr/preview/mmwrhtml/00051880.htm

Cuív P, Keogh D, Clarke P, O'Connell M. 2008. The *hmuUV* genes of *Sinorhizobium meliloti* 2011 encode the permease and ATPase components of an ABC transport system for the utilization of both haem and the hydroxamate siderophores, ferrichrome and ferrioxamine B. Molecular Microbiology 70:1261-1273.

Deniau C, Gilli R, Izadi-Pruneyre N, Létoffé S, Delepierre M, Wandersman C, Briand C, Lecroisey A. 2003. Thermodynamics of heme binding to the HasA hemophore: effect of mutations at three key residues for heme uptake. Biochemistry 42:10627-10633.

Dilworth M, Carson K, Giles R, Byrne L, Glenn A. 1998. *Rhizobium leguminosarum* bv. *viciae* produces a novel cyclic trihydroxamate siderophore, vicibactin. Microbiology 144:781-791.

Drechsel H, Jung G. 1998. Peptide siderophores. Journal of Peptide Science 4:147-181.

Elvehjem CA. 1931. The preparation of standard acid hematin solutions from hemin. J. Biol. Chem. 1931, 93:203-210

Ferguson A, Coulton J, Diederichs K, Welte W, Braun V, Fiedler H. 2000. Crystal structure of the antibiotic albomycin in complex with the outer membrane transporter FhuA. Protein Science 9:956-963.

Ferguson A, Hofmann E, Coulton J, Diederichs K, Welte W. 1998. Siderophore-mediated iron transport: crystal structure of FhuA with bound lipopolysaccharide. Science 282:2215-2220.

Freeman WM, Walker SJ, Vrana KE. 1999. Quantitative RT-PCR: pitfalls and potential. BioTechniques 26: 112-124.

Gao T, O'Brian M. 2005. Iron-dependent cytochrome C1 expression is mediated by the status of heme in *Bradyrhizobium japonicum*. Journal of Bacteriology 187:5084-5089.

Grandchamp G, Caro L, Shank E. 2017. Pirated siderophores promote sporulation in *Bacillus subtilis.* Applied and Environmental Microbiology 83:e03293-16.

Hammond SM, Lambert P, Rycroft A. 2012. The bacterial cell surface. Springer Science & Business Media. (chapter 6, pg. 194)

Hannauer M, Yeterian E, Martin L, Lamont I, Schalk I. 2010. An efflux pump is involved in secretion of newly synthesized siderophore by *Pseudomonas aeruginosa*. FEBS Letters 584:4751-4755.

Hans Fischer. 1941. "Hemin". Org. Synth. 21: 53.

Hill BD. 2014. Characterization of TonB in *Rhizobium leguminosarum* ATCC 14479 [thesis]. [Johnson City (TN)]: East Tennessee State University. Retrieved: 09/2015 http://dc.etsu.edu/etd/

Hoang T, Karkhoff-Schweizer R, Kutchma A, Schweizer H. 1998. A broad-host-range Flp-FRT recombination system for site-specific excision of chromosomally-located DNA sequences: application for isolation of unmarked *Pseudomonas aeruginosa* mutants. Gene 212:77-86.

Hogle S, Brahamsha B, Barbeau K. 2017. Direct heme uptake by phytoplankton-associated *Roseobacter.* Bacteria Systems 2:e00124-16.

Holmes RK. 2000. Biology and molecular epidemiology of diphtheria toxin and the *tox* gene. J. Infect. Dis. 181(Suppl. 1):S156-S167.

Horton RM, Cai ZL, Ho SN, Pease LR. 1990. Gene splicing by overlap extension: tailormade genes using the polymerase chain reaction. Biotechniques 8(5): 528-535.

Kalia A, Rattan A, Chopra P. 1999. A method for extraction of high-quality and high quantity

genomic DNA generally applicable to pathogenic bacteria. Analytical Biochemistry 275: 1-5.

Kloepper J, Leong J, Teintze M, Schroth M. 1980. Enhanced plant growth by siderophores produced by plant growth-promoting rhizobacteria. Nature. 286:885-886.

Kneen BE, Larue TA. 1983. Congo red absorption by *Rhizobium leguminosarum*. Applied Environmental Microbiology 45(1): 340-342.

Konishi H, Fujiya M, Tanaka H, Ueno N, Moriichi K, Sasajima J, Ikuta K, Akutsu H, Tanabe H, Kohgo Y. 2016. Probiotic-derived ferrichrome inhibits colon cancer progression via JNK-mediated apoptosis. Nature Communications 7:12365.

Kunkle CA, Schmitt MP. 2003. Analysis of the *Corynebacterium diphtheriae* DtxR regulon: identification of a putative siderophore synthesis and transport system that is similar to the *Yersinia* high-pathogenicity island-encoded yersiniabactin synthesis and uptake system. Journal of Bacteriology 185.23: 6826-6840.

Laemmli UK. 1970. Cleavage of structural proteins during the assembly of the head of bacteriophage T4. Nature. 227(5259):680-85.

Létoffé S, Delepelaire P, Wandersman C. 1996. Protein secretion in Gram-negative bacteria: assembly of the three components of ABC protein-mediated exporters is ordered and promoted by substrate binding. EMBO J. 15: 5804–5811.

Linberg R, Conover CD, Shum KL, Shorr RG. 1998. Hemoglobin based oxygen carriers: how much methemoglobin is too much?. Artif Cells Blood Substit Immobil Biotechnol. 26 (2): 133–48.

Liu J, Rutz J, Feix J, Klebba P. 1993. Permeability properties of a large gated channel within the

ferric enterobactin receptor, FepA. Proceedings of the National Academy of Sciences 90:10653-10657.

Loomis LD, Raymond KN. (1991). Solution equilibria of enterobactin and metal-enterobactin complexes. Inorganic Chemistry, 10, 906-911.

Loper JE, Buyer JS. 1991. Siderophore in microbial interaction on plant surface. Molecular Plant-Microbe Interaction 4(1): 5-13

Manhart JR, Wong PP. 1979. Nitrate reductase activities of rhizobia and the correlation between nitrate reduction and nitrogen fixation. Canadian Journal of Microbiology. 25: 1169-1174.

Marbach A, Bettenbrock K. 2012. Lac operon induction in *Escherichia coli*: Systematic comparison of IPTG and TMG induction and influence of the transacetylase LacA. Journal of Biotechnology. 157 (1): 82–8.

Martín-Moldes Z, Zamarro M, del Cerro C, Valencia A, Gómez M, Arcas A, Udaondo Z, García J, Nogales J, Carmona M, Díaz E. 2015. Whole-genome analysis of *Azoarcus sp*. strain CIB provides genetic insights to its different lifestyles and predicts novel metabolic features. Systematic and Applied Microbiology 38:462-471.

McAnulla C, Edwards A, Sanchez-Contreras M, Sawers RG, Downie JA. 2007. Quorum-sensing-regulated transcriptional initiation of plasmid transfer and replication genes in *Rhizobium leguminosarum* biovar *viciae*. Microbiology, 153:2074-2082.

Meija J. 2016. Atomic weights of the elements 2013 (IUPAC Technical Report).Pure Appl. Chem. (3): 265–91.

Messenger JM, Barclay R. 1983. Bacteria, Iron and Pathogenicity. Biochemical Education 11(2): 54-63.

Miethke M, Marahiel M. 2007. Siderophore-based iron acquisition and pathogen Control. Microbiology and Molecular Biology Reviews 71:413-451.

Miethke M, Pierik A, Peuckert F, Seubert A, Marahiel M. 2010. Identification and characterization of a novel-type ferric siderophore reductase from a gram-positive extremophile. Journal of Biological Chemistry 286:2245-2260.

Morton D, Williams P. 1989. Characterization of the outer-membrane proteins of *Haemophilus parainfluenzae* expressed under iron-sufficient and iron-restricted conditions. Microbiology 135:445-451.

Munro H. 1990. Iron regulation of ferritin gene expression. Journal of Cellular Biochemistry 44:107-115.

Muraki N, Aono S. 2016. Structural basis for heme recognition by HmuT responsible for heme transport to the heme transporter in *Corynebacterium glutamicum*. Chemistry Letters 45:24-26.

NCBI. 2017. National Center for Biotechnology Information, gene database. U.S. National Library of Medicine. Founded 1988. (Retrieved 01/2017) https://www.ncbi.nlm.nih.gov/gene/

Neumann E, Schaefer-Ridder M, Wang Y, Hofschneider PH. 1982. Gene transfer into mouse lyoma cells by electroporation in high electric fields. The EMBO Journal. 1 (7): 841–5.

Noya F, Arias A, Fabiano E. 1997. Heme compounds as iron sources for nonpathogenic *Rhizobium* bacteria. Journal of Bacteriology 179:3076-3078.

Ochsner UA, Johnson Z, Vasil ML. 2000. Genetics and regulation of two distinct haem-uptake systems, phu and has, in *Pseudomonas aeruginosa*. Microbiology, 146(1): 185-198.

Ott T, van Dongen J, Gu¨nther C, Krusell L, Desbrosses G, Vigeolas H, Bock V, Czechowski T, Geigenberger P, Udvardi M. 2005. Symbiotic leghemoglobins are crucial for nitrogen fixation in legume root nodules but not for general plant growth and development. Current Biology 15:531-535.

Pawelek P, Croteau N, Ng-Thow-Hing C, Khursigara C, Moiseeva N, Allaire M, Coulton J. 2006. Structure of TonB in complex with FhuA, *E.coli* outer membrane receptor. Science 312:1399-1402.

Peters N, Frost J, Long S. 1986. A plant flavone, luteolin, induces expression of *Rhizobium meliloti* nodulation genes. Science 233:977-980.

Pishchany G, Skaar E. 2012. Taste for Blood: Hemoglobin as a Nutrient Source for Pathogens. PLoS Pathogens 8:e1002535.

Postgate J. 1998. Nitrogen Fixation (3rd Ed.). Cambridge University Press. Cambridge, UK. Pg.1-15

Promega. 01/2017. Usage information for gotaq DNA polymerase PCR. https://www.promega.com/-/media/files/resources/protcards/gotaq-pcr-core-systems-quick- protocol.pdf)

Rachwał K, Boguszewska A, Kopcińska J, Karaś M, Tchórzewski M, Janczarek M. 2016. The regulatory protein RosR affects *Rhizobium leguminosarum* bv. *trifolii* protein profiles, cell surface properties, and symbiosis with clover. Frontiers in Microbiology 7: 1302.

Ramirez-Bahena M.H, Garcia-Fraile P, Peix A, Valverde A, Rivas R, Igual JM. 2008. Revision of the taxonomic status of the species *Rhizobium leguminosarum* (frank 1879) frank 1889AL, *Rhizobium phaseoli Dangeard*1926AL and *Rhizobium trifolii Dangeard* 1926AL. *R. trifolii* is a later synonym of *R. leguminosarum*. Reclassification of the strain

R. leguminosarum DSM 30132(=NCIMB 11478) as *Rhizobium pisi sp*. nov. International Journal of Systematic and Evolutionary Microbiology 58(11): 2484-2490.

Rhizobase. 01/2016. Kazusa genome resources. Kazusa DNA research institute, founded 1991. http://genome.annotation.jp/rhizobase

Rudnick RL, Gao S. 2003. Composition of the continental crust. The crust- Elsevier-Pergamon, Oxford 3: 1-64.

Rudolph G, Hennecke H, Fischer H. 2006. Beyond the Fur paradigm: iron-controlled gene expression in rhizobia. FEMS Microbiol Rev. 30(4):631-48.

Simon R, Priefer U, Pühler A. 1983. A broad host range mobilization system for *in vivo* genetic engineering: transposon mutagenesis in gram negative bacteria Bio/Technology, 1(9): 784-791

Smith A, Wilks A. 2015. Differential contributions of the outer membrane receptors PhuR and HasR to heme acquisition in *Pseudomonas aeruginosa*. Journal of Biological Chemistry 290:7756-7766.

Stevens JB, Carter RA, Hussain H, Carson KC, Dilworth MJ, Johnston AWB. 1999. The *fhu* genes of *Rhizobium leguminosarum*, specifying siderophore uptake proteins: *fhuDCB* are adjacent to a pseudogene version of *fhuA*. Microbiol. 145: 593 - 601.

Sugiura Y, Nomoto K. 1984. Phytosiderophores structures and properties of mugineic acids and their metal complexes. Structure and Bonding. 58: 107–135.

Sund R. 1983. Accent on science. Chas. E. Merrill, Columbus, Ohio.

Takase H, Nitanai H, Hoshino K, Otani T. 2000. Impact of siderophore production on

Pseudomonas aeruginosa infections in immunosuppressed mice. Infection and Immunity 68:1834-1839.

Thompson JM, Jones HA, Perry RD, 1999. Molecular characterization of the hemin uptake locus (hmu) from *Yersinia pestis* and analysis of hmu mutants for hemin and hemoprotein utilization. Infect Immun 67: 3879–3892.

Tong Y, Guo M. 2009. Bacterial heme-transport proteins and their heme-coordination modes. Archives of Biochemistry and Biophysics 481:1-15.

Walker SA, Downie JA. 2000. Entry of *Rhizobium leguminosarum* bv. *viciae* into root hairs requires minimal nod factor specificity, but subsequent infection thread growth requires nodO or nodE. Molecular Plant Microbe Interaction 13(7):754-762.

Wandersman C, Delepelaire P. 2004. Bacterial iron sources: from siderophores to hemophores. Annual Review of Microbiology 58:611-647.

Wexler M, Yeoman K, Stevens J, De Luca N, Sawers G, Johnston A. 2002. The *Rhizobium leguminosarum tonB* gene is required for the uptake of siderophore and haem as sources of iron. Molecular Microbiology 41:801-816.

Wexler M, Todd JD, Kolade O, Bellini D, Hemmings AM, Sawers G, Johnston AWB. 2003. Fur is not the global regulator of iron uptake genes in *Rhizobium leguminosarum*. Microbiology. 149: 1357 - 1365.

Wright W, Little J, Liu F, Chakraborty R. 2013. Isolation and structural identification of the trihydroxamate siderophore vicibactin and its degradative products from *Rhizobium leguminosarum* ATCC 14479 bv. *trifolii*. Biometals 26(2):271-83.

Yamamoto S, Hara Y, Tomochika K, Shinoda S. 1995. Utilization of hemin and hemoglobin as

iron sources by *Vibrio parahaemolyticus* and identification of an iron-repressible hemin-binding protein. FEMS Microbiology Letters 128:195-200.

Yeoman K, Timony C, Downie J, Stevens J, Johnston A, DeLuca N, Wisniewski-Dye F. 2000. Analysis of the *Rhizobium leguminosarum* siderophore-uptake gene *fhuA*: differential expression in free-living bacteria and nitrogen-fixing bacteroids and distribution of an *fhuA* pseudogene in different strains. Microbiology 146:829-837.

Yue W, Grizot S, Buchanan S. 2003. Structural evidence for iron-free citrate and ferric citrate binding to the TonB-dependent outer membrane transporter FecA. Journal of Molecular Biology 332:353-368.

APPENDICES

Appendix A: Media and Buffers

Luria Broth (LB)

Tryptone	10.0g
Yeast Extract	5.0g
NaCl	10.0g

ddH_2O to 1L

Dissolve ingredients and autoclave.

For LB agar plates:

Agar	15.0g

Dissolve ingredients, pH to 7.0 and autoclave.

Yeast Extract Mannitol Broth (YEM)/Congo Red Agar (CR)

Mannitol	l4.0g
K_2HPO_4	0.2g
$MgSO_4$	0.08g
NaCl	0.04g
Yeast Extract	0.4g

ddH_2O to 400 mL

Dissolve ingredients; adjust pH to 6.8 and autoclave.

For Congo Red agar plates, add:

Agar 12.0g

1% Congo red dye 1 mL

Dissolve ingredients to final volume 500mL; adjust pH to 6.8 and autoclave

Modified Manhart and Wong (MMW) Media

Basal Media	Gm
Dextrose	6.0
Glutamate	1.5
KH_2PO_4	1.0
K_2HPO_4	0.764
$MgSO_4$	0.18
$CaSO_4 * 2H_2O$	0.13

Final volume of 1 Litre, pH to 6.8 and autoclave

Vitamin Solution (1000x concentrated)	mg
$Na_2EDTA*2H_2O$	550
$Na_2MoO_4*2H_2O$	250
H_3BO_3	145
$ZnSO_4*7H_2O$	108
CalciumPanthenate	50

Inositol	50
Thiamine HCl	40
Biotin	12
$CoCl_2*6H_2O$	10
Riboflavin	10
p-aminobenzoic Acid	10
Nicotinic Acid	10
Pyridoxine HCl	10
Vitamin B12	10
$CuSO_4*5H_2O$	4.37
$MnCl_2*4H_2O$	4.3

SDS-PAGE Solutions and Buffers

Running Gel Buffer pH = 8.8

Tris 36.6 g

ddH_2O to 200 mL

Stacking Gel Buffer pH = 6.8

Tris 3.0 g

ddH_2O to 50 mL

2x Loading Buffer

Stacking Gel Buffer 2.5 mL

10% SDS 4.0 mL

Glycerol 2.0 mL

2-mercaptoethanol 1.0 mL

Bromophenol blue 2.0 mg

ddH_2O 10 mL

Coomassie Blue Stock

Coomassie Blue R-250 2.0 g

ddH_2O 200 mL

Tank Buffer (4x)

Tris 12 g

Glycine 57.6 g

SDS 4 g

ddH_2O to 1L

Coomassie Stain

Coomassie Blue Stock 12.5 mL

Methanol 50 mL

Glacial acetic acid 10 mL

ddH_2O 100 mL

Destaining Solution

Methanol 500 mL

Glacial acetic acid 100 mL

ddH_2O 400 mL

10% SDS-PAGE Recipe

Volume

Ingredient	Stacking Gel	Running Gel
30% Bis-acrylamide	1.33 mL	6.66 mL
Running Buffer	0 mL	5.0 mL
Stacking Buffer	2.50 mL	0 mL
ddH_2O	6.1 mL	8.0 mL
10% SDS	100 uL	200 uL
TEMED	5 uL	10 uL
10% Ammonium Persulfate (APS)	50 uL	100 uL

Degas before addition of TEMED and 10% APS

Appendix B: Alignments

Alignment of putative *fhuA* with *R. leguminosarum* 3841 and *R. leguminosarum* J251

The query is the putative *fhuA* from *R. leguminosarum* ATCC.

Rhizobium leguminosarum fhuA gene

Sequence ID: AJ238208.1 **Length:** 2997 **Number of Matches:** 1

Range 1: 39 to 2997 GenBank Graphics Next Match Previous M

Score	Expect	Identities	Gaps	Strand
5134 bits(2780)	0.0	2916/2978(98%)	24/2978(0%)	Plus/Plus

```
Query  1    GACATACGCACTGTGACCGTGTTCGGAATCTCCCAGACGCCGAACTTGACGACCTTCCCA  60
Sbjct  39   GACAATCGCA-TGTG-CC-TGTGCGGAATC-ATGAG-CGCCGAACTTGACGACCTTCCCA  93

Query  61   CGGAGGTTCGGACCGAGGTCGATAATATTCGCCGCTATGAACGTCCATTGGCTATCCAAG  120
Sbjct  94   CGGAGGTTCGGACCGAGGTCGATAA-ATTCGCCGCTATGAACGTCGGTTGGCTATCCAAG  152

Query  121  GTGCTCTCGCGGGCCAAGCCTTCCGCAAGCGACCAAGACCTGCAGGAGCACGCGATGGCG  180
Sbjct  153  GT-CTTTCGCGGGCCAAGCCTTCCGCAAGCGACCAAGACCTGCAGGAGCACGCGATGGCG  211

Query  181  ATCTTCGCAGCCATCGAGGGGG-CCCAGCTGGTCGCGCGGGGCTGCCAGGACATCGGCAT  239
Sbjct  212  ATCTTCGCAGCCATCGAGGGGGCCCCAGCTGGTCCCGC-GGGCTGCCAGGACATCGGCAT  270

Query  240  CTATGACCGGACGATCCGGGCTTACCGAGCGACAGGTCTCTTCCCGTAATTGGCCGGCGG  299
Sbjct  271  CTATGACCGGACGATCCGGGCTTACCGAGCGACAGGTCTCTTCCCGTAATT-GCCGGCGA  329

Query  300  CTCAAATGGGAGTGGCAGTTGACTCAAGTGA-GGCGATGGTTGTTTTTGCGCAAGTTCCC  358
Sbjct  330  CTCTAATGGGAGTGGCAGTTG-CTCAAGTGAGGGCGATGG-T-CTTTTGCGCAAGT--CC  384

Query  359  GCCGGCCGACCTATCCGGCGAGCCACTTCAGACGGCATCTGCGGTCGAAAATACCCCTCCT  418
Sbjct  385  GCCGGCCGACCTATCCGGCGAGCCACTTCAG-CGGCATCTGCAGTCGAAATACCCCTCCT  443

Query  419  ACTCAGTCAGTTGATACTGCTGGCCGCGGGCGTGGTTCAAAATCAGCAGCAA-TAGAAGA  477
Sbjct  444  ACTCAGTCAGGTGATACT-CTGG-CGCGGGCGTGGTTCAAAATCAGCAGCAAATACGGGA  501

Query  478  TCGTCGGGTCCATCCCCGTCAAGACCGGCAGGTTGGCAGTCGTCTCGGTGCGCACTTGGT  537
Sbjct  502  TCGTCGGGTCCATCCCCGTCAAGACCGGCAGGTTGGCCATCGTCTCGGTGCGCGCTTGGT  561

Query  538  CTCGCGCGCGGCAGAACCGCCTCCGTT-GGCA-CCGCACAGACACGTTACGAGGCCTCGA  595
Sbjct  562  CTCGCGCGCGGCAGAACTGCCTCTGTTTGGCAGCCCCACAGA-ACGTTACGAGGCCTCG-  619

Query  596  ATTCTACGTGCAACCTGTTCGGGAGTGTTGAAGGCGTGGATTTATCGATTTAAAGGTGAC  655
Sbjct  620  ATTCTACGTGCAACCTGTTCGGGAGTGTTGAAGGCGTGGATTTATCGATTTAAAGGTGAC  679
```

Nucleotide 1- Nucleotide 597 aligned with *fhuA* of *R. leguminosarum* 8401 only as the sequence of *R. leguminosarum* J251 was not present. The query is the putative *fhuA* from *R. leguminosarum* ATCC.

Nucleotide 597- Nucleotide 1256 aligned with *R. leguminosarum* 8401. The box above is the putative start codon. The arrows show the differences in the nucleotide sequence. The query is the putative *fhuA* from *R. leguminosarum* ATCC.

Nucleotide 1257- Nucleotide 2096 aligned with *R. leguminosarum* 8401. Arrows show the changes in the nucleotide sequences. The query is the putative *fhuA* from *R. leguminosarum* ATCC.

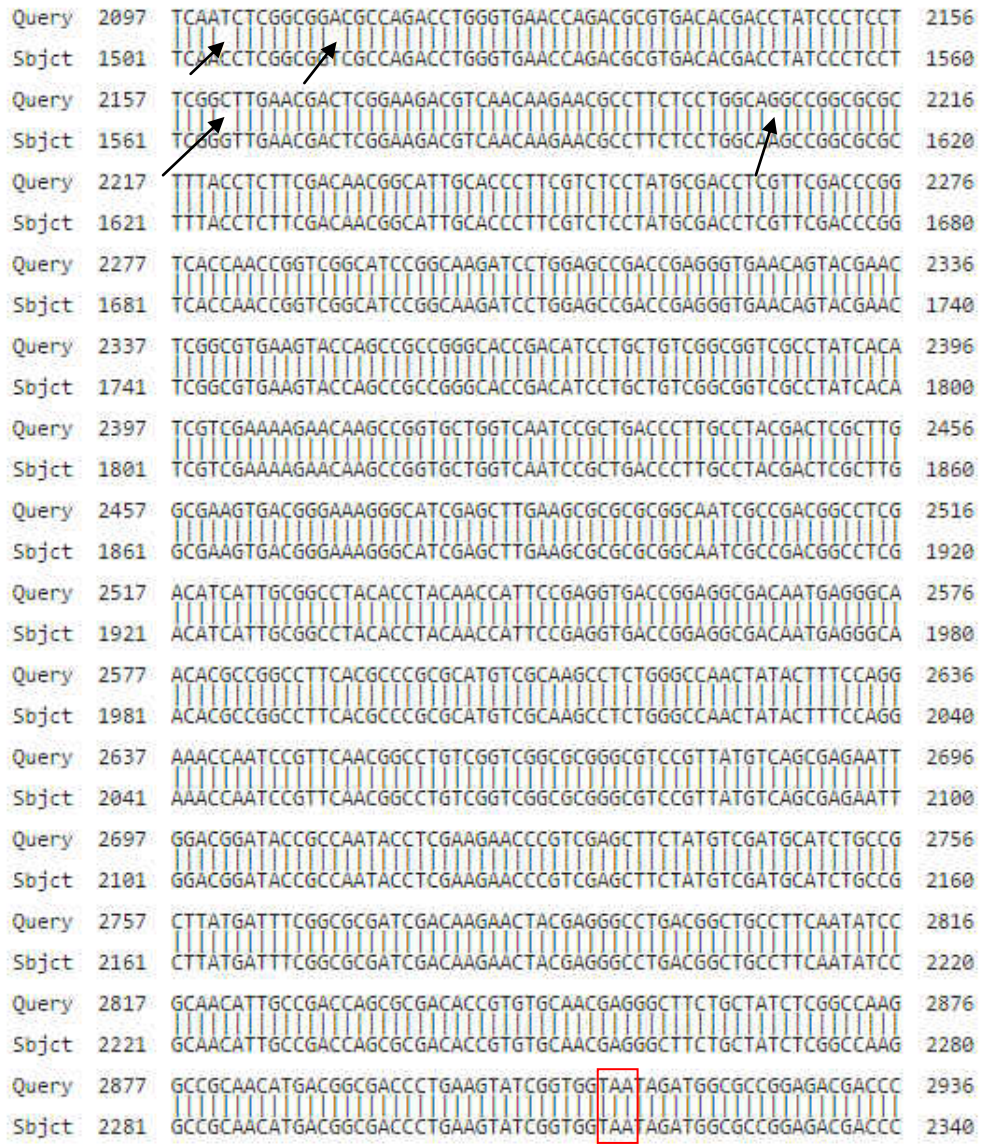

Nucleotide 2097 - Nucleotide 2936 aligned with *R. leguminosarum* 8401.The box shows the putative stop codon. Arrows show the changes in nucleotides. The query is the putative *fhuA* from *R. leguminosarum* ATCC.

Nucleotide 2937- Nucleotide 3746 aligned with *R. leguminosarum* J251, did not align with 8401 as the sequence data from 8401 is not available.

Alignment with *rosR* transcriptional regulator gene and *fhuF* siderophore-iron reductase

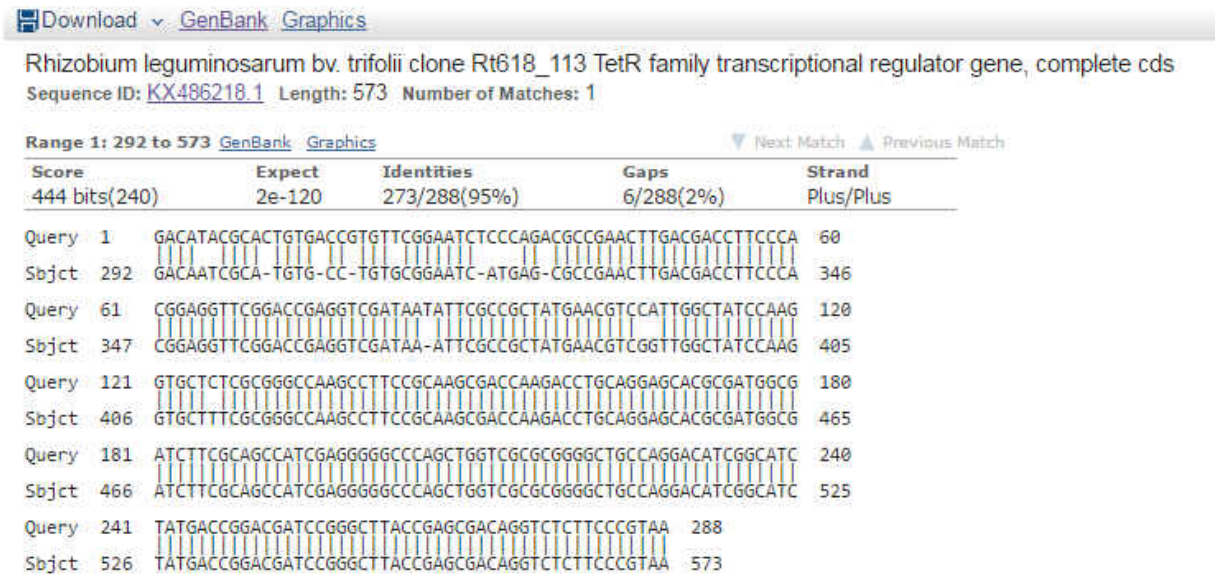

The fragment in front of the putative *fhuA* aligned with *rosR.* Whole gene has to be yet sequenced. Only a small fragment of 288 bp aligned with the known *rosR*. Query sequence is the sequence of the putative *rosR.* Remaining part of the gene needs to be sequenced further.

Alignment of the putative *fhuF* gene with the *fhuF* gene from *R. leguminosarum trifoli* 24.2. The complete sequencing yet has to be done. The query is the putative *fhuF* from *R. leguminosarum* ATCC.

VITA
SUSHANT KHANAL

Personal Data:	Date of Birth: March 14, 1992 Place of Birth: Bhaktapur, Nepal
Education:	Masters of Science (M.S.) in Biology, 2018. Concentration: Microbiology, East Tennessee State University. Johnson City, Tennessee, USA. Bachelors of Science (B.Sc.) in Biotechnology, 2013, SANN International College, Gairidhara-Kathmandu, Nepal (Affiliated Purbanchal University). High School (10+2) Major: Science, HSEB, 2008, AdarshaVidyaMandir Higher Secondary School (AVM) Lalitpur, Nepal. School Leaving Certificate (until Grade 10), 2007, SOS Hermann Gmeiner School, Bhaktapur-Nepal
Awards:	First place in poster presentation in Appalachian Student Research Forum (ASRF), 2016. Thesis/dissertation scholarship from ETSU, 2017. Graduate Assistantship/tuition scholarship at East Tennessee State University, 2015-2017.
Professional Experience:	Teaching Assistant/Graduate Assistant: East Tennessee State University (ETSU), Department of Health Sciences, 2015-2017. Research Assistant: Nepal Agriculture Research Council (NARC) at Animal Health and Research Division (AHRD), 2014-2015. Executive member: Biotech Association of Nepal for Research and Development (BANRD), 2011-2012.

Photo journalist: Government of Nepal, Ministry of information and communication, 2012-2014.

Presentations:

Khanal S. and Chakraborty R., 2016. “Characterization of *fhuA* like receptors for vicibactin transport and investigation of hemoglobin bound iron uptake in *R. leguminosarum* ATCC 14479.” Appalachian Student Research Forum, East Tennessee State University, Johnson City, TN, 2016.